DOKUZ EYLUL UNIVERSITY
GRADUATE SCHOOL OF NATURAL AND APPLIED SCIENCES

BIOSORPTION OF ZINC (II) IONS ONTO POWDERED WASTE SLUDGE IN BATCH AND FED-BATCH REACTORS

by
Sinem ÇIKLA

November, 2005
İZMİR

BIOSORPTION OF ZINC (II) IONS ONTO POWDERED WASTE SLUDGE IN BATCH AND FED-BATCH REACTORS

A Thesis Submitted to the
Graduate School of Natural and Applied Sciences of Dokuz Eylül University
In Partial Fulfillment of the Requirement for the Degree of Master of Science in Environmental Engineering, Environmental Technology Program

by
Sinem ÇIKLA

November, 2005
İZMİR

M.Sc THESIS EXAMINATION RESULT FORM

We certify that we have read this thesis and **"BIOSORPTION OF ZINC (II) IONS ONTO POWDERED ACTIVATED SLUDGE IN BATCH AND FED-BATCH REACTORS"** completed by **Sinem ÇIKLA** under supervision of **Prof.Dr. Fikret KARGI** and that in our opinion it is fully adequate, in scope and in quality, as a thesis for the degree of Master of Science.

Prof.Dr. Fikret KARGI

Supervisor

(Committee Member)

(Committee Member)

Approved by the

Graduate School of Natural and Applied Sciences

Prof.Dr. Cahit HELVACI
Director

ACKNOWLEDGMENTS

I would like to greatly thank to my supervisor Prof. Dr. Fikret Kargı for his valuable advises, incomparable helps, continuous supervision and considerable concern in carrying out the study. It has been a great honor and privilege for me to work with him.

I also would like to thank to research assistants Yunus Pamukoğlu, Serkan Eker and Serpil Özmıhçı for their help in my laboratory studies.

At the same time I thank to my best friend Gökhan Çabuk who helped me in preparing my thesis.

Furthermore, I greatly acknowledge my family, for being always with me in every single steps of this thesis with their encouragement.

Sinem ÇIKLA

BIOSORPTION OF ZINC (II) IONS ONTO POWDERED WASTE SLUDGE IN BATCH AND FED-BATCH REACTORS

ABSTRACT

In this study, the removal of zinc ions from aqueous solution using powdered waste sludge (PWS) under different experimental conditions was investigated in batch shake flasks and fed-batch reactors. Waste sludge from a paint industry wastewater treatment plant of DYO, Izmir was used for biosorption of zinc (II) ions becuase of its high biosorption capacity. The powdered waste sludge (PWS) was pre-treated with 1% H_2O_2 to improve the biosorption capacity. The effects of the initial zinc(II) ion and PWS concentration, particle size, agitation speed, temperature and pH on the rate and extent of zinc (II) biosorption were investigated.

Removal of zinc by adsorption increased with increasing PWS concentration, agitation speed, temperature and pH. The performance of biosorption of zinc ions onto pre-treated PWS samples were investigated for five different particle sizes of between 53 and 231μm using 1 g l^{-1} PWS concentration and 100 mg l^{-1} Zn^{2+} concentration at 25 ^{0}C. The extent of biosorption of zinc ions increased and the final Zn^{2+} concentration in solution decreased with decreasing particle size (D_p) because of larger external surface area of PWS at small particle sizes. From the batch shake flask experiments, optimum conditions for biosorption of zinc (II) ions were found to be 150 rpm, an average particle size of 64 μm and pH=5 with 24 hours of contact time.

The biosorption kinetics was tested for the pseudo-first order and pseudo-second order models at different experimental conditions. The rate constants of biosorption for both models were calculated. Good correlation coefficients were obtained for the pseudo-second order kinetic model of particle size, temperature, initial zinc and PWS concentrations data indicating that zinc biosorption process fitted to the pseudo-second order rate model better than the first order. Three different biosorption

isotherms were used to correlate the equilibrium biosorption data for different zinc and PWS concentrations and the isotherm constants were determined.
The Langmuir isotherm was found to fit the experimental data better than the other isotherms tested. Maximum biosorption capacity was found to be 82 mg Zn. g PWS^{-1}.

The operating parameters varied in fed-batch biosorption studies were feed flow rate, feed zinc concentration and the initial PWS concentration. Data confirmed that percent Zn^{2+} removal and biosorbed zinc concentration increased with increasing flow rate when initial PWS content was 3 g. Percent Zn^{2+} removal decreased and biosorbed zinc concentration increased with increasing initial zinc concentration. When initial PWS content increased, percent zinc biosorption and biosorbed zinc concentration increased. The results also indicated that biosorption efficiency can be improved by using high flow rates, low zinc (II) concentration in the feed and high PWS concentrations.

Keywords: biosorption; isotherms; kinetics; powdered waste sludge (PWS); zinc (II) ions

KESİKLİ VE KESİKLİ BESLEMELİ REAKTÖRLERDE ÇİNKO (II) İYONLARININ TOZ ATIK ÇAMUR ÜZERİNE BİYOSORPSİYONU

ÖZET

Bu çalışmada, farklı koşullarda toz arıtma çamuru (TAÇ) kullanarak sulu ortamlardan çinko (Zn) iyonlarının biyosorpsiyonla giderimi kesikli çalkalayıcı ve kesikli beslemeli reaktörlerde incelenmiştir. Yüksek biyosorpsiyon kapasitesi nedeniyle DYO boya endüstrisi atıksu arıtma tesisinden temin edilen arıtma çamurları çinko iyonlarının biyosorpsiyonunda kullanılmıştır. Biyosorpsiyon kapasitesini arttırmak için toz arıtma çamuru 1% H_2O_2 ile ön arıtıma tabii tutulmuştur. Başlangıç çinko (II) iyonu ve toz arıtma çamuru (TAÇ) konsantrasyonlarının, TAÇ' unun tanecik çapı, çalkalama hızı, sıcaklık ve pH'ın çinko giderim verimi üzerine etkileri saptanmıştır.

Biyosorpsiyon ile çinko giderimi toz arıtma çamuru konsantrasyonu, çalkalama hızı, sıcaklık ve pH'ın artmasıyla birlikte artmıştır. 25 ^{0}C'de 1 g l^{-1} toz arıtma çamuru ve 100 mg l^{-1} çinko kullanılarak, 53 ve 231 µm arasındaki beş farklı tanecik çapında ön arıtıma tabi tutulmuş TAÇ örnekleri üzerine çinko (II) iyonlarının biyosorpsiyonu kesikli deneylerle incelenmiştir. Küçük parçacık çaplarında TAÇ'ın daha geniş dış yüzey alanına sahip olması nedeniyle, parçacık çapının azalmasıyla birlikte çinko iyonlarının biyosorpsiyon verimi artmış ve çözeltideki son Zn^{2+} konsantrasyonları azalmıştır. Optimum biyosorpsiyon koşulları 24 saat temas süresi ile kesikli çalkalayıcı deneyleri sonucunda 150 rpm, 64 µm ortalama parçacık çapı ve pH=5 olarak bulunmuştur.

Biyososrpsiyon kinetiğnin incelenmesinde birinci derece ve ikinci derece kinetik modelleri farklı deneysel koşullarda kullanılmış ve her iki model için biyosorpsiyon hız sabitleri hesaplanmıştır. İkinci derece kinetik modeli kullanıldığında TAÇ ve Zn^{2+} konsantrasyonları, parçacık büyüklüğü ve sıcaklık değişimi deneylerinde yüksek korelasyon değerlerine ulaşılmıştır. Çinko ve TAÇ konsantrasyonlarının değiştirildiği deneylerde dengedeki biyosorpsiyon verileri için üç farklı

biyosorpsiyon izotermi kullanılmış ve izoterm sabitleri belirlenmiştir. Deneysel veriler kullanılarak değerlendirilen izotermler arasında Langmuir izoterminin diğer izotermlere kıyasla daha uygun olduğu saptanmıştır. Maksimum biyosorpsiyon kapasitesi 82 mg Zn g TAÇ$^{-1}$ olarak bulunmuştur.

Kesikli beslemeli adsorpsiyon çalışmalarında çinko çözeltisi debisi, giriş çinko ve TAÇ konsantrasyonları değiştirilmiştir. Deneysel sonuçlara göre, başlangıç TAÇ miktarı 3 g olduğunda, çinko giderim yüzdesi ve katı faz çinko konsantrasyonu, debinin artmasıyla artmıştır. Başlangıç çinko konsantrasyonunun artmasıyla çinko giderim yüzdesi azalmış ve katı faz çinko konsantrasyonu ise artmıştır. Başlangıç TAÇ miktarı arttırıldığında, biyosorblanan çinko konsantrasyonu ve çinko giderim verimi artmıştır. Deneysel sonuçlar göstermektedir ki, yüksek çinko biyosorpsiyon kapasitelerine ulaşmak için, biyosorpsiyon prosesi yüksek çinko çözeltisi debisinde, düşük çinko ve yüksek TAÇ konsantrasyonlarında işletilmelidir.

Anahtar kelimeler: Biyosorpsiyon; izoterm; kinetik; toz arıtma çamur (TAÇ); çinko iyonu

CONTENTS

CHAPTER ONE
INTRODUCTION

1.1. Literature Review

Presence of heavy metals in wastewaters causes significant environmental problems. High concentrations of heavy metals are known to be toxic and carcinogenic to living organisms. When heavy metals are present even in a very low concentration, their concentration may be elevated through bio-magnification to a level that they start to exhibit toxic characteristics. Therefore, heavy metals are major pollutants in many industrial wastewaters and are toxic to human and aquatic life.

Heavy metals in wastewaters have increased to toxic levels because of the human and industrial activities. Mine drainage, metal industries, petroleum refining, tanning, photographic processing and electroplating are some of the main industrial sources of heavy metals. Erosion of surface deposits of metal minerals, agricultural runoff, and acid rain contribute to heavy metals in wastewater naturally.

Adverse effects of heavy metal ions present in some chemical industry wastewaters such as pulp and paper, petrochemicals, refineries, fertilizers, steel and otomobile industries on the performance of biological treatment systems and on the receiving environment have been observed by many investigators (Kratochvil & Volesky, 1998; Aksu 2005).

Uncontrolled discharge of heavy metal containing wastewaters to the environment can be detrimental to humans, animals and the plants. As a result, removal and recovery of heavy metals from industrial wastewaters before biological treatment has gained considerable attention in recent years to protect the environment. Lead, mercury, chromium, cadmium, copper, zinc, selenium, iron, nickel, mercury are the most frequently found heavy metals in industrial wastewaters (Fergusson, 1990).

There are many processes that can be used for the removal of heavy metals from wastewaters. The conventional techniques commonly applied for the removal of heavy metals from wastewater include chemical and physical methods. Chemical methods are chemical precipitation/neutralization, coagulation / flocculation, solvent extraction and electro dialysis. Physical methods are ion exchange, membrane separation, adsorption and filtration. In chemical precipitation, chemicals such as ferrous sulfide, lime, caustic and sodium carbonate are usually used. However, these chemical and physical methods have significant disadvantages, including incomplete metal removal, production of large volume of sludge, requirements for expensive equipment and monitoring systems, high reagent or energy requirements and generation of toxic sludge or other waste products that require disposal. And also, when applied to dilute metal waste or lower concentrations of metals (<100 mg/L), these processes are either ineffective or not cost effective.

Methods used for removal of heavy metals from wastewaters can be classified as physical, chemical and biological. Physico-chemical methods such as precipitation, adsorption, ion exchange, and solvent extraction require high capital and operating costs and may produce large volumes of solid wastes (Kratochvil & Volesky, 1998).

Because of these disadvantages, a biological treatment which is called biosorption based on organisms or plants could be an alternative method to clean up industrial wastewaters containing heavy metals. Other processes are not suitable for wastewaters with high metal concentration, and are very sensitive to the characteristics of the effluent, such as temperature, pH and chemical composition.

Biological materials may be used for biosorption of heavy metals from solution. Biological materials accumulate heavy metals from wastewater through metabolically mediated or physico-chemical pathways of uptake (Fourest & Roux, 1992). Some advantages of biosoption for removal of heavy metals over chemical and physical methods can be summarized as follows:

1. Excess sludge from wastewater treatment plants may be used as biosorbent
2. Low cost, free availability and possible reuse of the biosorbent
3. High biosorption capacity because of large surface area of sludge organisms
4. Selective adsorption of metal ions
5. Operation over a broad range of environmental conditions (pH, ionic strength, temperature)

Different kinds of biomaterials such as digested sludge, activated sludge, and biomass waste may be used to remove heavy metals from wastewaters by biosorption. The use of microorganisms as biosorbents for heavy metals offers a potential alternative to recovery of heavy metals from industrial wastewaters. The special surface characteristics of microorganisms enable them to adsorb heavy metal ions from solutions. Bacteria, algae, fungi and yeast are some of the microorganisms that can efficiently accumulate heavy metals.

Furthermore, either live or dead microorganisms or their derivatives can be used for biosorption. Complex metal ions are adsorbed onto the surface of organisms by the functional groups located on the outer surface of the biosorbents. The use of dead microbial cells is more advantageous for water treatment because dead organisms are not affected by toxic wastes, they do not require a continuous supply of nutrients and they can be regenerated and reused for many cycles. But, the use of dead biomass in powdered form presents some difficulties, such as mass loss after regeneration, difficulty in the separation of biomass after biosorption, and low strength and small particle size that cause problems in column systems. So, dead biomass can be immobilized in a supporting material to solve these problems. Support materials used for immobilization must be rigid, chemically inert and cheap. And also, support materials should bind cells firmly, should have high loading capacity and a loose structure for overcoming diffusion limitations. The application of immobilization on dead biomass in a biopolymeric or polymeric matrix may enhance biosorption performance, biosorption capacity, increase mechanical strength and facilitate separation of biomass from metal-bearing solution. The number of binding sites easily accessible to metal ions in solution is greatly reduced when biomass is

immobilized. The majority of sites will lie within the bead after reducing of binging sites.

Large numbers of studies were reported in literature on biosorption of heavy metals onto different organisms. Most of those studies were done using pure cultures of bacteria, yeasts and molds (Yetis et al., 1998; Galli, Di Mario, Rapana, Lorenzoni & Angelini, 2003; Ozdemir, Ozturk, Ceyhan, Isler & Cosar, 2003; Davisa, Voleskya & Mucci, 2003; Sag and Kutsal, 2000; Sag, Tatar & Kutsal, 2003). Biomass from activated sludge reactors operating at different dilution rates was used by Arican, Gokcay & Yetis (2002) to investigate the effect of sludge age on Ni^{2+} removal by batch biosorption tests. Linear adsorption isotherms were obtained at all dilution rates indicating the presence of equilibrium between biomass and the nickel ions.

Goel, Kadirvelu, Rajagopal & Garg (2005) studied the dependence of adsorption on adsorbent (activated carbon and modified activated carbon) and adsorbate (lead) characteristics by means of both batch and column studies under various conditions. According to isotherm analysis for column mode adsorption studies, the extent of Pb(II) removal was found to be higher in the treated activated carbon. Removal of Pb(II) onto adsorbent depends on adsorbent concentration, and hydraulic loading rate, feed concentration and adsorbent bed height for the continuous-flow column operations. The data generated from column studies was correlated with the Bohart–Adams model. Adsorption capacity for 6 mg/l feed concentration of Pb(II) at hydraulic loading rate of 7,5 $m^3/(h.m^2)$ and 0,4 m bed height was found to be 2,89 mg/g in the column experiments, which indicated that adsorption capacity of modified activated carbon in column experiments was far less than that of batch experiments.

The removal of chemical grade methylene blue and commercial red basic 22 by $CaCl_2$ treated beech sawdust was studied by Batzias & Sidiras (2004) using untreated beech sawdust as control. The batch and column adsorption kinetics of the two dyes were used to estimate the adsorption capacity of the untreated and treated beech sawdust. The adsorption capacity coefficient values were determined using the

Bohart and Adams' bed depth service model. The results showed that $CaCl_2$ treatment enhanced the adsorption capacity of the adsorbent.

Yan (2001) investigated the potential of the fungus *Mucor rouxii* to remove lead, cadmium, nickel and zinc from aqueous solutions in batch and column systems. Live *M. rouxii* biomass exhibited a higher biosorption capacity than autoclaved biomass for metal ions. Because of its filamentous form, biomass had a high surface area. Autoclaved biomass pretreated with alkaline solution exhibited improved metal removal capacity. Biomass immobilized in form of beads was able to remove metal ions from aqueous solutions. Experiments showed that pretreated and powdered biomass had a higher metal biosorption capacity than beads. The biosorption capacity of beads was 3,66, 1,12, 0,25, 1,35 mg g^{-1} for lead, cadmium, nickel and zinc, respectively. In biosorption kinetic studies Ho's model (pseudo-second order) was found to be better than Lagergren model.

Bux, Atkinson & Kasan (1999) investigated and compared the biosorptive capacities of waste activated and waste digested sludge. Surface charge of each was determined in order to relate electro- negativity with bio-sorption capacity. Activated sludge was found to be more effective than digested sludge for removal of zinc from a metal plating effluent. Sludge bio-sorption capacity increased with initial zinc concentration.

Xu (2002) used *Laminaria japonica*, which is commonly called kelp, as a biosorbent for heavy metal removal. Kelp was found to have superior biosorption capacity over many natural biomaterials investigated such as seaweed, water hyacinth and activated sludge. He used fixed-bed column operations with kelp for the biosorption of Cd, Cu, Ni and Zn. The equilibrium biosorption capacity of heavy metal ions was found in the order of Cd>Cu>Zn>Ni.

Al-Asheh (1997) used *Aspergillus carbonarius* and plant materials such as canola meal (CM), pine bark and moss for heavy metal removal by biosorption. The effects of temperature, adsorbent and metal concentrations and pH on metal ion adsorption

were investigated using batch and continuous processes. The uptake of metal ions per unit mass of adsorbent decreased with an increasing adsorbent concentration. Pre-heating of *A. carbonarius* biomass to higher temperatures prior to utilization decreased its metal sorption capacity. The affinity *A. carbonarius* for different metal ions was found to be in the order of $Cu^{+2}>Cr^{+2}>Cd^{+2}$. Decreasing CM particle sizes resulted in an increase in uptake of metal ions. The affinity of CM for the sorption of the tested metals followed the order of $Zn^{+2}>Cr^{+2}>Cu^{+2}>Cd^{+2}>Ni^{+2}$. The affinity of moss for heavy metal biosorption was in the order of $Cr^{+2}>Cu^{+2} >Zn^{+2}>Ni^{+2}> Cd^{+2}$. The adsorption capacity of pine bark was found to be in the following order $Cu^{+2}>Zn^{+2}>Cd^{+2}>Ni^{+2}$. These results demonstrated that in a mixture of metal ions, the adsorption of one metal was affected by the presence of the others and also by the type of adsorbent used.

The ability of dried anaerobic activated sludge to adsorb phenol and chromium (VI) ions in a batch system was investigated by Aksu & Akpınar (2001). The optimum initial pH for both chromium (VI) ions and phenol biosorption was determined to be 1,0. The cells of dried anaerobic activated sludge bacteria were effective for simultaneous removal and separation of phenol and chromium (VI) ions from aqueous effluents.

The binding of heavy metal ions (Cd, Cu, Zn), light metal ions (Ca, Na) and protons to biomass of the brown alga *Sargassum* were investigated by Schiewer (1996). The mechanism of metal binding was confirmed to be ion exchange. Biosorption equilibrium, batch kinetics and column applications were also studied.

Biosorption of Pb(II) and Cu(II) ions were investigated by Sağ et al.(2003) using activated sludge as biosorbent in batch and continuous-flow stirred tank reactors. The Freundlich model described the experimental equilibrium uptake of Pb(II) and Cu(II) ions by the resting activated sludge better than the Langmuir model. The results of the competitive biosorption studies showed that the Pb(II) [or Cu(II)] interfered with the uptake of Cu(II) [or Pb(II)].

Gabriel, Baldrian, Hladíková & Háková (2001) investigated biosorption of copper to the pellets of different fungal species in batch and continuous column experiments. Different molds yielded comparable biosorption capacities for copper (5 to 8 mg Cu g biomass^{-1}).

Byerley & Scharer (1987) studied uranium(VI) biosorption by different bacteria, yeasts, molds, algea and activated sludge. A Langmuir-type isotherm was found to be suitable with a maximum biosorption capacity of 146 mg U per g biomass for the activated sludge.

Adsorption of three metal ions, Cu, Cd and Zn in a bi-component mixture system onto activated sludge organisms was investigated by Hammaini, González, Ballester, Blázquez & Muñoz (2002). The empirical isotherms indicated a competitive uptake with Cu being preferentially adsorbed followed by Cd and Zn.

Liu et al. (2003) studied the feasibility of aerobic granules as a novel type of biosorbent for cadmium removal from industrial wastewater. A kinetic model was developed to describe Cd^{2+} biosorption and the results showed that the Cd^{2+} biosorption on aerobic granule surface was closely related to both initial Cd^{2+} and granule concentrations.

Utkiger, Chen, Tabak, Bishop & Govind (2000) studied the equilibrium biosorption of Zn(II) and Cu(II) by non-viable activated sludge in a packed column adsorber. In binary mixture studies with Cu(II) and Zn(II), equilibrium was reduced by about 30% for each metal ion indicating some competition between the two metals.

Aksu, Açıkel, Kabasakal & Tezer (2002) also studied biosorption of chromium (VI) and nickel (II) ions, both singly and in combination by dried activated sludge in a batch system as a function of initial pH and metal ion concentrations. The optimal initial pH values for single chromium(VI) and nickel (II) biosorptions were

determined to be 1,0 and 4,5, respectively. A multi-component Freundlich model was found to be satisfactory to represent the equilibrium experimental data.

Norton, Baskaran & McKenzie investigated the potential to remove zinc ions from aqueous solutions by biosorption using biosolids. The biosorptive capacity of dry, unground biosolids was determined to be 0,564 mM/(g dry biosolids) in batch experiments. Kinetic experiments showed that the metal uptake equilibrium took 5 h for initial zinc concentrations below 0,3 mM and 24 h for 1,5 mM zinc solutions. The optimum pH values for zinc biosorption were found to be between 4 and 6.

Various types of waste biomass such as bacteria, yeast, molds, marine algea and activated sludge were compared for biosorption of copper, zinc and nickel ions by Bakkaloglu et al. (1998). Bacteria and molds were found to be more effective biosorbents as compared to the other biomass tested.

Hamadi, Chen, Farid & Lu (2002) studied the biosorption of chromium with tyres (TAC), sawdust (SPC) and activated carbon (CAC). It was reported that the second order reaction rate constants for TAC, SPC and CAC at 22 ^{0}C were 0,0296 g/mg min, 0,0369 g/mg min, 0,0377 g/mg min. The first order reaction rate constants of TAC, SPC and CAC at 22 ^{0}C were 0,0113 min^{-1}, 0,0127 min^{-1}, 0,0071 min^{-1}, respectively. Singh, Rastogi & Hasan studied the biosorption of cadmium with rice polish. The reported pseudo-first order adsorption rate constants for cadmium at 20, 30, 40 ^{0}C were 0,00608 min^{-1}, 0,00571 min^{-1}, and 0,00536 min^{-1} , respectively.

The iron biosorption capacity of a *Streptomyces rimosus* biomass was studied by Selatnia, Boukazoula, Kechide, Bakhti & Chergui. Langmuir constants of q_m and b were determined as 125 mg g^{-1} and 0,00952 l mg^{-1} . The Freundlich constants of k and n^{-1} were 27,76 and 0,2694. Correlation coefficients (R^2) were 0,9904 for the Langmuir and 0,8346 for the Freundlich isotherm. Apparently, the Langmuir isotherm represented the equilibrium data better than the Freundlich isotherm.

Aksu (2000) studied the biosorption of reactive dyes (Reactive Blue 2 – RB2 and Reactive Yellow 2 – RY2) onto dried activated sludge. The maximum capacity Q^0 determined from the Langmuir isotherm defines the total capacity of the biosorbent as 333,3 mg g^{-1} for RY2 and as 250 mg g^{-1} for RB2 at 25 ^{0}C. The value of b was 0,0067 for RB2 and 0,0029 for RY2. Freundlich constants of K and n were 1,4 mg g^{-1} and 1.16 for RB2 and 3,14 and 1,34 for RY2. The removal of lead ions from aqueous solution using natural clinoptilolite was investigated by Bektaş & Kara (2003). Freundlich and Langmuir isotherm constants and correlation coefficients at different conditions were calculated and compared. The maximum capacities of clinoptilolite for lead was calculated as 111,11 mg g^{-1} at pH 5 and b was found to be 0,0683 l mg^{-1} for the Langmuir isotherm. Freundlich constants of K and n were 10,65 mg g^{-1} and 0,3762. Correlation coefficient (R^2) for the Langmuir isotherm was higher than that of the Freundlich isotherm. The experimental results showed that the equilibrium process was described well by the Langmuir isotherm model.

In none of the literature studies biosorption of zinc (II) ions onto pre-treated powdered activated sludge (PAS) was studied extensively. Therefore, it is the major objective of this study to investigate the zinc ion removal from aqueous solutions by using different activated sludge samples obtained from different wastewater treatment plants. Activated sludge from a paint industry (DYO, Izmir) wastewater treatment plant was found to be superior to the others tested and was used for biosorption of zinc ions for further studies. After the adsorbent selection, the powdered waste sludge (PWS) obtained from the paint industry wastewater treatment plant was pre-treated by different chemicals to improve the biosorption capacity. The experimental studies are divided in two parts. The first part is batch shake flask experiments and the second part is fed-batch applications. The pre-treated PWS was used biosorption of zinc (II) ions in batch shake flask experiments and fed-batch operations. Effects of major physical and chemical parameters such as zinc and PWS concentrations, pH, temperature, agitation speed and PWS particle size on zinc biosorption performances were investigated. Kinetics and equilibrium of the zinc biosorption onto PWS were studied in batch shake flask experiments. Zinc ions and PWS concentrations and flow rate were changed as variables in fed-batch operations.

1.2. Theoretical Background

1.2.1. Kinetic Modeling

Adsorption of heavy metals from liquid phase to solid may be considered as a reversible phenomenon with an equilibrium state being established between the two phases. After adsoption takes places, the concentration of adsorbate remaining in solution drops till a dynamic equilibrium is reached. The time needed to reach the equilibrium is called equilibrium time. Equilibrium time is important to determine the sorption kinetics. The models of adsorption kinetics correlate the adsorbate uptake rate. The kinetics models are important in treatment process design. First and second order rate models can be used to describe the kinetics of heavy metal biosorption.

The pseudo- first order kinetic model or namely the Lagergreen model (Ho & McKay, 1998, 1999) has the following form;

$$\ln (1- q / q_e) = - k_1 t \quad \text{or} \quad q = q_e (1- \exp (-k_1 t)) \qquad \text{eq.1}$$

where q_e is the equilibrium solid phase concentration of zinc ions which is a constant for a given condition. When $\ln (1- q / q_e)$ was plotted against time, a straight line is obtained with a slope of 'k_1', the first-order rate constant.

The pseudo-second order kinetic model as developed by Ho & McKay (1998, 1999) has the following form:

$$\frac{t}{q} = \frac{1}{k_2 q_e^2} + \frac{t}{q_e} \qquad \text{eq.2}$$

where 'k_2' is the pseudo-second order rate constant, q_e is the equilibrium solid phase zinc ion concentration. q_e values were obtained from biosorption profiles for each experimental condition. A plot of 't/q' versus time (t) would yield a line with a slope

of $1/q_e$ and an intercept of $1/(k_2 q_e^2)$, if the second order model is a suitable expression.

1.2.2. Adsorption Isotherms

Adsorption isotherms indicate that equilibrium is established for the adsorbed compound on the biosorbent and unadsorbed component in solution. An adsorption isotherm represents a relationship between solid phase and solution phase concentration of an adsorbent at an equilibrium condition under a particular temperature. Three different biosorption isotherms were used to correlate the equilibrium data. The biosorption isotherms used were the Langmuir, Freundlich and the generalized biosorption isotherms.

The most widely used isotherm equation for modeling equilibrium is the Langmuir equation. This model suggests a monolayer sorption onto a surface with a homogeneous distribution over the adsorbent surface. Langmuir isotherm has the following form:

$$q = X / M = q_m C / (K + C) \qquad \text{eq.3}$$

which may be written in linearized form as follows:

$$\frac{1}{q} = \frac{1}{q_m} + \frac{K}{q_m}\,\frac{1}{C} \qquad \text{eq.4}$$

where, X is the amount of zinc ions adsorbed (mg); M is the amount of biosorbent (PWS) used (g); q is the equilibrium zinc ion concentration on the biosorbent (mg g^{-1}); q_m is the maximum biosorption capacity of the adsorbent for zinc ions (mg g^{-1}); C is the liquid phase equilibrium concentration of the zinc ions (mg l^{-1}) and K is the saturation constant (mg l^{-1}).

The Freundlich expression is an empirical equation based on sorption on a heterogeneous surface and binding sites are not equivalent or independent. Freundlich isotherm has the following form:

$$q = KC^{1/n} \quad \text{eq.5}$$

or in linearized form equation 5 can be written as;

$$\ln q = \ln K + (1/n) \ln C \quad \text{eq.6}$$

where K is the Freundlich capacity constant (mg g^{-1}); n is the affinity constant; q is the equilibrium zinc ion concentration in solid phase (mg g^{-1}) and C is the equilibrium zinc ion concentration in aqueous phase (mg l^{-1}).

The third isotherm tested for correlation of the equilibrium data was the generalized biosorption isotherm equation which has the following form;

$$q = q_m C^n/(K+C^n) \quad \text{eq.7}$$

Equation 7 can be written as follows in linearized form;

$$\ln ((q_m/q)-1) = \ln K - n \ln C \quad \text{eq.8}$$

where K is the saturation constant (mg l^{-1}); n is the cooperative binding constant; q_m is the maximum biosorption capacity of the adsorbent (mg g^{-1}); q (mg g^{-1}) and C (mg l^{-1}) are the equilibrium zinc ion concentrations in the solid and liquid phases, respectively.

Prepared zinc solution was added slowly into the PWS containing well mixed reactor without effluent removal in fed-batch operation. As the feed zinc solution was added slowly, the liquid volume in the reactor increased with time linearly. A variety of mathematical models have been developed to design fed-batch adsorption system.

The system of fed batch reactor which was used in this study was different from other column operations. So, Bohart and Adams equation is modified for this study which is generally used for columns. Since no effluent is removed from the system, the depth of the bed increases with time until the system reaches equilibrium.

According to the Bohart–Adams model (Eckenfelder, 1989; Cooney, 2000), the following equation is used to predict the performance of adsorption columns:

$$t_b = \frac{N_o X}{C_o V_o} - \frac{1}{K C_o} \ln\left[\frac{C_o}{C_b} - 1\right] \qquad \text{eq.9}$$

where, t is the operation time to break point (h); Co the influent adsorbate concentration (kg/m^3); C_b the effluent concentration at the breakthrough point (kg/m^3); N_o the adsorption capacity of the adsorbent (kg solute/ m^3 of bed); X the bed depth of column (m); V_o the linear flow rate (m/h); K is the rate constant (m^3/(kg. h)). The following definitions are used to modify eq.9

$$N_o = q_s (1-\varepsilon) \qquad X A_o = V_{bed} = \frac{V_{adsorbent}}{(1-\varepsilon)} \qquad \text{eq.10}$$

where, q_s is the adsorption capacity of the adsorbent (kg solute/m^3 adsorbent); (1-ε) is the adsorbent volume fraction (m^3 adsorbent/ m^3 bed), A_o is the cross section area of bed (m^2). Bohart–Adams equation takes the following form after substitution of eq. 10 into eq.9.

$$t_b = \frac{q_s (1-\varepsilon)}{C_o V_o A_o} (X A_o) - \frac{1}{K C_o} \ln\left[\frac{C_o}{C_b} - 1\right] \qquad \text{eq.11}$$

Further arrangement yields,

$$t_b = \frac{q_s (1-\varepsilon)}{C_o Q} \frac{V_{adsorbent}}{(1-\varepsilon)} - \frac{1}{K C_o} \ln\left[\frac{C_o}{C_b} - 1\right] \qquad \text{eq.12}$$

Adsorbent volume is defined as

$$V_{adsorbent} = \frac{m_{adsorbent}}{\rho_{adsorbent}} \qquad \text{eq.13}$$

Substitution of eq.13 into eq.12 yields

$$t = \frac{q_s}{C_o Q} * \frac{m_{adsorbent}}{\rho_{adsorbent}} - \frac{1}{K C_o} \ln \left[\frac{C_o}{C_b} - 1\right] \qquad \text{eq. 14}$$

where, $m_{adsorbent}$ is mass of the adsorbent (kg), $\rho_{adsorbent}$ is the density of dry adsorbent (kg adsorbent/m^3 adsorbent).By defining qs' as follows one can write eq.14 as follows;

$$q'_s = \frac{q_s}{\rho_{adsorbent}} \qquad \text{eq.15}$$

where q'_s is the adsorption capacity of the dry adsorbent, PWS (kg solute/kg adsorbent) and $\rho_{adsorbent}$ is the density of dry adsorbent (kg adsorbent/m^3 adsorbent).

$$t_b = \frac{q'_s}{C_o Q} m_{adsorbent} - \frac{1}{K C_o} \ln \left[\frac{C_o}{C_b} - 1\right] \qquad \text{eq.16}$$

where, t_b is the operation time to break point (h); C_o the influent solute (zinc ion) concentration (kg/m^3); C_b the effluent solute concentration at break through (kg/m^3); q'_s the adsorption capacity of the adsorbent (kg solute/kg adsorbent); $m_{adsorbent}$ is the mass of adsorbent, PWS (kg); Q is the feed flow rate (m^3/h); K is the adsorption rate constant (m^3/(kg h)).

1.3. Objectives and Scope

Major objectives of this thesis can be summarized as follows;

1. to select an effective waste sludge as biosorbent for the removal of zinc (II) ions by using batch shake flask experiments
2. to examine the effect of various pretreatment methods on zinc removal capacities of the selected waste sludge.
3. to determine the effects of major operating conditions such as metal and adsorbent concentrations, pH, temperature, rotational speed on biosorption performance of the selected PWS.
4. to investigate zinc biosorption onto selected PWS by fed-batch operation
5. to determine the kinetic and isotherm constants by using shake flask experimental data.
6. to determine the biosorption capacity and the rate constants in fed-batch biosorption experiments..

In the first part of the experiments batch shake flasks were used to evaluate the zinc removal capacities of different PWS samples. Waste sludge samples obtained from different wastewater treatment plants were tested for their zinc ion biosorption capabilities. Waste sludges obtained from DYO paint industry, Izmir Pak-Maya Yeast Industry, Güzelbahçe and Çiğli Domestic Wastewater Treatment Plant of İzmir were used for this purpose. Three different pre-treatment solutions were used as 1% H_2SO_4, 1% NaOH and 1% H_2O_2 to improve the biosoption capacities of the selected (DYO sludge) powdered waste sludge (PWS). In batch shake flask studies, effects of zinc ions and PWS concentrations, PWS particle size, pH, temperature and rotational speed were investigated. Kinetics of zinc biosorption onto PWS was investigated by using the PWS samples with particle size of 64 μm. The pseudo first and second order rate expressions were used to correlate the experimental data. The kinetic constants were determined for both models. Three different biosorption isotherms were used to correlate the equilibrium biosorption data and the isotherm constants were determined.

In the second and final part of the thesis, fed-batch experiments were performed to determine the adsoption capacity of PWS. The system was stirred and operated until the equilibrium was reached. The adsoption capacities of zinc and the performance of the fed batch process were investigated by changing the zinc ion concentrations, PWS concentration and the feed flow rate. A mathematical model describing the dynamics of metal uptake in fed batch operation was used and the constants were determined by using the experimental data.

CHAPTER TWO
MATERIALS AND METHODS

2.1. Batch Biosorption Experiments

Eight different sets of batch shake flask experiments were performed to investigate the biosorption of zinc ions onto PWS. Free zinc concentrations in the solution were measured every hour by using an atomic absorption spectrometer. Flask experiments were done in duplicates. The samples (5 ml) withdrawn from the erlenmeyers every hour were centrifuged at 8000 rpm (7000 g) to remove solids. The clear supernatants were analyzed for zinc ion contents using an Atomic Absorption Spectrometer (ATI Unicam 929 AA Spectrometer) at 213,9 nm wavelength.

2.1.1. Selection of Powdered Waste Sludge

Powdered waste sludges used in this work as adsorbent were obtained from DYO paint industry, Izmir Pak-Maya Yeast Industry, Güzelbahçe and Çiğli Domestic Wastewater Treatment Plant of İzmir, Turkey. The waste sludge was dried at 100 ^{0}C in an oven for 24 h and then crushed and sieved to different size fractions with particle diameters between 140 – 200 mesh (109 μm).

2.1.1.1. Experimental Procedure

Experiments were carried out on a gyrotary shaker in 500 ml flasks with 200 ml reaction volume at T=25 ^{o}C, pH=5 and 150 rpm for 24 hours. The pH of the adsorbate solution was adjusted by adding 0,1 M HCl or 0,1 M NaOH. Adsorbent concentration was kept constant at 1 g/200 ml and initial zinc concentration of each flask was 100 mg l^{-1}. Control flasks contained only zinc ions without ant adsorbent. Samples were removed from the flaks periodically for analysis. Samples were centrifuged for 15 min at 8000 rpm.

2.1.2. Selection of Pretreatment Method

Pretreatment experiments were done with waste sludge samples from a paint industry wastewater treatment plant (DYO, Izmir, Turkey) because of the higher zinc biosorption capacity of this sludge. The sludge was dried, ground and sieved to desired particle size to obtain the powdered activated sludge (PWS) samples. The pre-treatment experiments were done with 1% H_2SO_4, NaOH, and H_2O_2 solutions.

2.1.2.1. Experimental Procedure

The PWS samples were pre-treated using three different pre-treatment solutions of 1% H_2SO_4, NaOH, and H_2O_2. 200 ml pre-treatment solution was mixed with 2 g of PWS in a 500 ml erlenmeyer flask and placed on a gyratory shaker at 150 rpm and 25 ^oC for 6 hours for pre-treatment. Pre-treated PWS was washed with deionized water on a filter paper until the filtrate pH was neutral. Pre-treated and washed PWS samples were dried at 80 ^oC, reground and sieved to different mesh sizes of between 140 and 200 mesh with average particle size of 109 µm. Then, again zinc ions (in form of $ZnCl_2$) and PWS were added to the flasks of 500 ml to yield 100 mg l^{-1} Zn^{2+} and 1g l^{-1} PWS in the solution of 200 ml and pH was adjusted to 5. Also, a control flask was prepared which contained only zinc ions. The flasks were incubated in a gyratory shaker at 25 ^oC for 24 hours. Samples were removed from the flasks periodically for analysis.

2.1.3. Effect of pH

Paint industry sludge was used after pre-treatment with 1% H_2O_2 in pH studies. Initial solution pH was adjusted to 3, 4, 5, 6, 7 and 8.

2.1.3.1. Experimental Procedure

Zinc(II) solutions were prepared by diluting 1000 mg l^{-1} of stock Zinc(II) solution which was obtained by dissolving exact quantity of $ZnCl_2$ in distilled and deionized

water. The zinc solution with desired concentration (100 mg l^{-1}) was prepared from stock solution by mixing 20 ml zinc (II) stock solution and 180 ml de-ionized water. Then 0.2 g pretreated PWS (109 μm) was added into the 500 ml erlenmeyer flasks. To adjust the initial pH, either 0.1M NaOH or 0.1M HCl solutions were used for pH adjustment. The flasks containing zinc solution and PWS were placed in a shaker at 25 ^{0}C and a control flask was placed without PWS. The reaction time was 24 h and a rotation speed of 150 rpm was used. The samples were removed from the flasks every hour for zinc ion analysis.

2.1.4. Effect of Particle Size

Pre-treated and washed PWS samples were dried at 80 ^{o}C, reground and sieved to different mesh sizes of between -270 and 60 mesh with average particle sizes between 53 and 231 μm.

2.1.4.1. Experimental Procedure

The average particle sizes which were used in particle size experiment were 53, 64, 109,178 and 231 μm. 0,2 g of PWS samples with different particle size were contacted with the known concentration (100 mg l^{-1}) of 200 ml zinc solution in erlenmeyer flasks at pH 5. The flasks were placed on a gyratory shaker at 25 ^{0}C and 150 rpm for 24 hours.

2.1.5. Effect of Agitation Speed

This experiment was performed at different agitation (rotation) speeds ranging from 50 to 200 rpm using an incubator shaker. Pretreated PWS with the average particle size of 64 μm was used in this set of experiments.

2.1.5.1. Experimental Procedure

Incubator shaker was operated at different agitation speeds as 50, 75, 100, 150, 200 rpm. Zinc(II) ions and pretreated PWS were added to the flasks to yield 100 mg

l^{-1} Zn^{2+} and 1g l^{-1} PWS in the solution. pH was adjusted to 5. The flasks were incubated at 25 C.

2.1.6. Effect of Initial zinc (II) concentrations

A set of experiments were performed at different initial zinc(II)concentrations, 50, 100, 150, 200, 250, 300 and 350 mg l^{-1} using PWS (1 g /L) with average particle size of 64 µm which was pretreated prior to use.

2.1.6.1. Experimental Procedure

The prepared stock zinc(II) solution (1000 mg l^{-1}) was diluted to the desired concentrations. In experiments with variable zinc ion concentrations, 0,2 g of PWS with a particle size of 64 µm was added to 200 mg l^{-1} zinc(II) solution at pH =5 while zinc ion concentrations were varied between 50 and 350 mg l^{-1}.The samples and control flasks were placed on a shaker at 150 rpm at 25 ^{0}C for 24 hours. Samples (5ml) were withdrawn at suitable time intervals and centrifuged before analysis.

2.1.7. Effect of PWS concentrations

PWS samples were pretreated, ground and sieved to the size fraction between 200 and 270 mesh with an average particle size of 64 µm were used along with zinc ion concentration of 200 mg l^{-1} in this set of experiments. PWS concentrations were 0,25, 0,5, 1, 1,5, 2, 2,5 and 3 g l^{-1} in different flasks.

2.1.7.1. Experimental Procedure

Powdered waste sludge (PWS) concentration was varied between 0.25 and 3 g l^{-1} in this set of experiments while initial zinc ion concentration was 200 mg l^{-1}. The pH was adjusted to 5 and PWS particle size was 64 µm. The other conditions were the same as the previous experiments (25 C, 150 rpm).

2.1.8. Effect of Temperature

Experiments were also performed at different temperatures ranging from 30 to 50 ^{0}C. Variable temperature experiments were done using a gyratory shaker with temperature control. The temperature of shaker was controlled periodically by a thermometer.

2.1.8.1. Experimental Procedure

Biosorption experiments were carried out for 24 h at temperatures 35, 40, 45 and 50 ^{0}C and at room temperature of 30 ^{0}C. A 0,2 g of pretreated PWS was added to 200 ml volume of zinc(II) solution with an initial concentration 100 mg l^{-1} and agitated at 150 rpm. Initial pH was adjusted to 5.

2.2. Fed-batch Biosorption Experiments

2.2.1. Experimental Setup

Figure 2.1.1 depicts a schematic of experimental setup. The system consists of a feed reservoir, an agitated reaction tank placed on a magnetic stirrer, pipes and serum bottle feeding mechanism. An adsorption tank of 15 cm diameter and 30 cm height with a total volume of 5,3 liter was used throughout the studies. Zinc solution was fed to the reactor by using a serum bottle feeding mechanism with adjusted flow rates varying between 0,05-0,5 l h^{-1} by using an adjustable switch. A plastic bottle (2,5 liter) was used as the zinc solution reservoir.

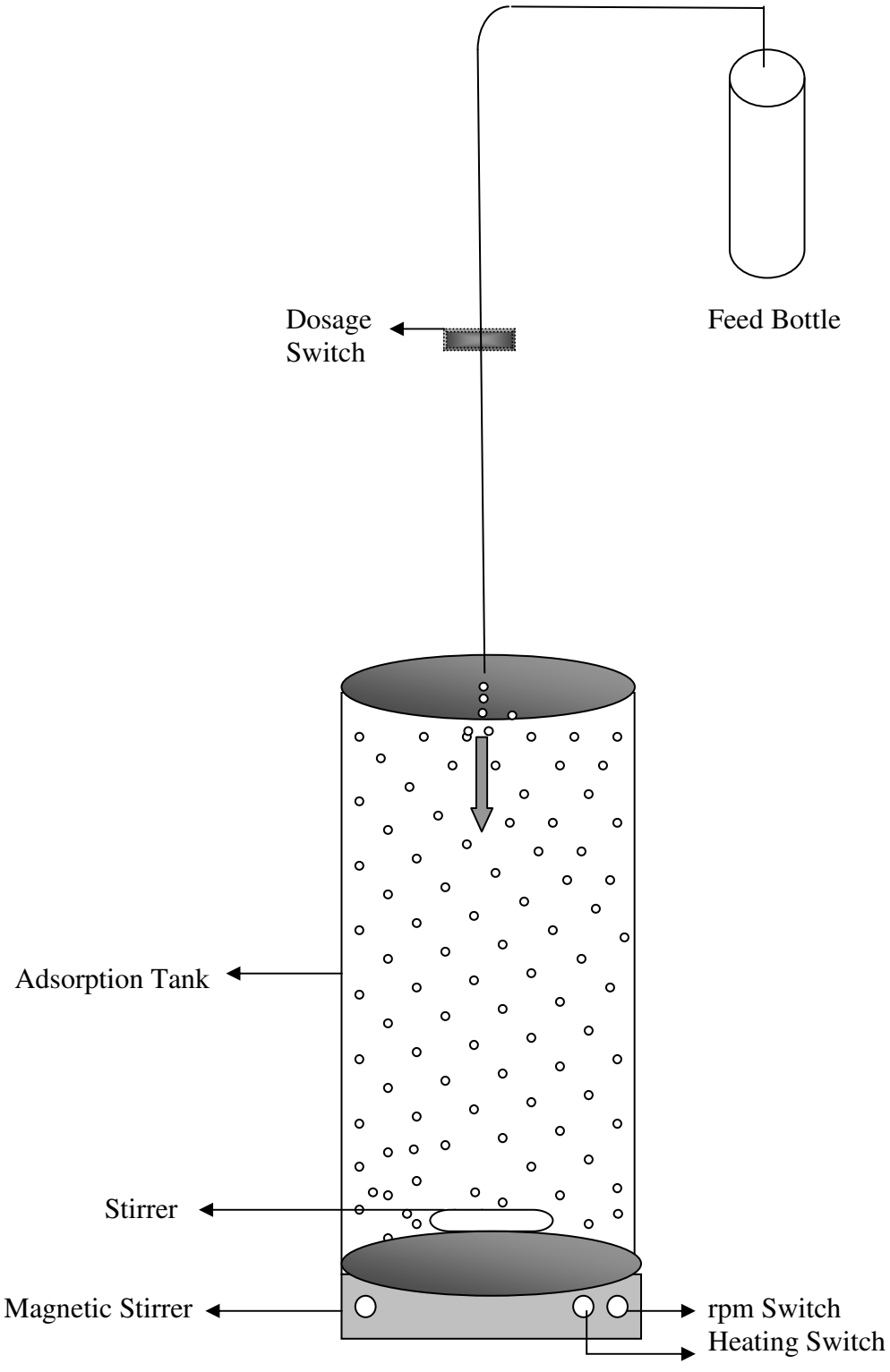

Figure 2.1.1. Schematic diagram of the fed-batch experimental setup.

2.2.2. Experimental Procedure

The fed-batch system was operated by changing the flow rate, feed zinc and PWS concentrations. In the first set of experiments, zinc concentration (100 mg l^{-1}) and pretreated PWS concentration (3 g) were kept constant while the flow rate of zinc solution was changed in the range of 0,05-0,5 l h^{-1}. The flow rate was adjusted by adjusting the serum feed switch. In the second set of experiments, the feed zinc ion concentration was changed at 37,5, 75, 125, 175, 225, 275 mg l^{-1} while the feed flow rate and PWS concentration were 0,2 l h^{-1} and 3 g, respectively. In the last set of fed-batch biosorption experiments, powdered waste sludge concentration was varied between 0,5 and 5 g l^{-1} while the flow rate (0,25 l h^{-1}) and feed zinc concentration (200 mg l^{-1}) were kept constant.

Initially, the adsorption tank was filled with 1 liter of distilled water and pretreated powdered waste sludge (3 g) with the average particle size of 64 µm was added to the tank. Zinc solution was fed to the adsorption tank using a serum bottle feeding mechanism. The initial volume of distilled water for the flow rate of 0,4 and 0,5 l h^{-1} was 0,5 liter because of the high flow rate.

For all fed-batch adsorption experiments, the studies were performed at a room temperature of nearly 25 ^{0}C . The initial pH of the adsorption tank was adjusted 5 using 1 % H_2SO_4 and 1 % NaOH.

The samples (5 ml) were taken from the adsorption tank every hour until the zinc concentration has reached equilibrium. The samples were centrifuged at 8000 rpm (7000 g) to remove solids before analysis. The clear supernatants were analyzed for zinc ion contents using an Atomic Absorption spectrometer (ATI Unicam 929 AA Spectrometer) at 213,9 nm wavelength.

CHAPTER THREE
RESULTS AND DISCUSSION

3.1. Selection of Adsorbent

An economical and easily available adsorbent would make an adsorption-based process an attractive alternative for the removal of heavy metals from wastewaters. Biomass such as powdered waste sludge, plants, organisms provide a good capacity for the adsorption of heavy metals due to their high surface area. The surface chemistry and the chemical characteristics of adsorbate, such as polarity, ionic nature and functional groups determine the nature of bonding mechanisms as well as the extent and strength of adsorption. Biosorption is essentially the passive and physicochemical binding of chemical species to biopolymers. . The polymeric structure of biomass surfaces has a negative charge because of the ionization of organic groups. So, metallic cations are attracted to negatively charged sites at the surface of the biomass cell, a number of anionic ligands participate in binding the metal.

In this part of the study, waste sludges obtained from different wastewater treatment plants in İzmir were used for removal of zinc (II) ions from aqueous solution by biosorption in order to select the most suitable adsorbent. The sludgees were obtained from DYO paint industry, Izmir Pak-Maya bakers yeast industry, Güzelbahçe and Çiğli domestic wastewater treatment plants. Adsorption experiments were conducted in shake flasks with 1 g l^{-1} PWS and 100 mg l^{-1} zinc concentration at 25 C, pH = 5 and 150 rpm.

Figure 3.1 depicts time course of variations of biosorbed (solid phase) zinc ion concentration for different PWS samples over a period of 24 hours. Biosorbed zinc ion concentration (mg Zn $gPWS^{-1}$) increased with time for all waste sludges. The greatest increases in biosorbed zinc ion concentration typically occurred within 10 minute. Biosorbed zinc ion concentration increased to 49 mgZn $gPWS^{-1}$ within 6

hours when DYO paint industry sludge was used and no adsorption was observed afterwards. When Güzelbahçe domestic wastewater treatment sludge was used as adsorbent, biosorbed zinc ion concentration increased to 41 mgZn $gPWS^{-1}$ at the end of six hours.

Variations of Zn^{2+} removal efficiency with time for different adsorbents are shown in Figure 3.2. Percent zinc removal within 10 minute was % 21 for DYO paint industry sludge and % 14 for Çiğli domestic wastewater treatment sludge. At the end of 24 hours, adsorption was completed with the % 49 zinc removal efficiency for DYO paint industry sludge.

Izmir Pak-Maya Yeast Industry and Çiğli domestic wastewater treatment sludges did not result in satisfactory zinc removals by biosorption. Güzelbahçe domestic wastewater treatment sludge didn't perform as well as DYO paint industry sludge. These adsorbents were found inefficient and therefore, were not used in further experiments. The sludge obtained from DYO paint industry in Izmir, Turkey was found to be superior to the other sludges tested and therefore was used for further studies.

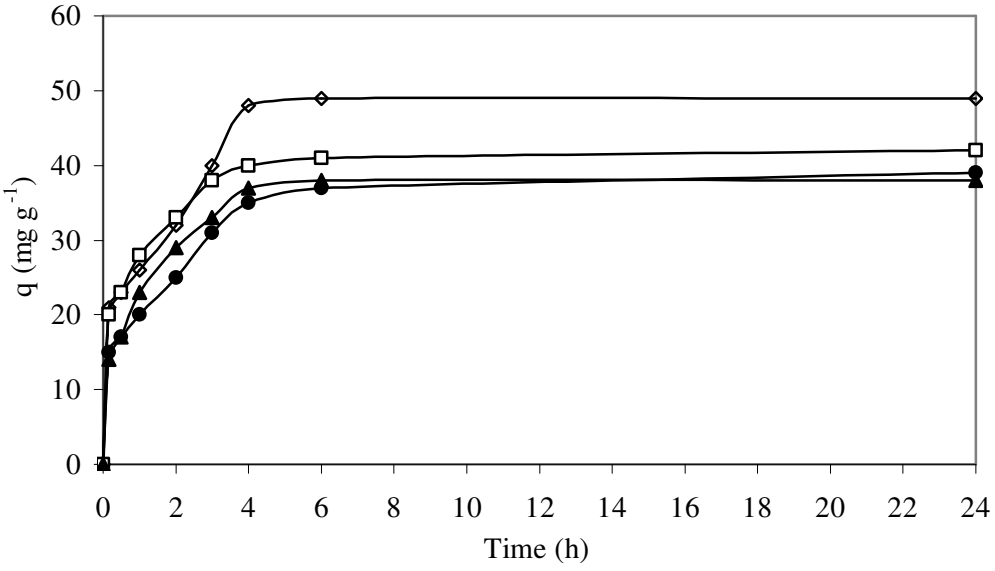

Figure 3.1 Variation of biosorbed zinc ion concentration with time for different biosorbents. ● Pak-Maya yeast industry sludge, ◊ DYO paint industry sludge, □ Güzelbahçe Domestic Wastewater Treatment Plant sludges, ▲ Çiğli Domestic Wastewater Treatment Plant sludge

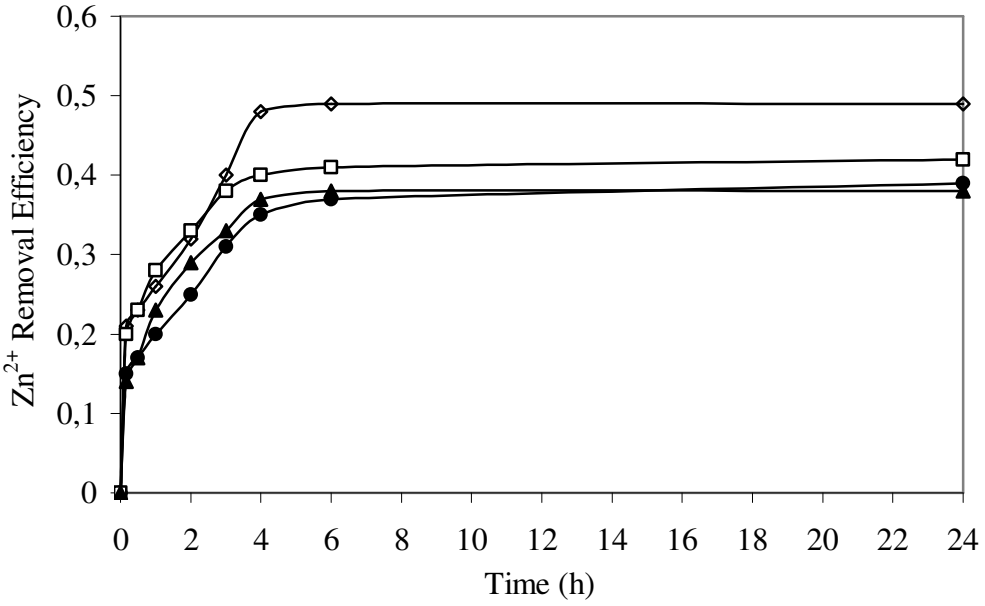

Figure 3.2 Variation of Zn^{2+} removal efficiency with time for different biosorbents. ● Pak-Maya yeast industry sludge, ◊ DYO paint industry sludge, □ Güzelbahçe Domestic Wastewater Treatment Plant sludges, ▲ Çiğli Domestic Wastewater Treatment Plant sludge

3.2. Pre-treatment Methods

Three different pre-treatment solutions were used as 1% H_2SO_4, 1% NaOH and 1% H_2O_2. Powdered waste sludge from the DYO paint industry was pretreated with these solutions to enhance adsorption capacity of biosorbents. Pretreatment experiment was done with 1 g l^{-1} PWS and 100 mg l^{-1} zinc concentration at 25 ^{0}C and 150 rpm for 24 hours.

Figure 3.3 depicts variation of solid phase (biosorbed) zinc ion concentrations with time for different pre-treatment methods. Pretreatment of PWS was found to be beneficial for biosorption of zinc ions. The system reached equilibrium in six hours. Biosorbed zinc ion concentration increased 63 mgZn $gPWS^{-1}$ within six hours when H_2O_2 pretreatment was used. When NaOH was used, biosorbed zinc ion concentration was 58 mgZn $gPWS^{-1}$. Only 48 mgZn $gPWS^{-1}$ was obtained when PWS was pretreated with 1% H_2SO_4.

Figure 3.4 summarizes the Zn^{2+} removal efficiency results obtained with PWS by using different pretreatment solutions. According to the results, the best zinc removal performance was obtained with H_2O_2 where zinc removal was 64% at the end of 24 hours. Therefore, PWS from DYO paint industry pretreated with 1% H_2O_2 was determined to be the best choice among the others tested and was used in further experiments.

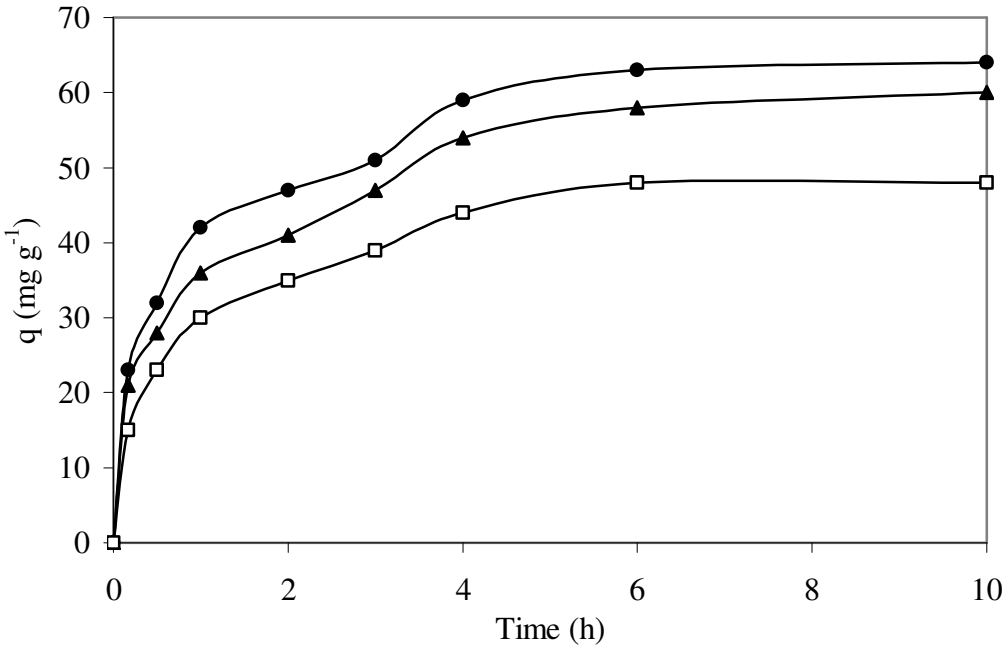

Figure 3.3 Variation of solid phase (biosorbed) zinc ion concentrations with time for different pretreatment solutions. ● H_2O_2, ▲ NaOH, □ H_2SO_4 (1%).

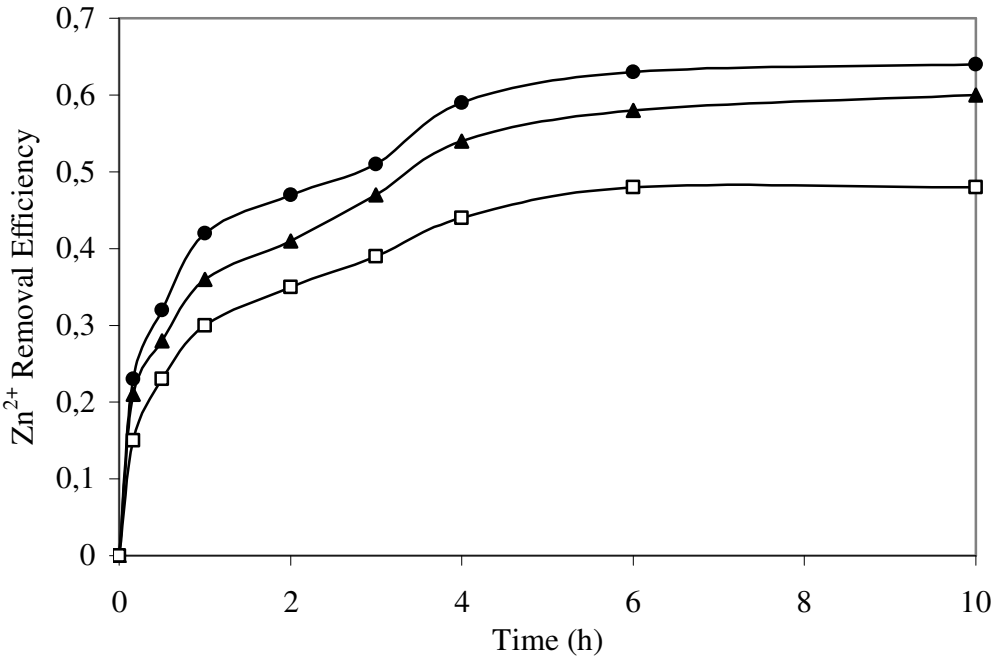

Figure 3.4 Variation of percent zinc ion removals with time for different pretreatment solutions.
● H_2O_2, ▲ NaOH, □ H_2SO_4

3.3. Effect of Operating Conditions

3.3.1. Initial pH effects

pH is an important parameter affecting the rate and the extent of biosorption of metal ions onto biosorbents such as PWS. Variation of pH may affect the surface charge of biosorbent and also the solubility of metal ions. Some metal ions are known to precipitate in form of hydroxides at high pH values such as pH>6. For this reason the effects of initial pH on biosorption of Zn^{2+} ions onto PWS was investigated for pH values between 3 and 8 while PWS and Zn^{2+} concentrations were 1 g l^{-1} and 100 mg l^{-1}, respectively and the PWS particle size was 109µm.

Figure 3.5 depicts variation of solid phase (biosorbed) zinc ion concentrations with time for different initial pH values. Biosorbed Zn^{2+} concentration increased with time at all pH levels tested and equilibrium was reached after six hours of incubation. At low pH values such as pH=3, due to high (H^+) ion concentrations in solution the

surfaces of PWS would be neutralized (which is normally negatively charged) or positively charged prohibiting binding of positively charged zinc ions onto the surfaces of PWS. As a result, the extent of biosorption was rather low at low pH values. However, the equilibrium solid phase Zn^{2+} ion concentration increased with increasing pH because of increasingly negative charges on the surfaces of the PWS at high pH values which attracted positively charged Zn^{2+} ions more strongly. The only mechanisms for zinc ion removal at pH values above 5 is not biosorption, but also precipitation of Zn^{2+} ions in form of $Zn(OH)_2$. Precipitation of zinc begins around pH 6. As can be seen from Figure 3.5, zinc ion removal from solution was almost completed within 2 hours for pH values 7 and 8 because of precipitation while biosorptions for pH values below 7 lasted for about six hours. pH of 6 is the critical point for zinc ions because of zinc hydroxide precipitation. Therefore, it can be said that the optimum pH for biosorption of zinc ions is about pH =5 above which Zn^{2+} ions precipitate in form of $Zn(OH)_2$.

Zn^{2+} removal efficiencies at equilibrium are plotted against time for different pH's in Figure 3.6. Percent zinc ion removal increased with increasing pH. At low pH values such as pH = 3 the extents of Zn^{2+} removal were low yielding % 36 removal efficiency at the end of 6 hours because of neutralization of negative surface charges of PWS by high H^+ ion concentrations at low pH values. The extent of Zn^{2+} ion removal increased up to 60 % as the pH increased to 5. The equilibrium solid phase Zn^{2+} ion concentration at pH=6 were similar with pH=5. For pH values above 7, the extent of zinc ion removal was extremely high because of precipitation of zinc ions in form of $Zn(OH)_2$ in addition to biosorption.

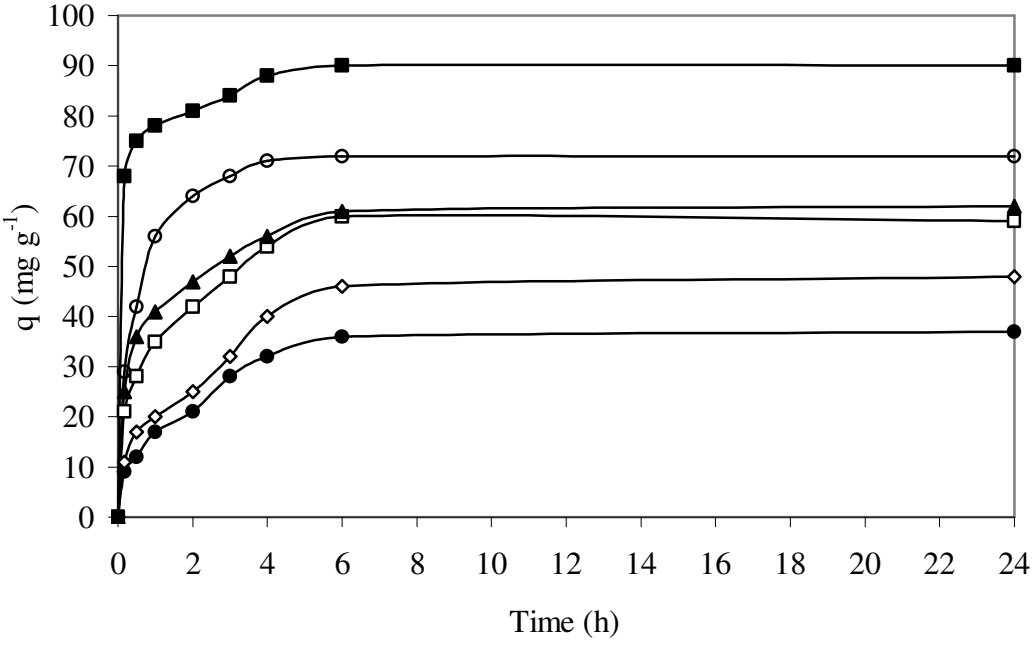

Figure 3.5 Variation of biosorbed zinc ion concentration with time at different pH's. pH : ● 3, ◊ 4, □ 5, ▲ 6, ○ 7, ■ 8

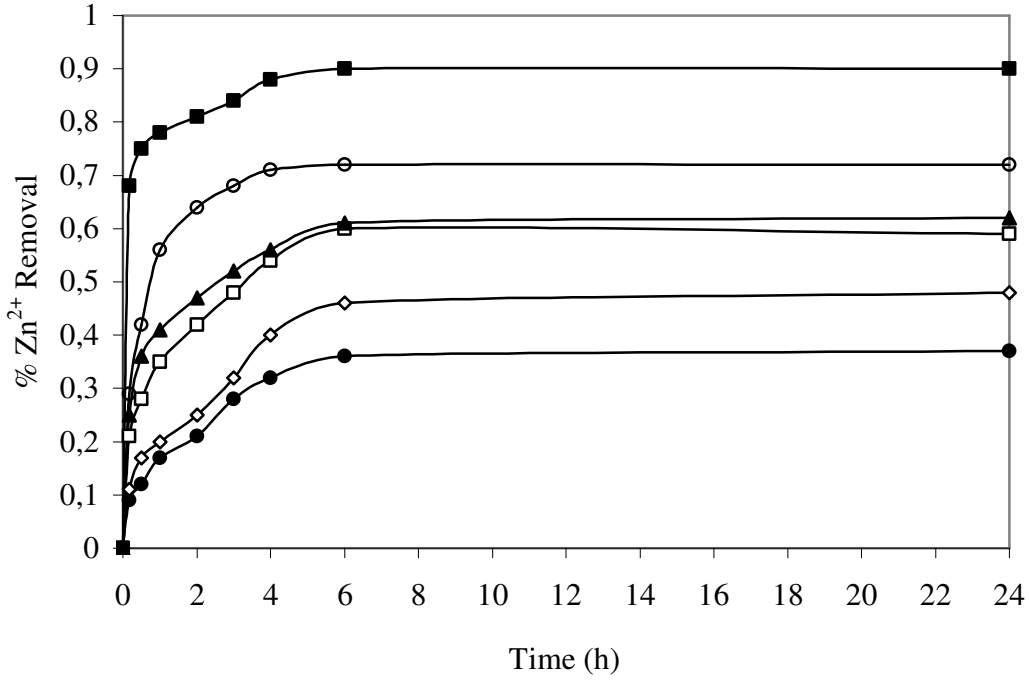

Figure 3.6 Variation of percent zinc ion removals with time at different pH's.
pH : ● 3, ◊ 4, □ 5, ▲ 6, ○ 7, ■ 8

Variation of the equlibrium solid phase zinc ion concentration with initial pH is depicted in Figure 3.7. Increases in pH from 3 to 8 resulted in increased Zn^{2+} concentrations in the solid phase. Biosorption onto PWS (biosorbent) surfaces was lower than the others at pH=3 because of neutral or positively charged PWS surfaces at low pH (high H^+ ions) values. Increased pH values resulted in increasingly negative charges on PWS surfaces yielding higher extent of zinc ion biosorption at pH values around 5. At pH levels above 6 the biosorbed Zn^{2+} concentrations seemed to be high (>70 mg g^{-1}) because of precipitation of zinc ions in form of $Zn(OH)_2$ which cannot be attributed to biosorption. Therefore, the optimum pH for soluble zinc (II) ion biosorption onto PWS was pH= 5 yielding nearly 59 mg g^{-1} biosorption. Further experiments were performed at pH=5 in order to avoid zinc ion precipitation.

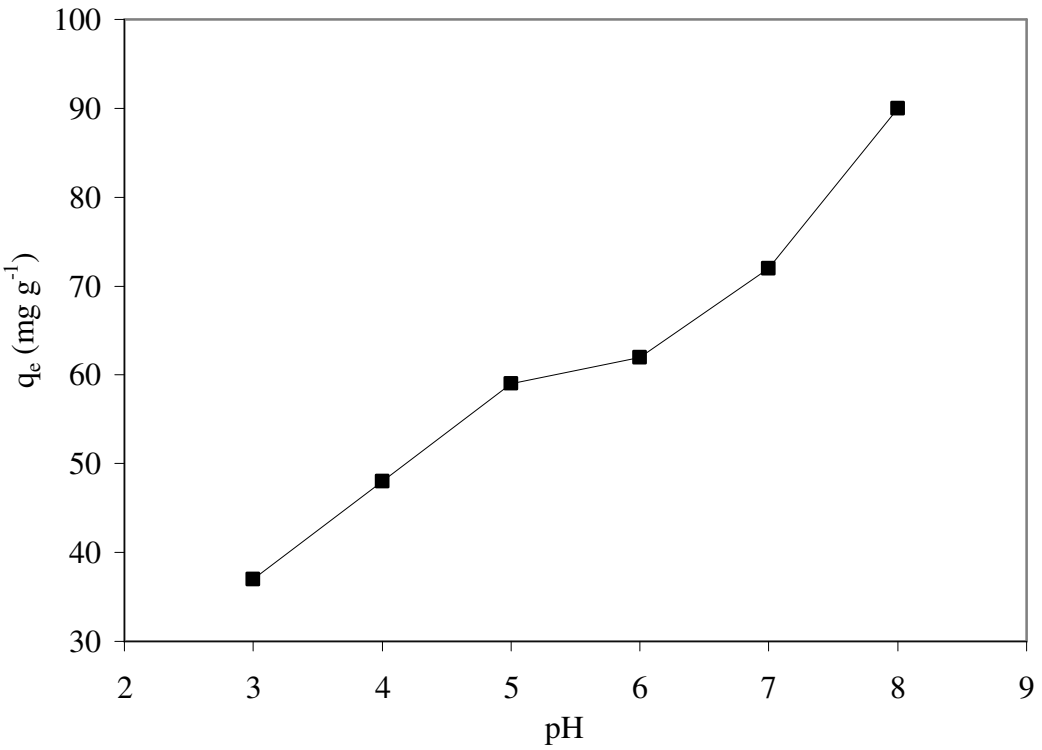

Figure 3.7 Variation of equilibrium solid phase (biosorbed) zinc ion concentration with pH.

The kinetics of biosorption of zinc ions onto pre-treated PWS samples were investigated at different initial pH values. Two different kinetic models were used for correlation of biosorption data. The pseudo- first order kinetic model or namely the Lagergreen model was investigated first. Equation 1 was used to correlate the experimental data.

Biosorbed zinc ions reached equilibrium after six hours of incubation and the pre-equilibrium data were used in kinetic studies. The experimental data was plotted in form of ln (1- q/q_e) versus time for different pH values and a group of lines with different slopes were obtained as shown in Figure 3.8. The kinetic constants for the pseudo-first order model were determined from the slopes of the lines presented in Figure 3.8.

Variations of the first-order rate constants (k) with pH are depicted in Figure 3.9. The rate constant increased with increasing pH due to increasingly negative charges on adsorption surfaces. The figure shows that Zn^{2+} ions removal was obtained by adsorption up to pH=5 but Zn^{2+} ions removed by adsorption and precipitation above pH=5. The highest first order rate constant was nearly 1,027 h^{-1} obtained at pH=8.

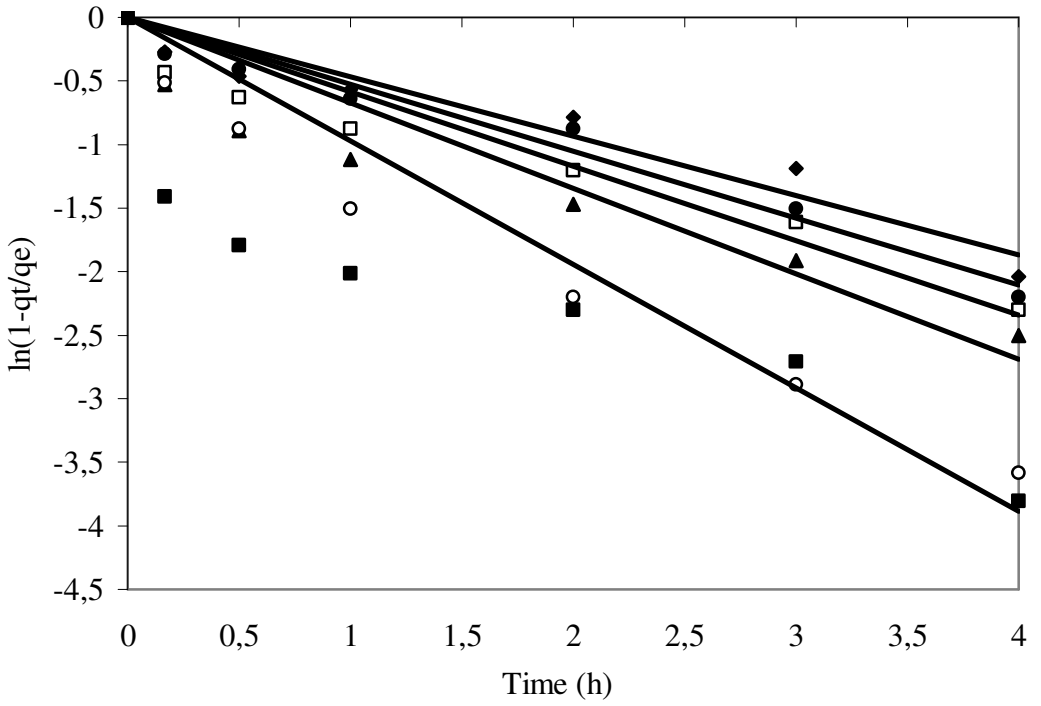

Figure 3.8 A plot of ln (1- q_t / q_e) versus time according to the pseudo-first order biosorption kinetics.
pH: ● 3, ◊ 4, □ 5, ▲ 6, ○ 7, ■ 8

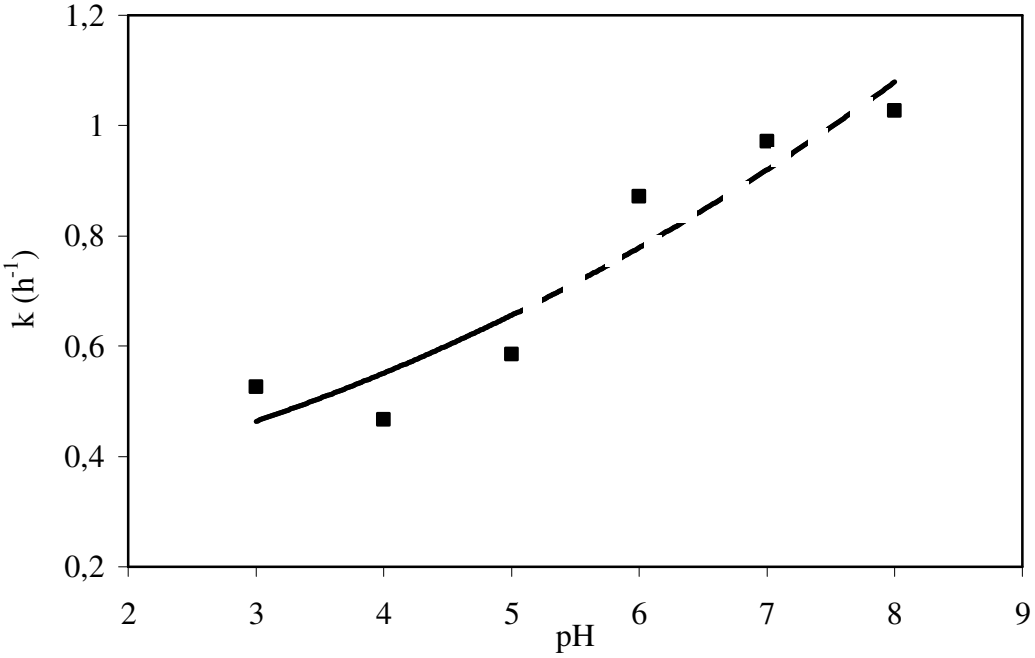

Figure 3.9 Variation of of the pseudo-first order biosorption rate constant (k) with pH. Solid line is for adsorption and the dotted line is for adsorption plus precipitation of Zn^{2+} ions.

Pseudo-second order kinetic model (Ho model) was also used to correlate experimental data obtained at different pH's. The experimental data was plotted in form of 't/q' versus time for different pH values using equation 2 and a group of lines with different intercepts were obtained as shown in Figure 3.10. The kinetic constants for the pseudo-second order model were determined from the y-axis intercepts of the lines presented in Figure 3.10.

Variations of the pseudo-second order rate constants (k) with pH is depicted in Figure 3.11. The rate constant increased with increasing pH except pH=4. Equilibrium solid phase zinc concentration (q_e) is found from Figure 3.5 and used to find rate constants. Equilibrium solid phase zinc concentration (q_e) incresead with increasing pH values yielding q_e values between q_e = 36 mg Zn $gPAS^{-1}$ to q_e = 90 mg Zn $gPAS^{-1}$. The figure shows that Zn^{2+} ions removal was obtained by adsorption up to pH=5 but Zn^{2+} ions removed by adsorption and precipitation above pH=5.

The highest rate constants for the pseudo-first and second order kinetics were 1,027 h^{-1} and 0,077 $(mg/g)^{-1}.h^{-1}$, respectively for pH=8. Pseudo-first order kinetic model was found to represent the experimental data better than the second order model yielding higher correlation coefficient.

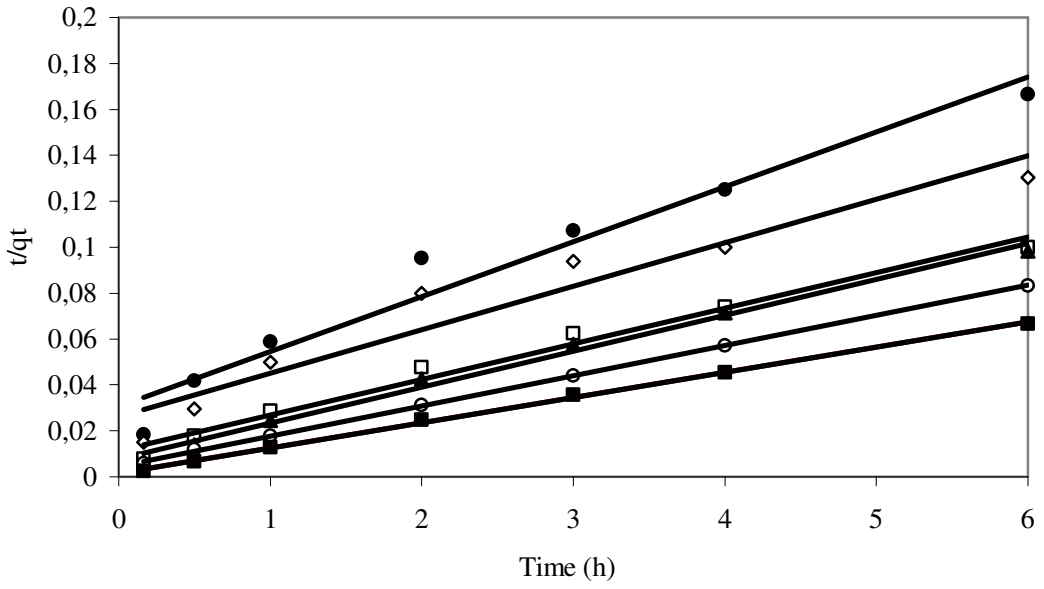

Figure 3.10 A plot of t / q_t versus time according to the pseudo- second order biosorption kinetics.
pH: ● 3, ◊ 4, □ 5, ▲ 6, ○ 7, ■ 8

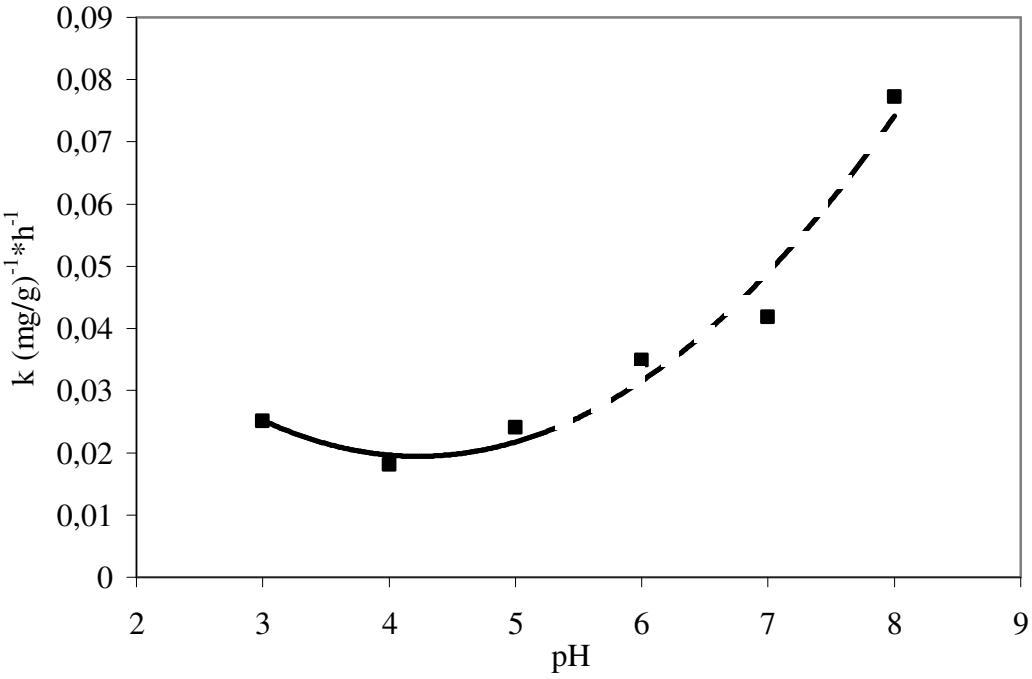

Figure 3.11 Variaton of pseudo-second order biosorption rate constant (k) with pH. Solid line is for adsorption and the dotted line is for adsorption plus precipitation of Zn^{2+} ions.

3.3.2. Effect of Particle Size

The kinetics of biosorption of zinc ions onto pre-treated PWS samples were investigated for five different particle sizes of between 53 and 231µm Time course of variations of aqueous and solid phase (biosorbed) concentrations of zinc ions were obtained for each particle. The experiments were done under the same environmental conditions as the other experiments (pH= 5, 25 C and 150 rpm) with 100 mg l^{-1} zinc and 1g l^{-1} PWS concentrations. Figure 3.12 depicts time course of variations of biosorbed (solid phase) zinc ion concentration for different particle sizes over a period of 24 hours. Biosorbed zinc ion concentration (mg Zn $gPWS^{-1}$) increased with time for all particle sizes. However, small particle sizes (large external surface area) resulted in higher rates and extent of zinc ion removal. Biosorption was almost complete within the 6 hours of incubation. Equilibrium solid phase zinc ion concentrations were 54, 61 and 68 mg g^{-1} for the average particle sizes 231, 109 and D_p<53 µm, respectively. Apparently, reductions in particle size resulted in increases

in external surface area of PWS particles yielding more binding sites for zinc ion adsorption and therefore, more efficient biosorption.

Percent zinc (II) ion removals were plotted versus time for each size fractions (Figure 3.13). Percent zinc removals increased with decreasing particle size. Increases in percent biosorption were much steeper at low specific surface areas (large particle sizes). Apparently, biosorption of zinc ions onto PWS particles was limited by the availability of biosorbent surface area. Percent Zn(II) removals increased from 0,46 to 0,70 at the end of 24 hours for the average particle sizes 231 and D_p<53 µm, respectively ($Zn^{2+}{}_o$=100 mg l^{-1}). Zinc ion removal efficiencies for the average particle sizes of 178, 109 and 64µm were 56%, 61%, 64% after six hours of incubation.

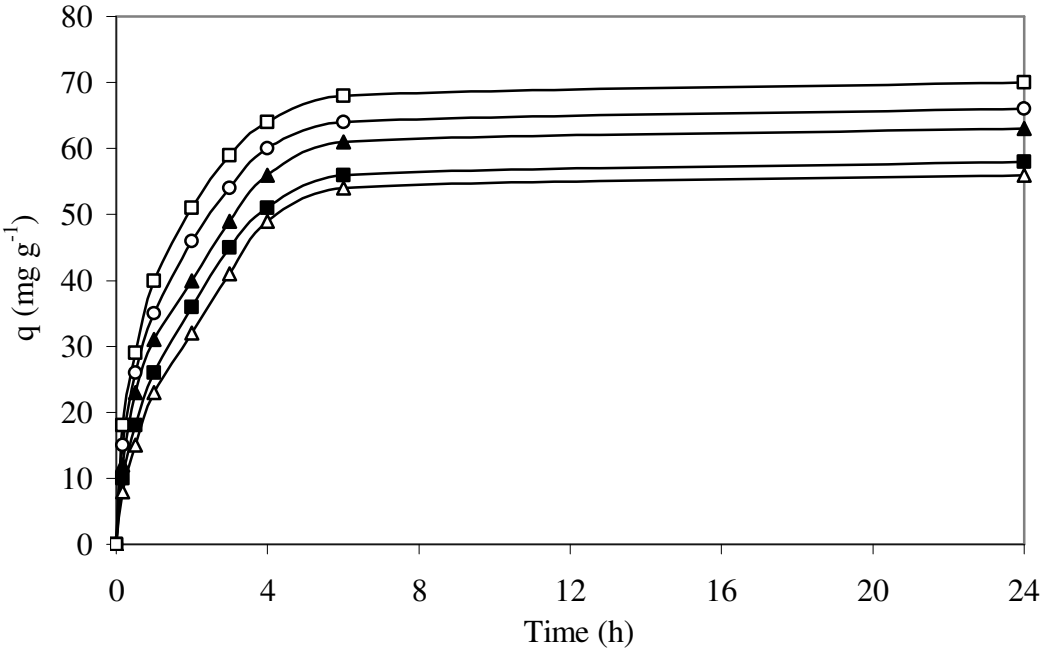

Figure 3.12 Variation of biosorbed (solid phase) zinc ion concentration with time for different particle sizes of PWS. Average $D_{p:}$ □ < 53 µm , ○ 64 µm , ▲ 109 µm, ■ 178 µm , Δ 231 µm

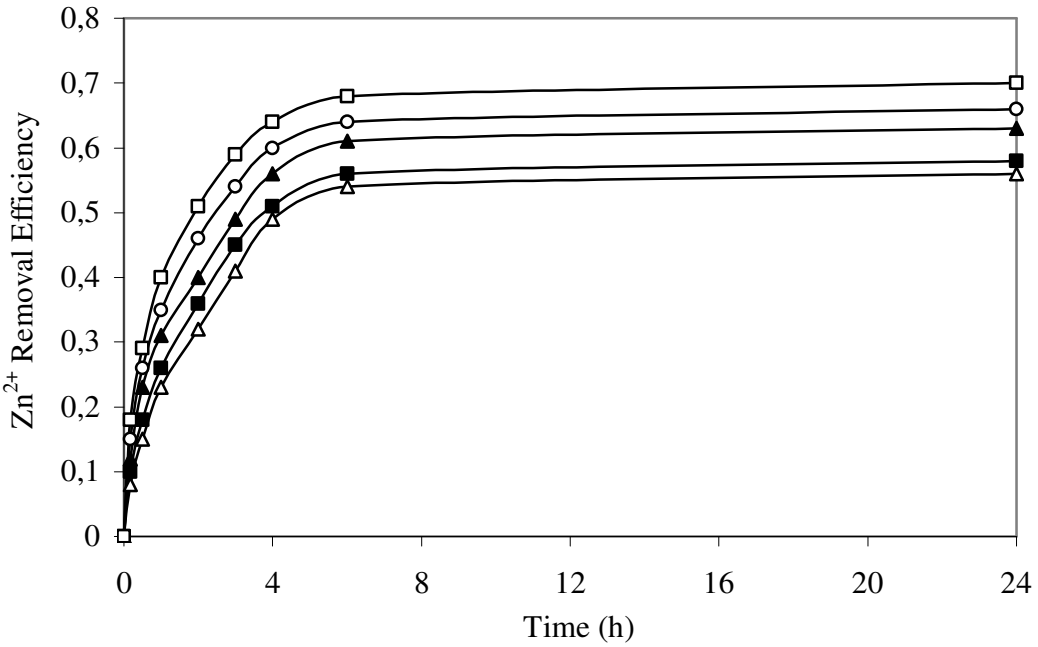

Figure 3.13 Variation of zinc ion removal efficiencies with time for different particle sizes of PWS. Average D_p : □ <53 µm, ○ 64 µm , ▲ 109 µm, ■ 178 µm , Δ 231 µm

The experimental data was plotted in form of ln (1- q/q_e) versus time for different particle sizes and a group of lines with different slopes were obtained as shown in Figure 3.14 to determine the pseudo-first order rate constants by using equation 1. The kinetic constants for the pseudo-first order model were determined from the slopes of the lines presented in Figure 3.14.

Variation of the first-order rate constants (k) with the particle size is depicted in Figure 3.15. The rate constants increased with decreasing particle size due to larger total surface area of particles with smaller particle sizes. The highest first order rate constant was nearly 0,71 h^{-1} obtained with a particle size of < 53µm which dropped to 0,54 h^{-1} at an average particle size of 231µm.

Results of variable particle size experiments were also correlated with the pseudo-second order model and the rate constants were determined by using equation 2. The experimental data was plotted in form of 't/q' versus time for different particle sizes and a group of lines with different intercepts were obtained as shown in

Figure 3.16. Equilibrium solid phase zinc concentration (q_e) is found from Figure 3.12 and used to find rate constants.

Variations of the pseudo-second order rate constants (k) with the particle size is depicted in Figure 3.17. The rate constant decreased with increasing particle size due to smaller total surface area of particles with large particle sizes. The highest second order rate constant was nearly 0,024 $(mg/g)^{-1}h^{-1}$ obtained with a particle size of 53µm which dropped to 0,015 $(mg/g)^{-1}h^{-1}$ at an average particle size of 231µm. So that the pseudo-second order model fitted better than pseudo-first order model yielding high rate constants.

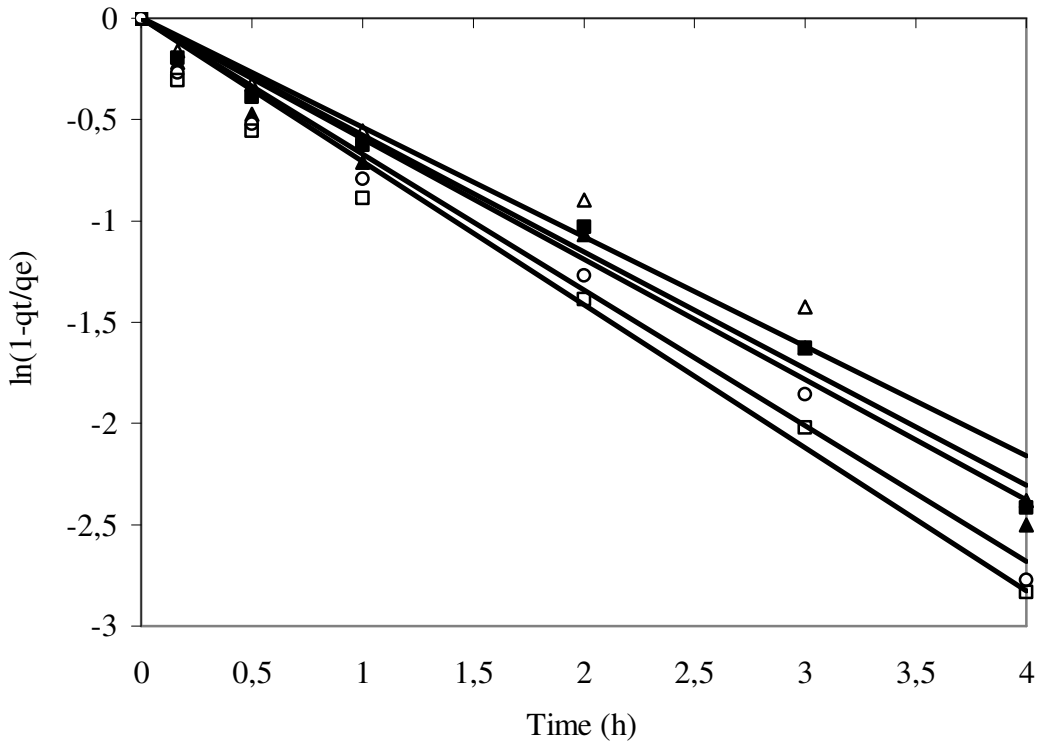

Figure 3.14 A plot of ln (1- q_t / q_e) versus time according to the pseudo-first order biosorption kinetics. $D_{p:}$ < □ 53 µm , ○ 64 µm , ▲ 109 µm, ■ 178 µm , Δ 231 µm

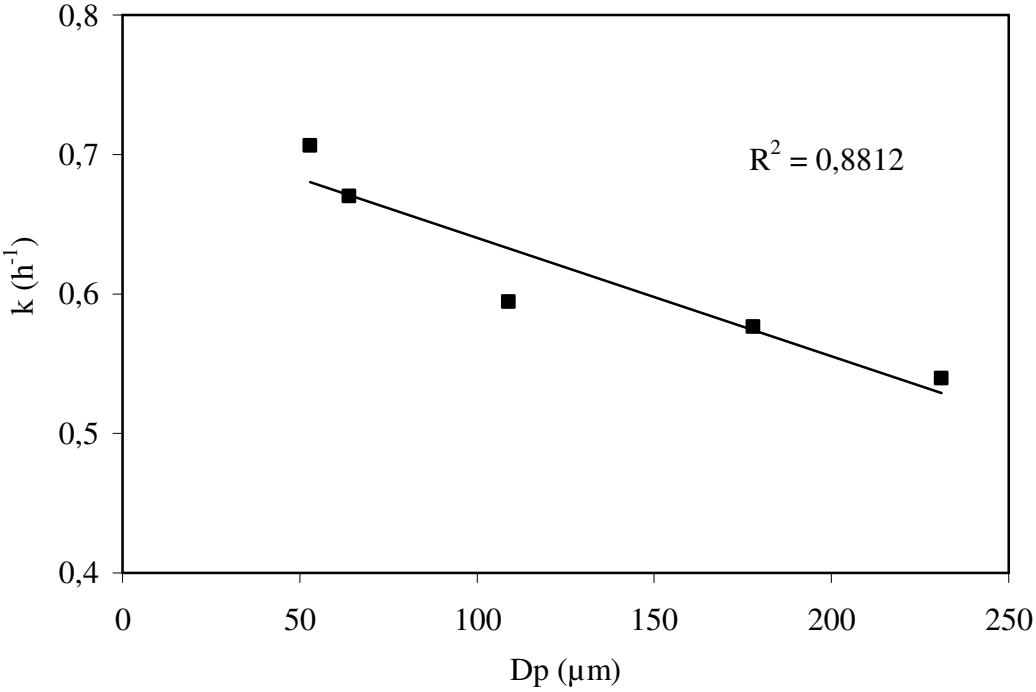

Figure 3.15 A plot of pseudo-first order biosorption rate constant (k) versus particle size (D_p)

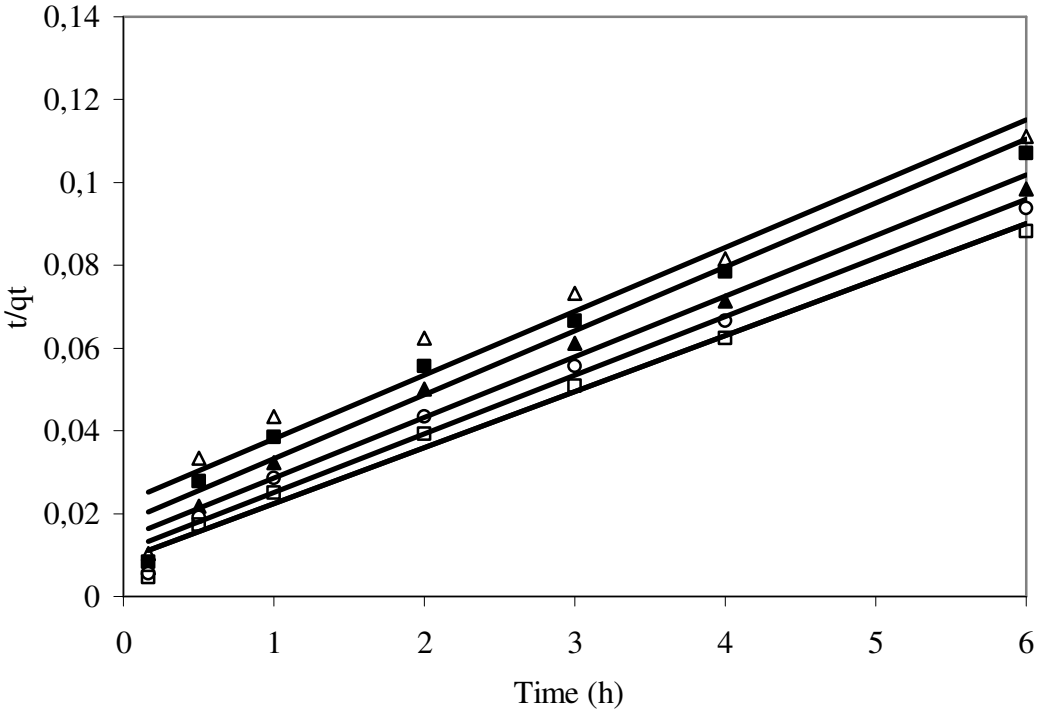

Figure 3.16 A plot of t / q_t versus time according to the pseudo- second order biosorption kinetics. D_p: □ 53 µm , ○ 64 µm , ▲ 109 µm, ■ 178 µm , Δ 231 µm

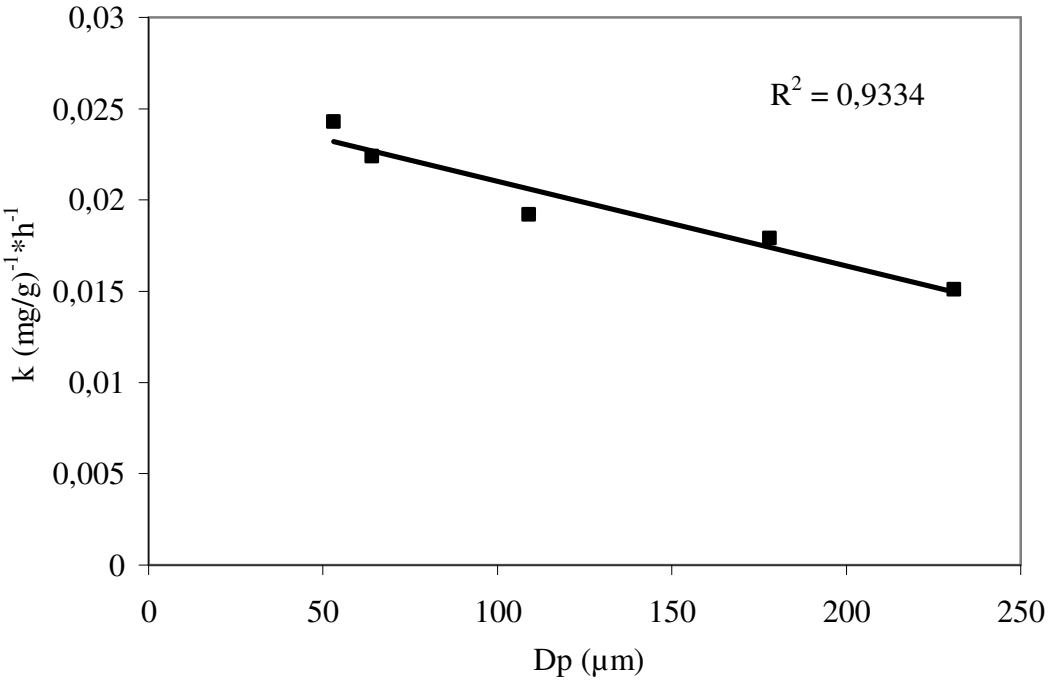

Figure 3.17 A plot of pseudo-second order biosorption rate constant (k) versus particle size (D_p)

3.3.3. Effects of agitation speed

Pretreated (1% H_2O_2) PWS with average particle size of 64µm was used at 1 g l^{-1} concentration along with 100 mg l^{-1} zinc at different rotational speeds ranging from 50 to 200 rpm. This set of experiments were performed at pH=5 and 25 ^{0}C.

Variations of the solid phase (biosorbed) zinc (II) ion concentrations with time are depicted in Figure 3.18 for different rotational speeds. Biosorbed zinc ion concentrations increased with time and reached equilibrium after six hours of incubation for all rotational speeds tested. At low rotational speeds such as 50 and 75 rpm, low final solid phase zinc ion concentrations such as 47 and 51 mg g^{-1} were obtained because of the inadequate mixing. At agitation speed such as 150 and 200 rpm, high solid phase zinc ion concentrations such as 64 and 69 mg g^{-1} were obtained due to better mixing.

Figure 3.19 depicts variations of Zn^{2+} removal efficiency with time for different rotational speeds. Percent zinc ion removals increased with increasing agitation

speed. The highest zinc removal efficiency of 69 % was obtained at the agitation speed of 200 rpm. High rotational speeds prevent precipitation of biosorbent and provide efficient mixing yielding better contact between the solid and liquid phases.

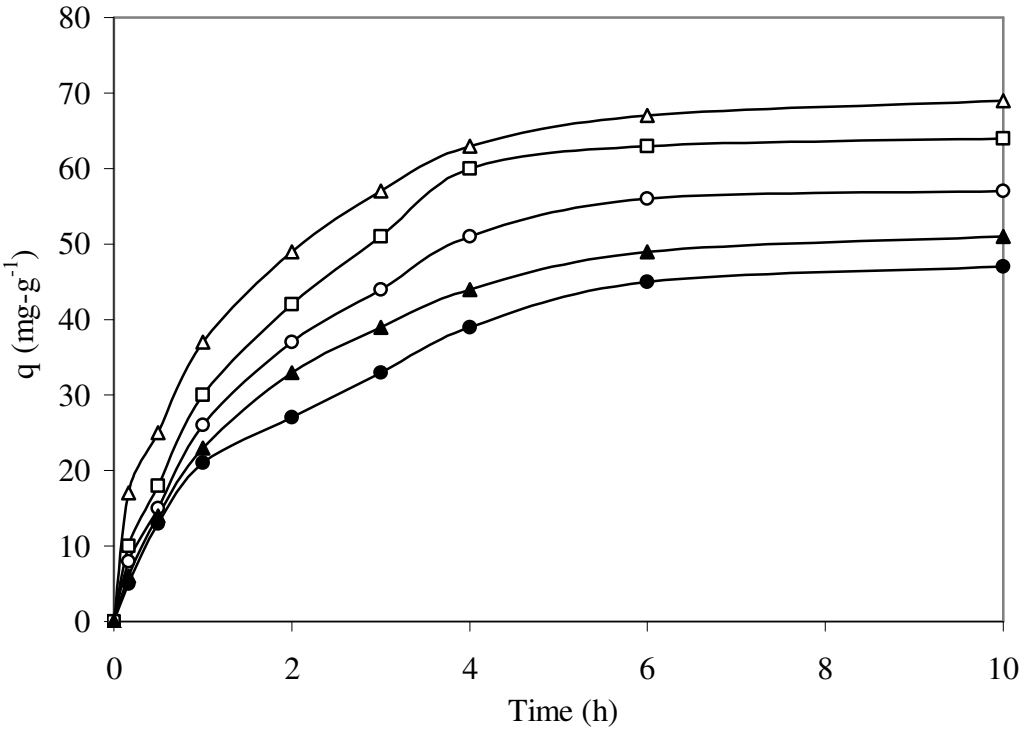

Figure 3.18 Variation of biosorbed (solid phase) zinc ion concentrations with time for different rotational speeds. ● 50 rpm, ▲ 75 rpm, ○ 100 rpm, □ 150 rpm, Δ 200 rpm

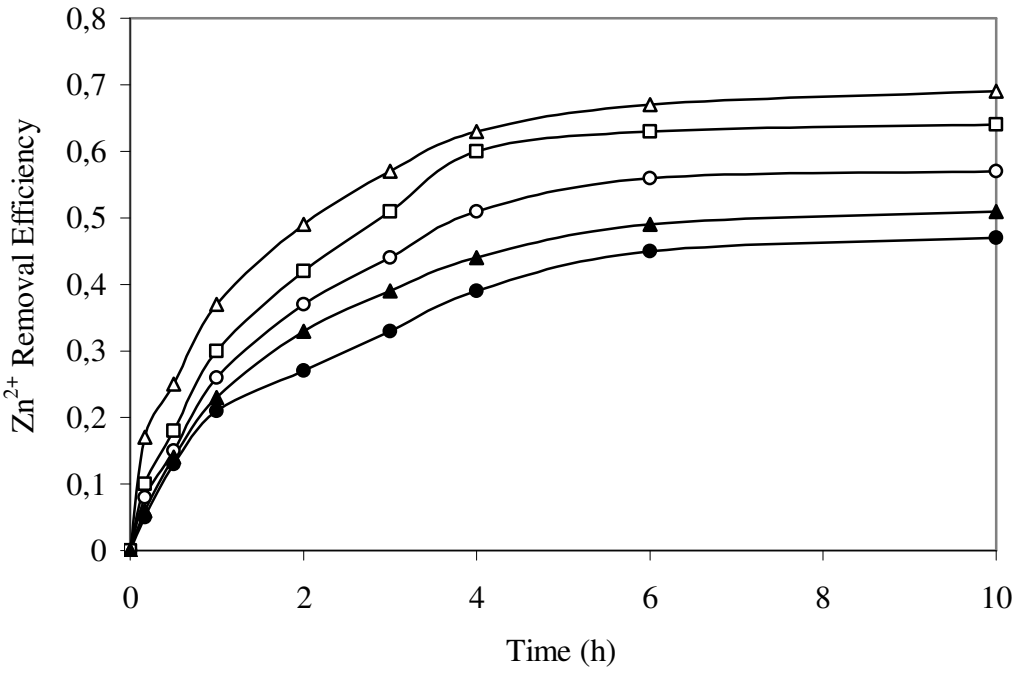

Figure 3.19 Variation of Zn^{2+} removal efficiency with time for different rotational speeds

● 50 rpm, ▲ 75 rpm, ○ 100 rpm, □ 150 rpm, Δ 200 rpm

In order to test the kinetic models for zinc ion biosorption, pseudo-first order, and pseudo-second order kinetic models were correlated with the experimental data obtained at different agitation speeds. The experimental data was plotted in form of ln (1- q/q_e) versus time for different agitation speed and a group of lines with different slopes were obtained as shown in Figure 3.20. The solid lines in Figure 3.20 are the best-fit lines with high correlation coefficients (R^2 >0,95). The first order rate constants were obtained from the slopes of the lines in Figure 3.20.

Variations of the first-order rate constants (k) with the rotational speed are depicted in Figure 3.21. The rate constant increased with increasing agitation speed due to homogeneous mixing at high rotational speeds. The pseudo-first order rate constants were 0,485 h^{-1} and 0,6835 h^{-1} for 50 and 200 rpm, respectively. Good correlation coefficients (R^2=0,9207) was obtained for the pseudo-first order rate expression indicating the fact that zinc biosorption follows the pseudo-first order kinetics.

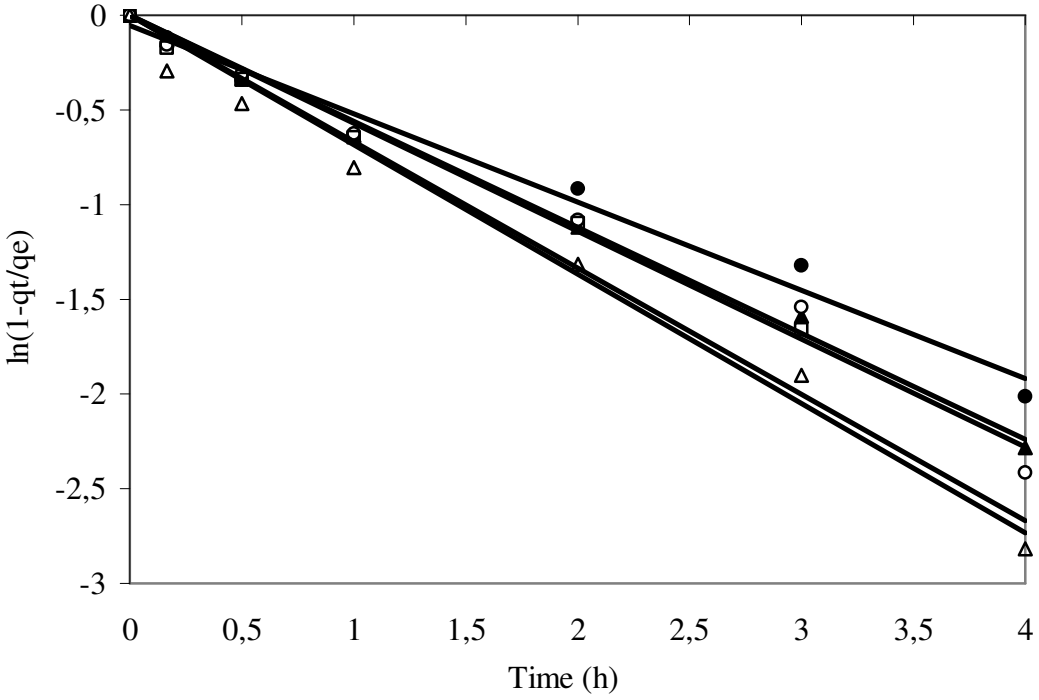

Figure 3.20 A plot of ln (1- q_t / q_e) versus time according to the pseudo-first order biosorption kinetics. ● 50 rpm, ▲ 75 rpm, ○ 100 rpm, □ 150 rpm, Δ 200 rpm

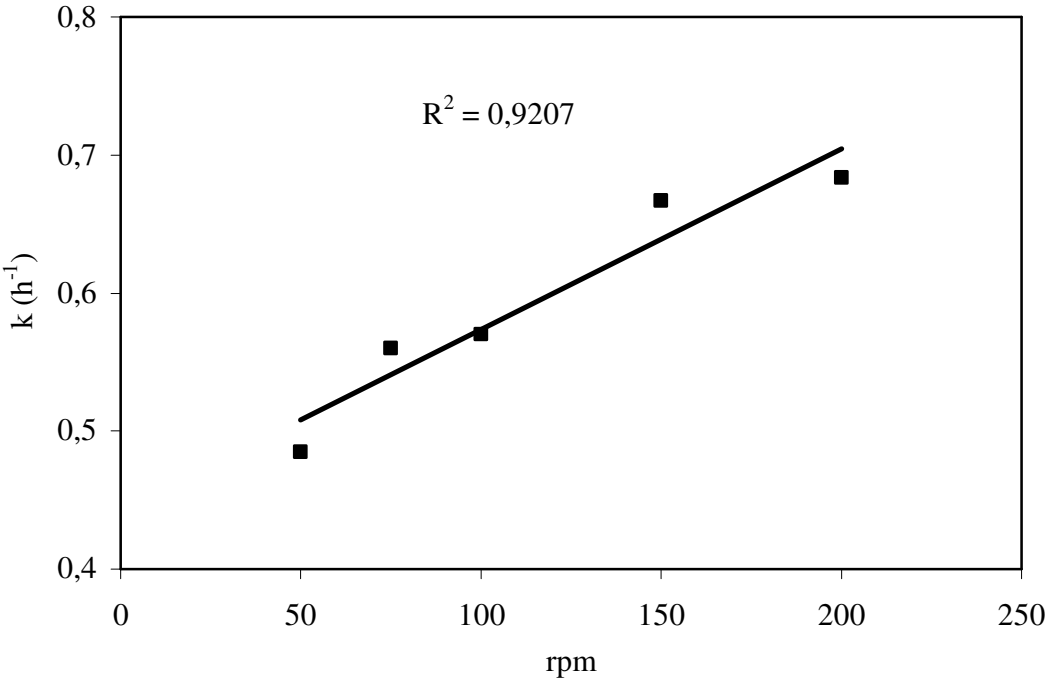

Figure 3.21 A plot of pseudo-first order biosorption rate constant (k) versus agitation speed

The rate constants for pseudo-second kinetics were determined by plotting t/q_t against t and shown in Figure 3.22. The rate constant (k) is obtained from the slope and intercept of equation 2.

Variations of the pseudo-second order rate constants (k) with agitation speed is depicted in Figure 3.23. Equilibrium solid phase zinc ion concentration increased from 45 to 67 mg g^{-1}, when the agitation speed was increased from 50 to 200 rpm which was found from Figure 3.18. These values were used in equation 2 to find pseudo-second order rate constants. The highest second order rate constant was nearly 0,018 $(mg/g)^{-1}h^{-1}$ obtained with the agitation speed of 200 rpm which dropped to 0,013 $(mg/g)^{-1}h^{-1}$ at 150 rpm. Pseudo-second order kinetics did not fit to the experimental data as well as the first order kinetics.

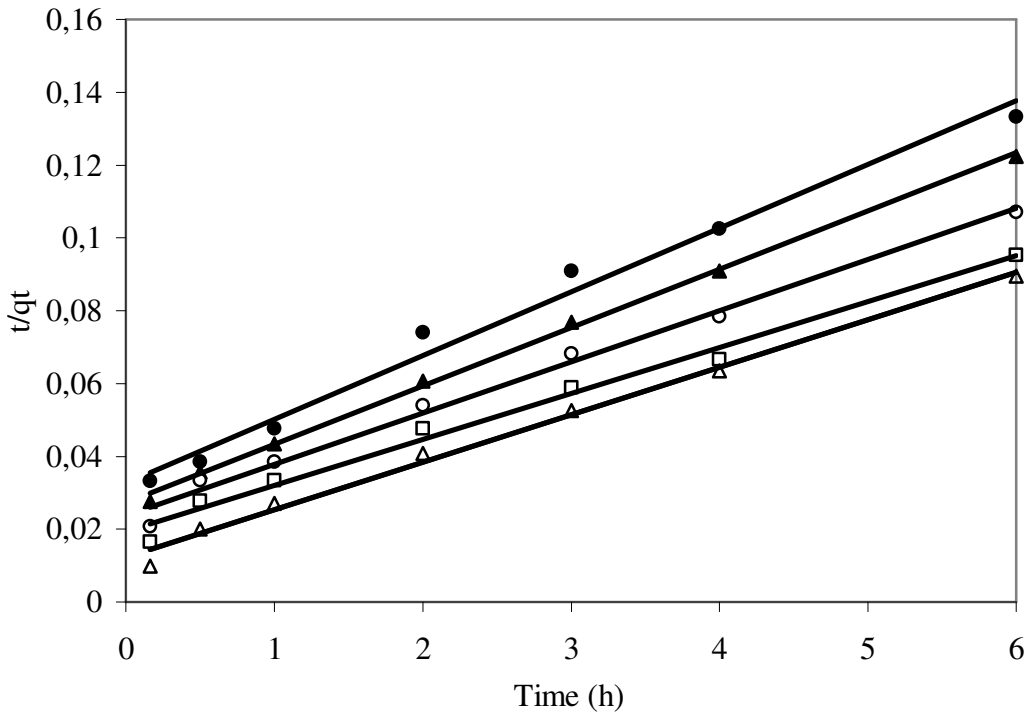

Figure 3.22 A plot of t / q_t versus time according to the pseudo- second order biosorption kinetics

● 50 rpm, ▲ 75 rpm, ○ 100 rpm, □ 150 rpm, Δ 200 rpm

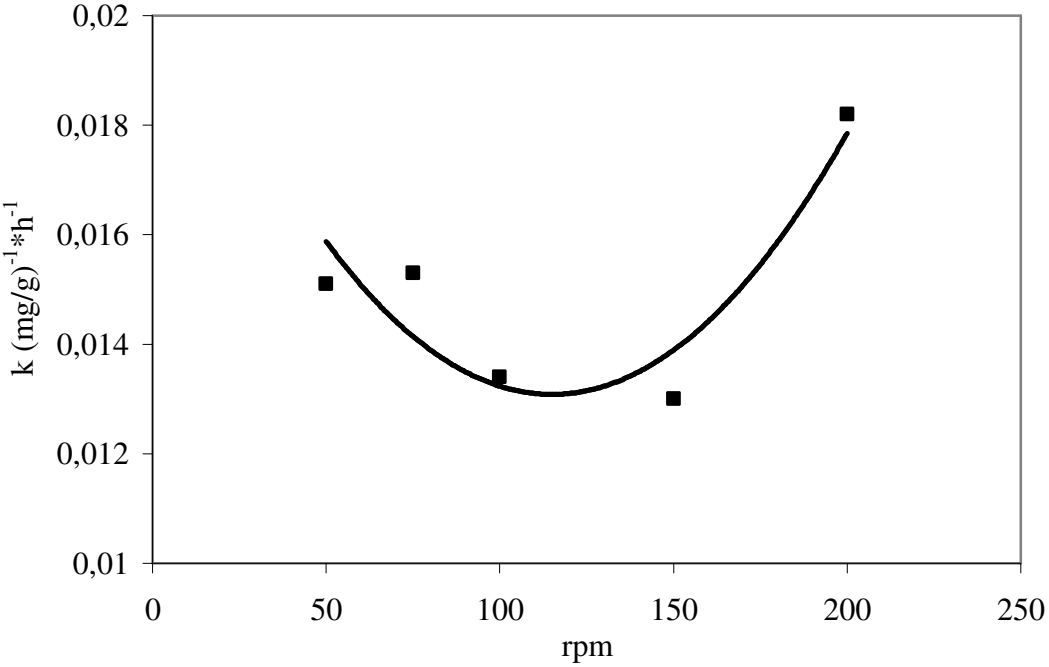

Figure 3.23 A plot of pseudo-second order biosorption rate constant (k) versus different agitation speeds

3.3.4. Effects of Initial Zn(II) Concentration

Zinc (II) ion concentrations were varied between 50 and 350 mg l^{-1} in this set of experiments while the PWS concentration, particle size and pH were constant at 1 g l^{-1}, 64 µm and pH = 5, respectively. Variations of the solid phase (biosorbed) zinc ion concentrations with time are depicted in Figure 3.24 for different initial zinc ion concentrations. Biosorbed zinc ion concentrations increased with time and reached equilibrium after six hours of incubation for all initial zinc ion concentrations tested. Zinc ions at 50 mg l^{-1} concentration were biosorbed completely onto binding sites on PWS surfaces at the end of 24 hours. At low initial Zn^{2+} concentrations such as 50 and 100 mg l^{-1}, the extent of biosorption was limited by zinc ion concentrations yielding 50 mg g^{-1} and 72 mg g^{-1} equilibrium solid phase concentrations. However, at high initial Zn^{2+} concentrations such as 300 and 350 mg l^{-1}, the extent of biosorption was limited by the concentration or the binding sites of the PWS yielding high equilibrium Zn^{2+} concentrations in the solid phase such as 94 and 86 mg g^{-1},

respectively. At constant PWS concentration, initial zinc ion concentration should be high enough to maximize biosorbed zinc ion concentration.

Variations of Zn^{2+} removal efficiency with time are depicted in Figure 3.25 for different initial zinc ion concentrations. Although the equilibrium zinc uptake and biosorbed zinc ion concentration increased with increasing initial zinc concentration from 50 to 350 mg l^{-1}, percent zinc ion removals decreased. Percent zinc ion removal decreased from 100% to 25% when the initial Zn^{2+} concentration was raised from 50 to 350 mg l^{-1}. At low initial Zn^{2+} concentrations such as 50 and 100 mg l^{-1}, all zinc ions were biosorbed onto the binding sites on PWS surfaces since binding sites were in excess of zinc ions yielding low zinc ions in solution such as 28 mg l^{-1} for 100 mg l^{-1} initial zinc concentration. However, at high initial zinc ion concentrations such as 300 and 350 mg l^{-1}, a large fraction of binding sites on PWS surfaces were occupied by zinc ions since zinc ions were in excess of the binding sites yielding high zinc ion concentrations in the solution at equilibrium and low percent zinc ion removals such as 31% and 25%, respectively.

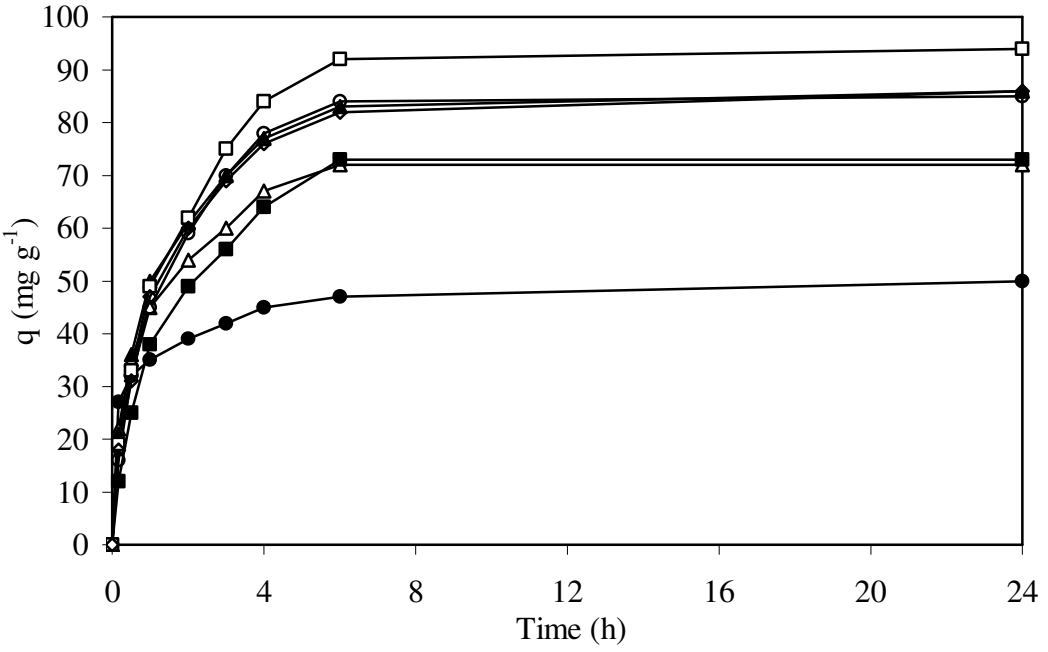

Figure 3.24 Variation of biosorbed (solid phase) zinc ion concentrations with time for different initial zinc ion concentrations. ● 50 mg l^{-1}, Δ 100 mg l^{-1}, ■ 150 mg l^{-1}, ▲ 200 mg l^{-1}, ○ 250 mg l^{-1}, □ 300 mg l^{-1}, ◊ 350 mg l^{-1}.

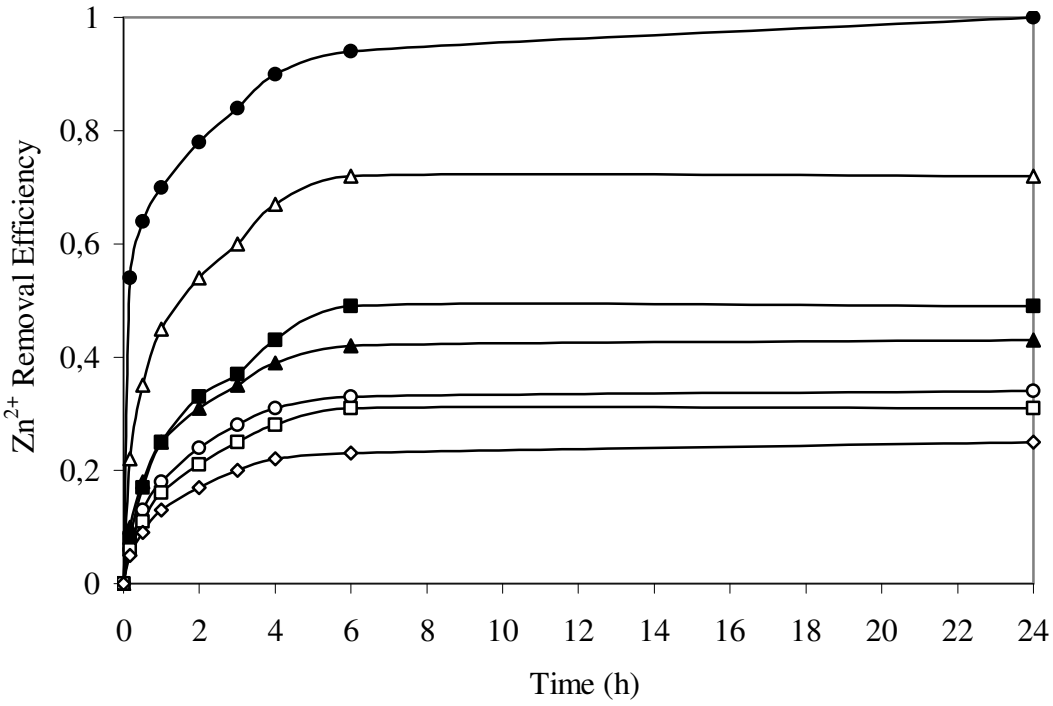

Figure 3.25 Variation of zinc ion removal efficiencies with time for different initial zinc ion concentrations. ● 50 mg l^{-1}, Δ 100 mg l^{-1}, ■ 150 mg l^{-1}, ▲ 200 mg l^{-1}, ○ 250 mg l^{-1}, □ 300 mg l^{-1}, ◊ 350 mg l^{-1}.

The pseudo-first order kinetic model was used to correlate the experimental data as shown in Figure 3.26. The kinetic constants for the pseudo-first order model were determined from the slopes of the lines presented in Figure 3.26. The results did not fit well to the Lagergreen model.

Variations of the first-order rate constants (k) with the initial zinc ion concentration are depicted in Figure 3.27. The correlation between the rate constant and the initial zinc ion concentrations was not good enough.

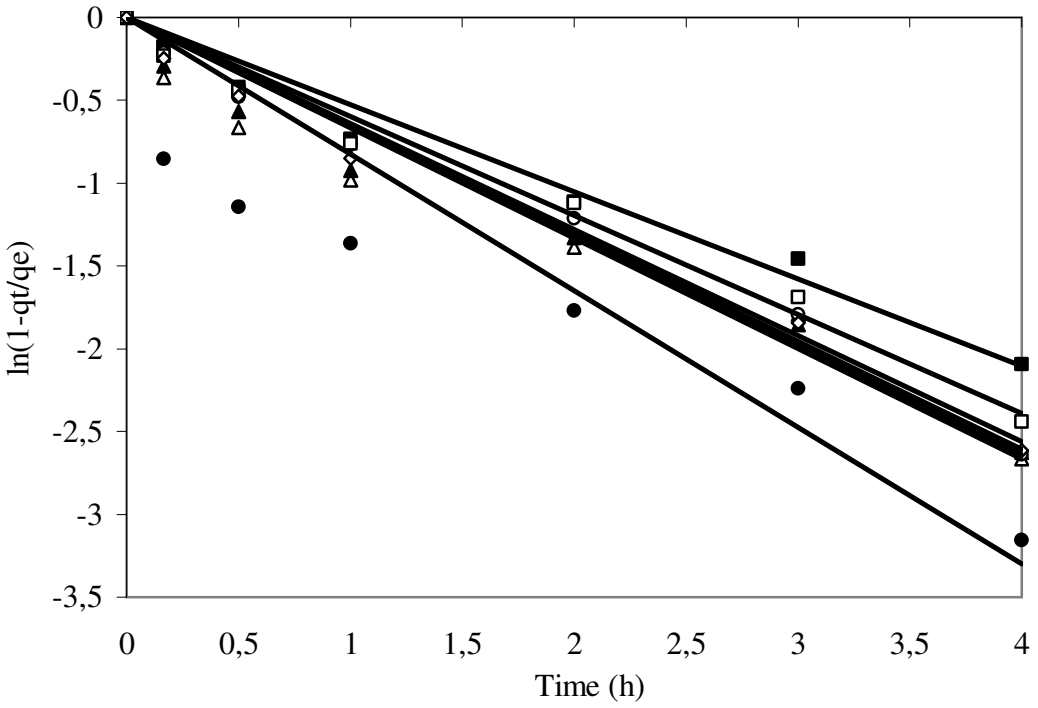

Figure 3.26 A plot of ln (1- q_t / q_e) versus time according to the pseudo-first order biosorption kinetics.● 50 mg l^{-1}, Δ 100 mg l^{-1}, ■ 150 mg l^{-1}, ▲ 200 mg l^{-1}, ○ 250 mg l^{-1}, □ 300 mg l^{-1}, ◊ 350 mg l^{-1}.

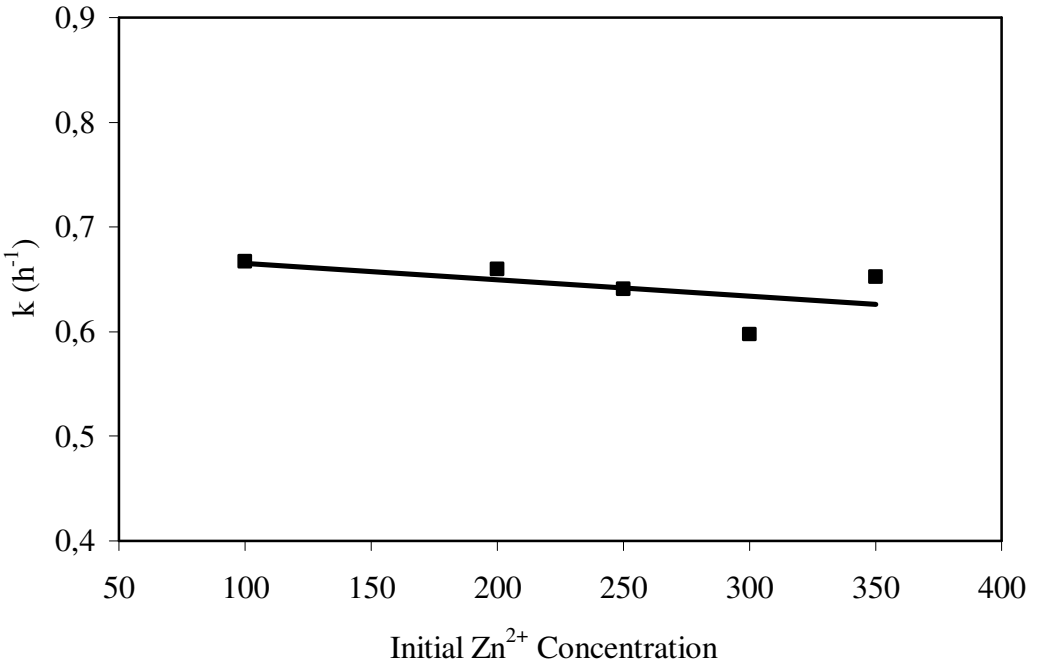

Figure 3.27 A plot of pseudo-first order biosorption rate constant (k) versus initial zinc ion concentration.

The experimental results were also correlated with the pseudo-second order kinetic model. The experimental data was plotted in form of 't/q' versus time for different initial zinc concentrations as shown in Figure 3.28. The rate constant (k) was obtained by using equation 2.

Variations of the pseudo-second order rate constants (k) with initial zinc ion concentration are depicted in Figure 3.29. The rate constants and the initial sorption rates decreased with increases in initial zinc concentration. Equilibrium solid phase zinc concentration (q_e) was obtained from figure 3.24. Nevertheless, equilibrium solid phase zinc ion concentration increased from 47 to 92 mg g^{-1}, when the initial Zn^{2+} concentration was increased from 50 and 300 mg l^{-1}. The equilibrium solid phase zinc ion concentration decreased to 82 mg g^{-1} when initial zinc concentration was 350 mg l^{-1} because of the limitation of binding sites on PWS surfaces. The solid lines in Figure 3.28 are the best-fit lines indicating high correlation coefficients (R^2 >0,97). The experimental data fitted to the pseudo-second order model better than the pseudo-first order model.

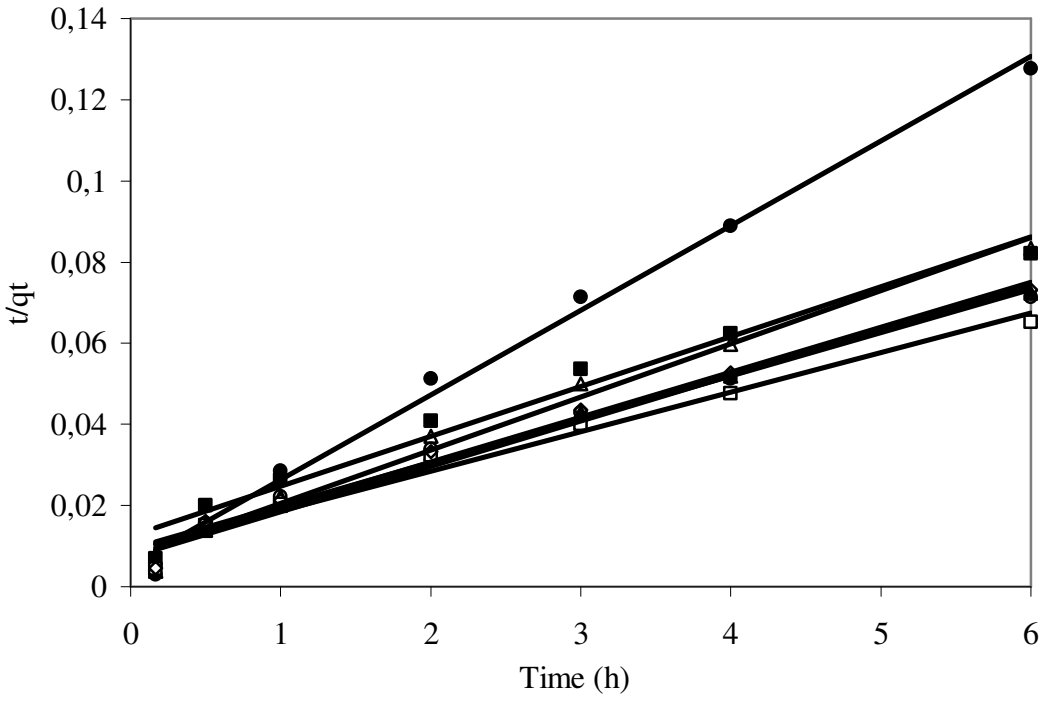

Figure 3.28 A plot of t / q_t versus time according to the pseudo- second order biosorption kinetics
● 50 mg l^{-1}, Δ 100 mg l^{-1}, ■ 150 mg l^{-1}, ▲ 200 mg l^{-1}, ○ 250 mg l^{-1}, □ 300 mg l^{-1}, ◊ 350 mg l^{-1}

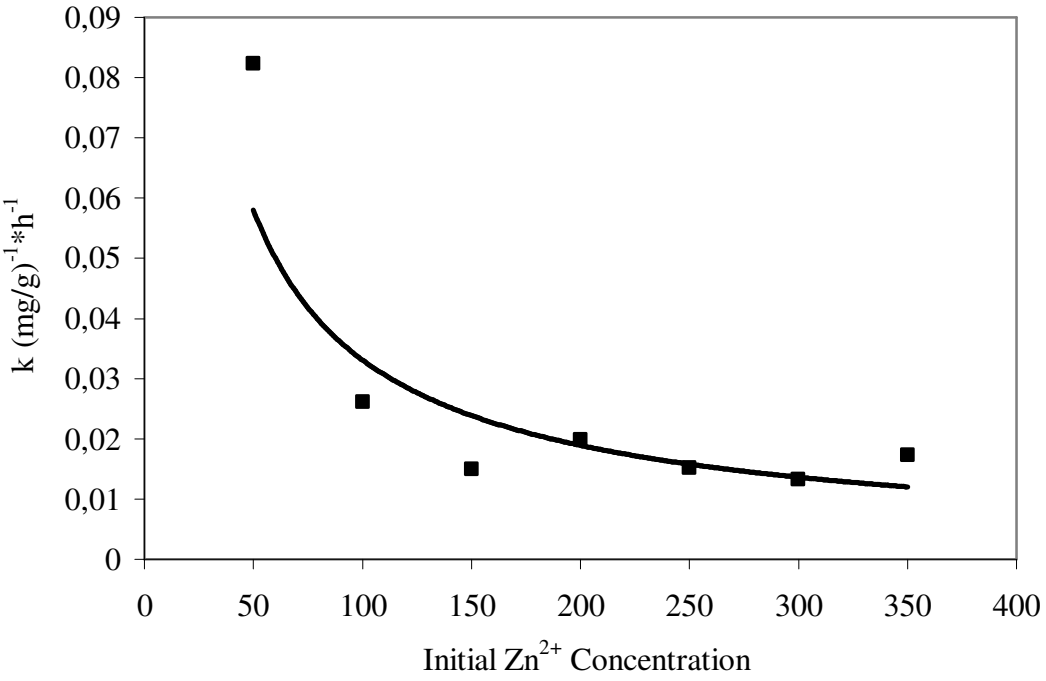

Figure 3.29 A plot of pseudo-second order biosorption rate constant (k) versus initial Zn^{2+} concentration

3.3.5. Effects of powdered waste sludge (PWS) concentration

The biosorbent (PWS) concentration was varied between 0,25 and 3,0 g l^{-1} in this set of experiments while the initial zinc ion concentration, PWS particle size and pH were constant at 200 mg l^{-1}, 64 µm and pH = 5, respectively. Variations of the solid phase (biosorbed) Zn^{2+} concentrations with time are depicted in Figure 3.30 for different biosorbent (PWS) concentrations. Biosorbed zinc ion concentrations increased with time and reached equilibrium after six hours of incubation for all biosorbent (PWS) concentrations tested. At low PWS concentrations such as 0,25 and 0,5 g l^{-1}, the available binding sites on biosorbent surfaces were occupied by zinc ions since zinc ion concentrations exceeded the binding sites yielding high equilibrium biosorbant Zn^{2+} ion concentrations such as 200 and 116 mg g^{-1}, respectively. However, at high biosorbent (PWS) concentrations such as 2,5 and 3,0 g l^{-1} , large binding sites were available on PWS surfaces and only a fraction of those binding sites were occupied by Zn^{2+} ions yielding low solid phase Zn^{2+}

concentrations such as 47 and 55 mg g^{-1}. The extent of biosorption was limited by zinc ion concentration at high PWS concentrations.

Variations of Zn^{2+} removal efficiency with time are depicted in Figure 3.31 for different biosorbent (PWS) concentrations. Percent zinc ion removal increased from 25% to 83% when the biosorbent (PWS) concentration was raised from 0,25 to 3,0 g l^{-1}. At low biosorbent concentrations such as 0,25 and 0,5 g l^{-1}, the extent of zinc biosorption was limited by the availability of the binding sites on the biosorbent (PWS) surfaces yielding low percent zinc ion removal such as 25 and 29% respectively at equilibrium. However, at high biosorbent concentrations such as 2,5 and 3,0 g l^{-1}, the binding sites on the biosorbent surfaces exceeded zinc ions in solution and large fractions of zinc ions were biosorbed onto the binding sites resulting in nearly 59 and 83% zinc ion removals, respectively. At an initial zinc ion concentration of 200 mg l^{-1}, the biosorbent (PWS) concentration should be higher than 3 g l^{-1} to obtain more than 83% zinc ion removal.

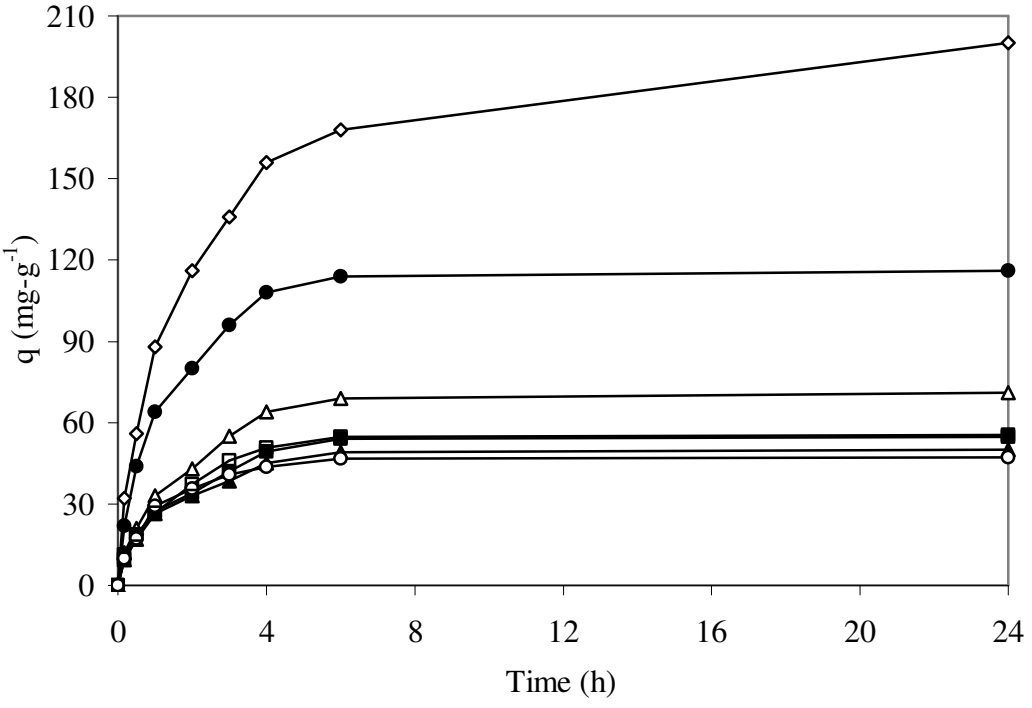

Figure 3.30 Variation of biosorbed zinc ion concentration with time for different PWS concentrations.

PWS (g l^{-1}): ◊ 0,25 , ● 0,5, Δ 1, ■ 1,5, ▲ 2, ○ 2,5, □ 3

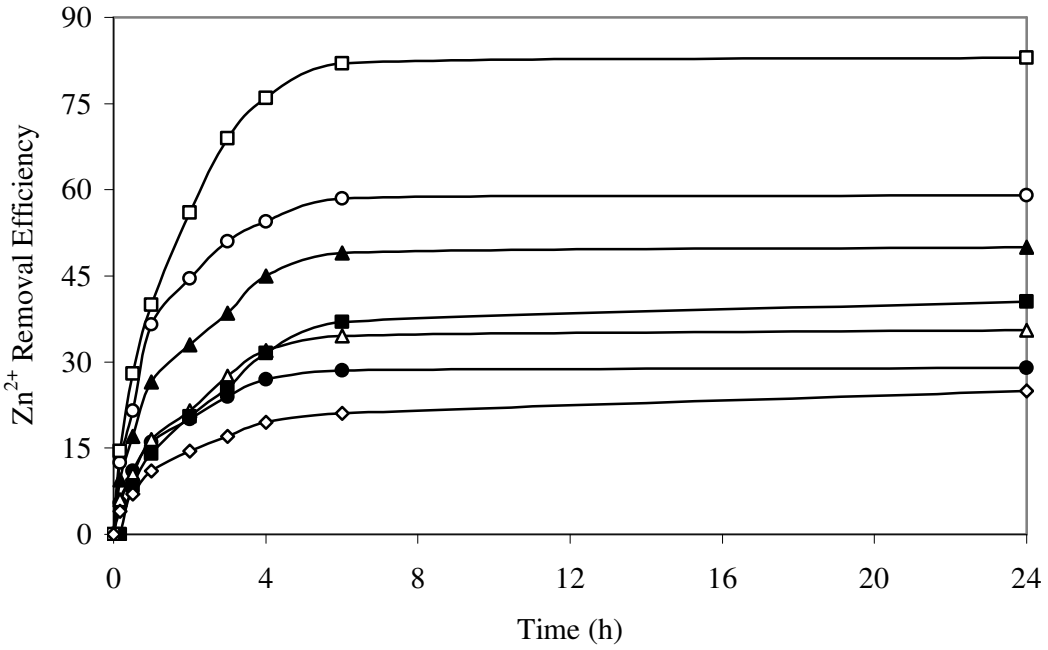

Figure 3.31 Variations of Zn^{2+} removal efficiency with time for different PWS concentrations

PWS (g l^{-1}): ◊ 0,25 , ● 0,5, Δ 1, ■ 1,5, ▲ 2, ○ 2,5, □ 3

The pseudo-first order kinetic model was used to correlate the experimental data. The experimental data was plotted in form of ln (1- q/q_e) versus time for different PWS concentrations and a group of lines with different slopes were obtained as shown in Figure 3.32. The kinetic constants for the pseudo-first order model were determined from the slopes of the lines. As shown in Figure 3.32, the correlations between the experimental data and the first order rate predictions were not good.

Variations of the first-order rate constants (k) with PWS concentrations are depicted in Figure 3.33. The straight line is the best fit line which does not fit to the experimental data. Apparently, the first order model does not represent the experimental data.

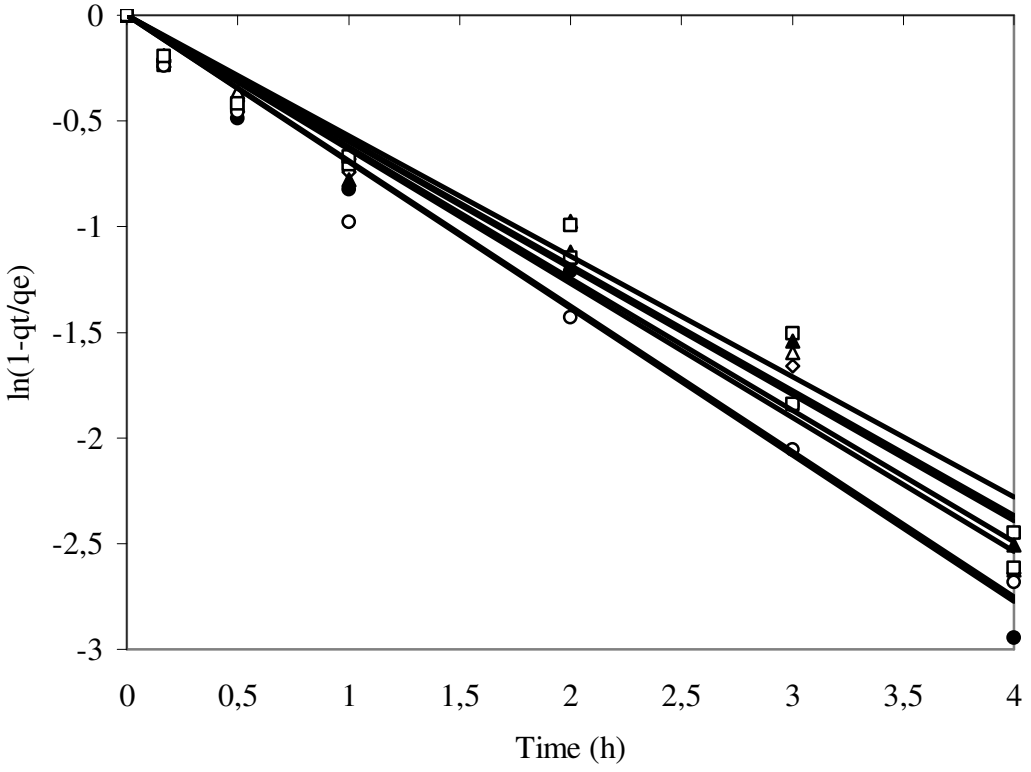

Figure 3.32 A plot of ln (1- q_t / q_e) versus time according to the pseudo-first order biosorption kinetics. PWS (g l^{-1}): ◊ 0,25 , ● 0,5, Δ 1, ■ 1,5, ▲ 2, ○ 2,5, □ 3

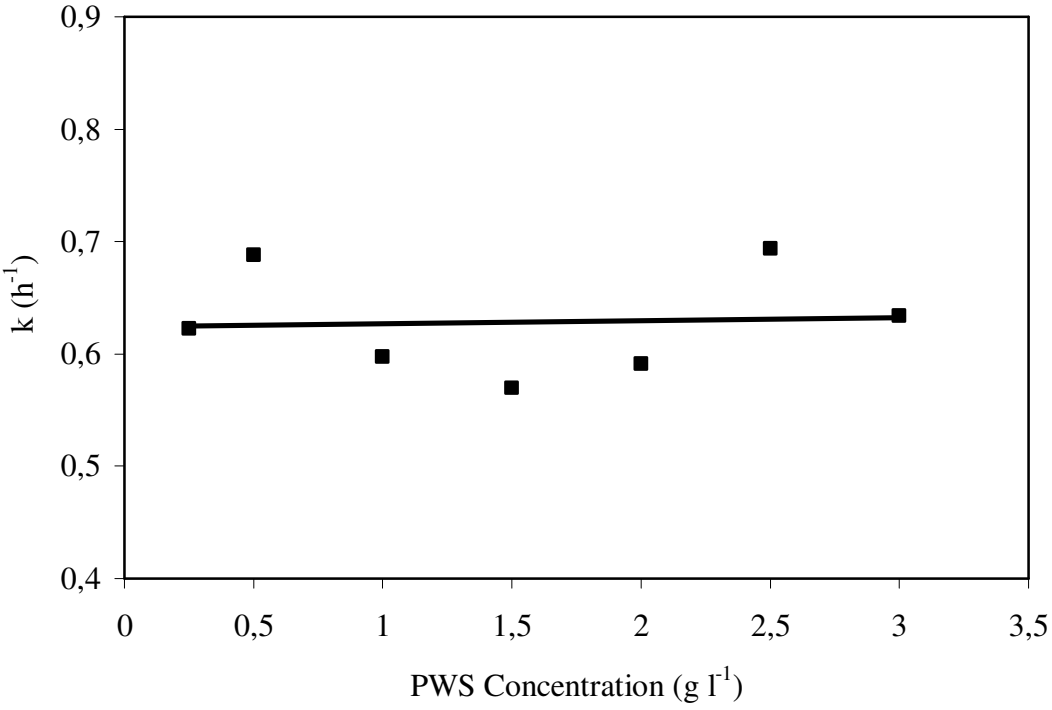

Figure 3.33 A plot of pseudo-first order biosorption rate constant (k) versus PWS concentration

Figure 3.34 shows a plot of the linearized form of the pseudo-second order model for the biosorption of zinc (II) ions onto PWS at different PWS concentrations. Equilibrium biosorption capacities (qe) for the pseudo-second order model were obtained from the Figure 3.30 and used in equation 2 to find rate constants (k).

Variations of the pseudo-second order rate constants (k) with different PWS concentration are depicted in Figure 3.35. There is a linear relationship between the pseudo-second order rate constant and the PWS concentration with a correlation coefficient of 0,87. The correlation coefficient obtained by using five experimental data without 2,5 and 3 g l^{-1} PWS. The values of the rate constants were found to increase from 0,007 to 0,024 $(mg/g)^{-1}$ h^{-1} as the PWS concentrations increased from 0,25 to 2 g l^{-1}. Equilibrium biosorption capacity (q_e) decreased from 156 to 50 mg g^{-1}, as the PWS concentrations increased from 0,25 to 3 g l^{-1}.

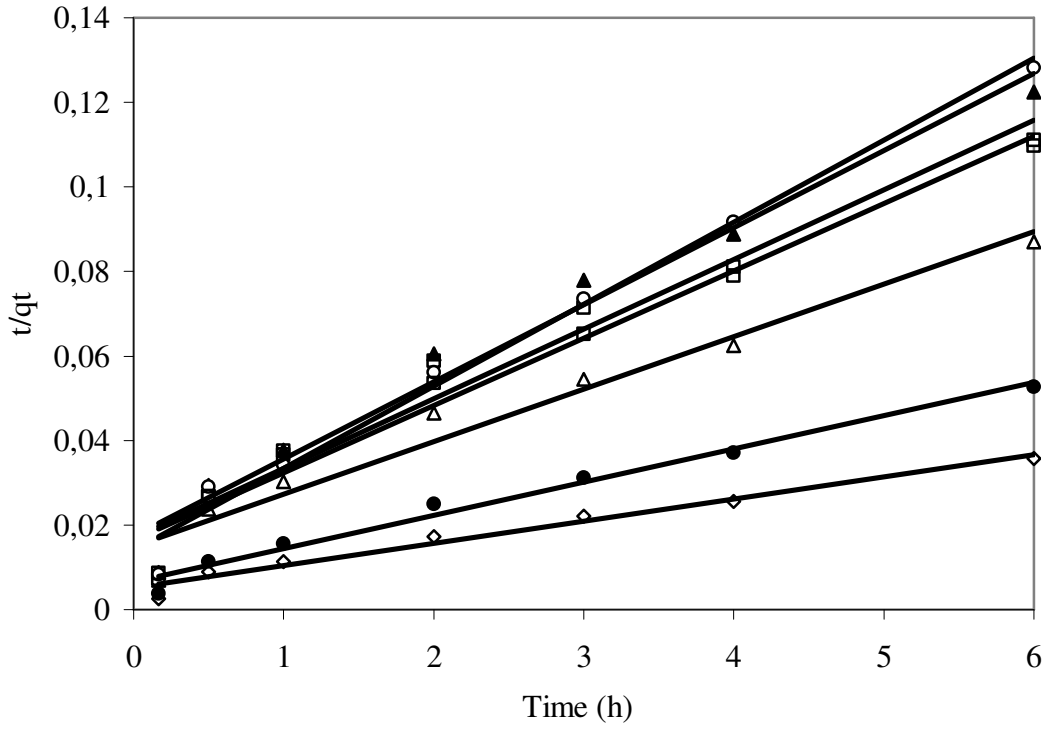

Figure 3.34 A plot of t / q_t versus time according to the pseudo- second order biosorption kinetics. PWS (g l^{-1}): ◊ 0,25 , ● 0,5, Δ 1, ■ 1,5, ▲ 2, ○ 2,5, □ 3

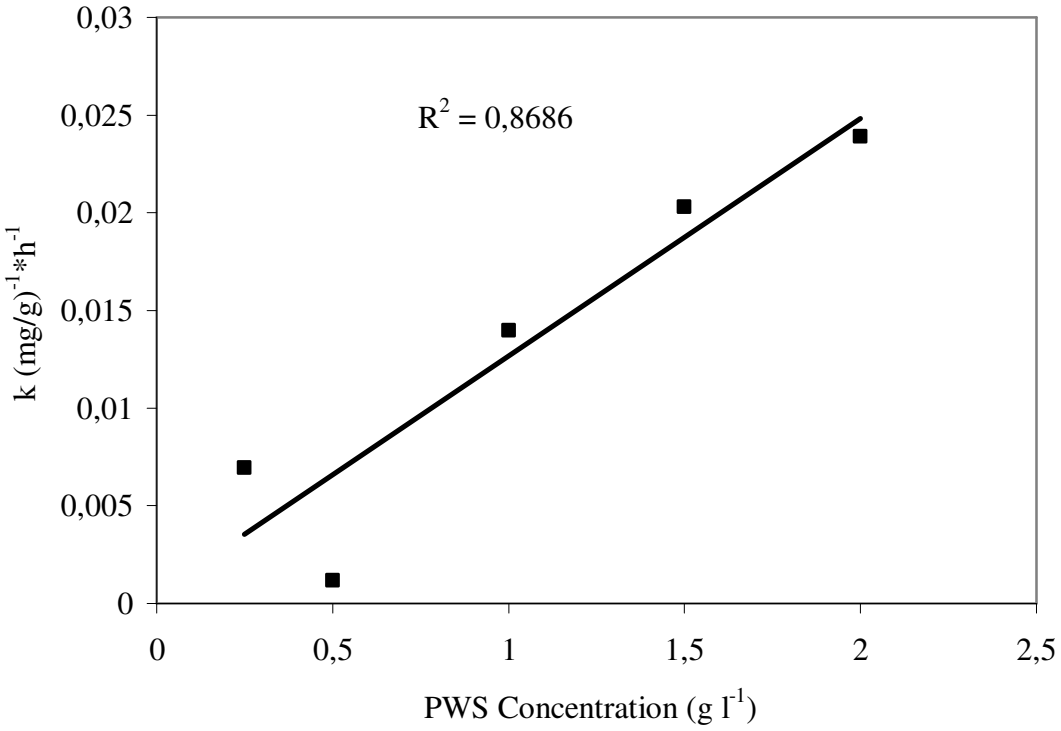

Figure 3. 35 A plot of pseudo-second order biosorption rate constant (k) versus PWS concentration

3.3.6. Effects of Temperature

Experiments were also performed at different temperatures 30, 35, 40, 45 and 50 ^{0}C with 1 g l^{-1} PWS concentration (64 µm) at zinc ion concentration of 100 mg l^{-1} and a pH of 5 at 150 rpm. Figure 3.36 depicts variation of solid phase (biosorbed) zinc ion concentrations with time for different temperatures. Equilibrium time for different temperatures was found to be 6 hours indicating thereby that the equilibrium time was independent of the temperature. Biosorbed Zn^{2+} concentration increased with time at all temperatures tested. Equilibrium solid phase zinc ion concentrations were 60, 66 and 73 mg g^{-1} when the temperature was 30, 40 and 50 ^{0}C, respectively. The increases in solid phase zinc ion concentrations with temperature were not significant.

Variations of Zn^{2+} removal efficiency with time are depicted in Figure 3.37 for different temperatures. The percentage of adsorption increased from 60 % to 73 % with an increase in temperature from 30 to 50 ^{0}C.

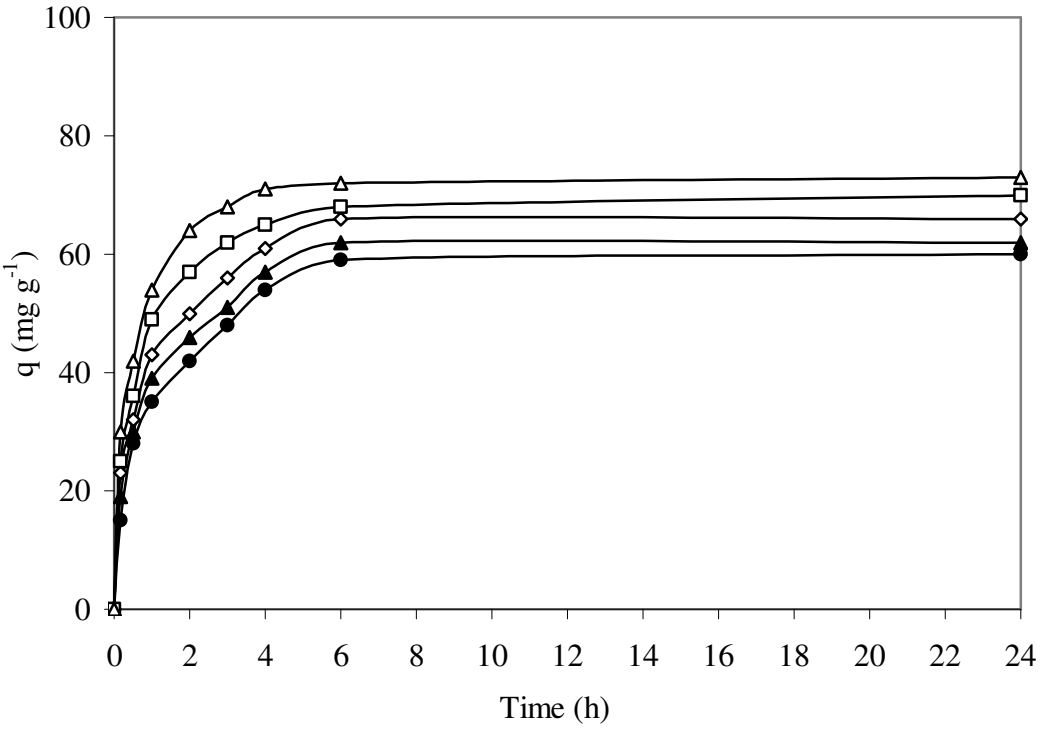

Figure 3.36 Variation of biosorbed (solid phase) zinc ion concentration with time at different temperatures. T (^{0}C): ● 30, ▲ 35, ○ 40, □ 45, Δ 50

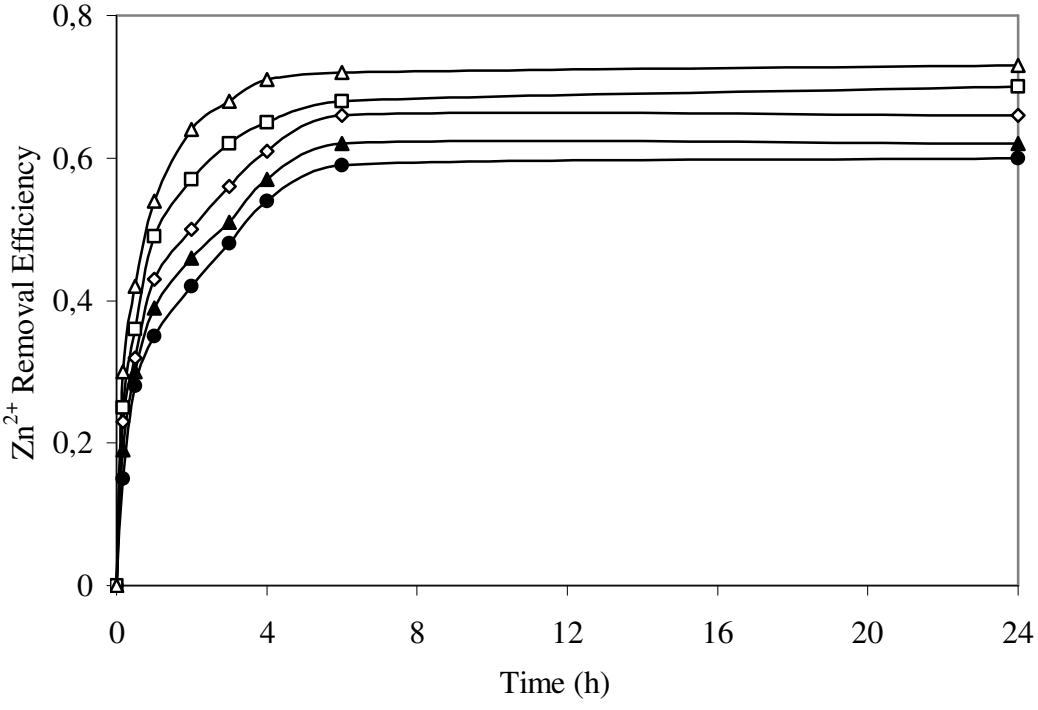

Figure 3.37 Variation of Zn^{2+} removal efficiency with time at different temperatures.
T (^{0}C): ● 30, ▲ 35, ○ 40, □ 45, Δ 50

The pseudo-first order model was used for correlation of the experimental data obtained at different temperatures. The experimental data was plotted in form of ln (1- q/q_e) versus time for different temperatures and a group of lines with different slopes were obtained as shown in Figure 3.38. The correlation coefficients R^2 and rate constant k are obtained from the slope of the line in Figure 3.38.

The first order rate constants (k) were plotted against temperature and a linear variation with high correlation coefficient (R^2= 0,8849) was obtained as shown in Figure 3.39. Values of pseudo-first order rate constants ranged from 0,6166 to 0,9663 h^{-1} when temperature was increased from 30 to 50 ^{0}C.

The increase in the pseudo-first order rate constants with increasing temperature may be described by the Arrhenius equation:

$$\ln k = \ln A - E_a/RT \qquad \text{eq. 17}$$

where k is the rate constant of biosorption (g/mg h), A is the frequency factor, E_a the activation energy of sorption (kcal mol^{-1}), R the gas constant (1,99 kcal/mol K) and T the solution temperature (K).

The first order rate constants (k) were plotted as a function of the reciprocal absolute temperature and a linear correlation was obtained as shown in Figure 3.40. The correlation coefficient was 0,8945. The activation energy of biosorption for the pseudo-first order model were determined from the slope of the line and found to be 4493,4 cal mol^{-1}.

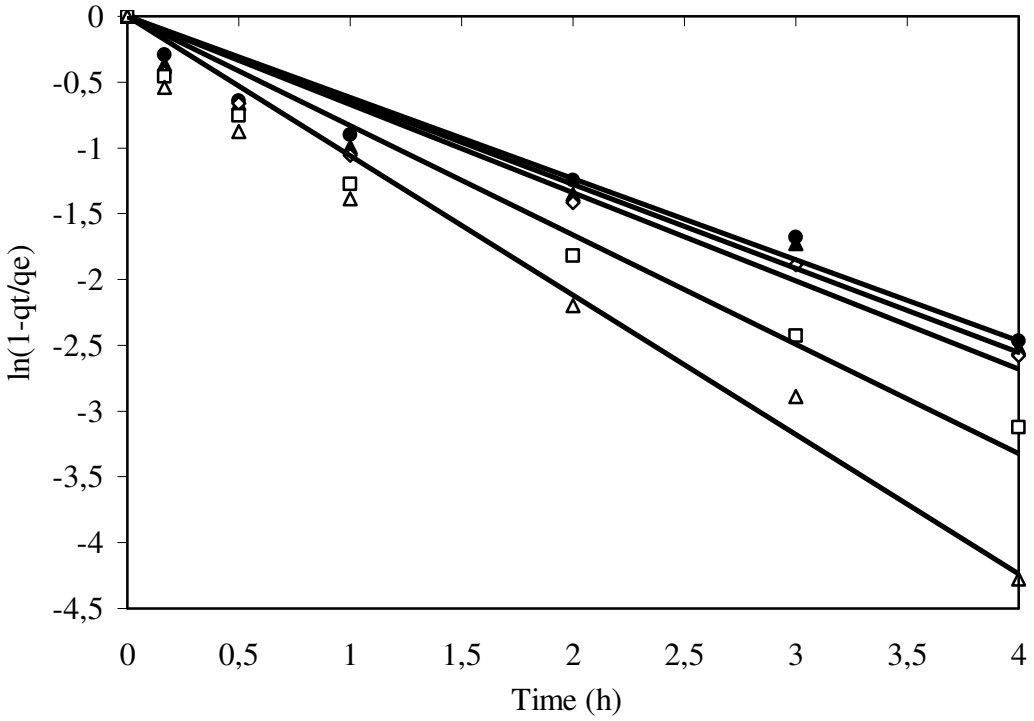

Figure 3.38 A plot of ln (1- q_t / q_e) versus time according to the pseudo-first order biosorption kinetics. Temperature (^{0}C): ● 30, ▲ 35, ○ 40, □ 45, Δ 50

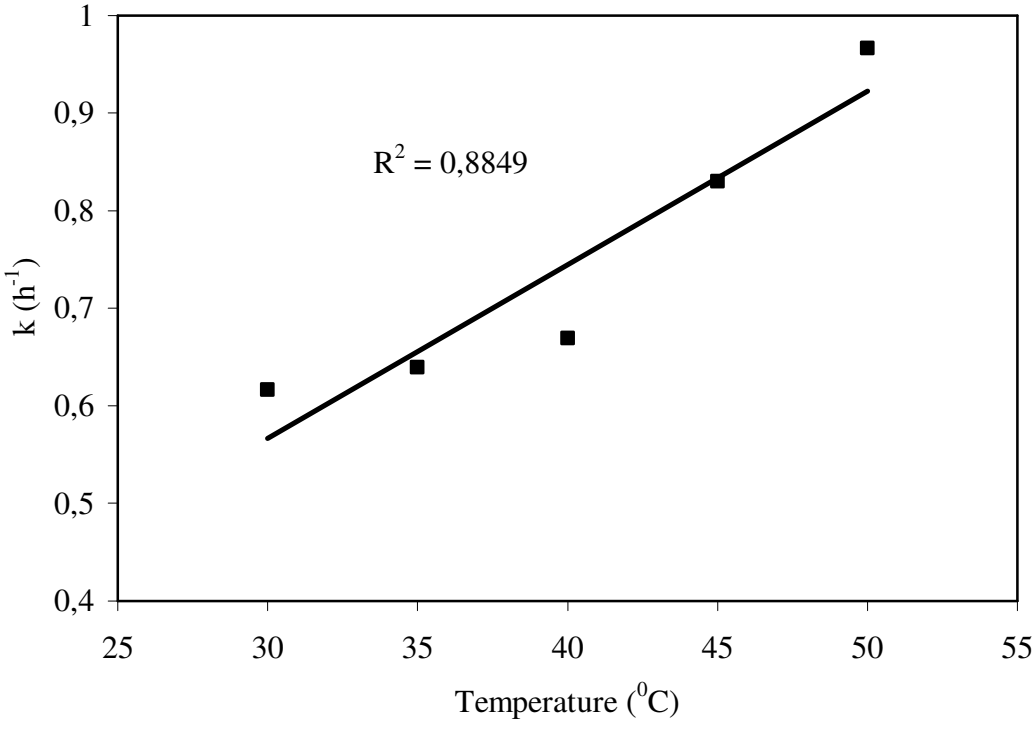

Figure 3.39 A plot of pseudo-first order biosorption rate constant (k) versus temperature

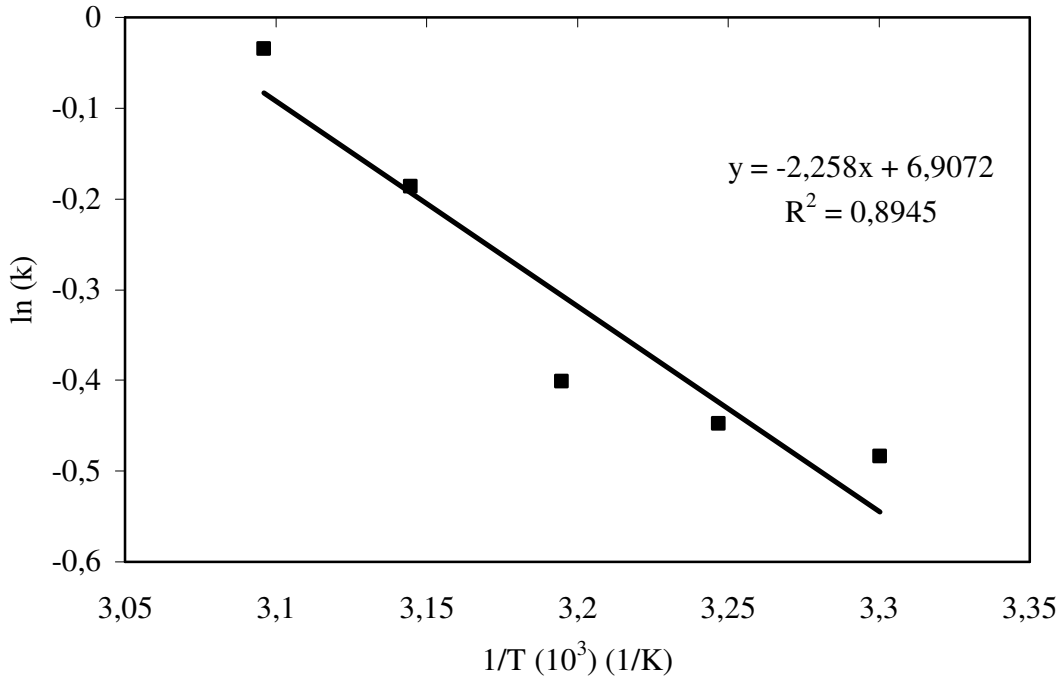

Figure 3.40 A plot of pseudo-first order biosorption rate constant (ln k) versus reciprocal absolute temperature (1/T).

Figure 3.41 shows a plot of the linearized form of the pseudo-second order model for the biosorption of zinc(II) at different temperature. The graph is plotted in the form of t/q_t versus time.

Variations of the pseudo-second order rate constants (k) with temperature are depicted in Figure 3.42 with high correlation coefficient (R^2=0,8943). The rate constants and the initial sorption rate increased with temperature. The equilibrium sorption capacity was not considerably affected by increasing temperature. Equilibrium solid phase zinc ion concentration increased from 59 to 72 mg g^{-1}, when the temperature was raised from 30 to 50 ^{0}C which was found from the Figure 3.36. Pseudo-second order kinetic model was found to represent the experimental data better than the first order model.

The variation in the extent of adsorption with respect to temperature has also been explained on the basis of thermodynamic parameters. To find the activation energy of adsorption, equation 17 was used for pseudo-second order rate constants. The rate

constants were plotted as a function of the reciprocal absolute temperature (K) and a linear variation was obtained as shown in Figure 3.43. The activation energy was found to be 6075,5 cal mol^{-1} using the slope of the line presented in Figure 3.43.

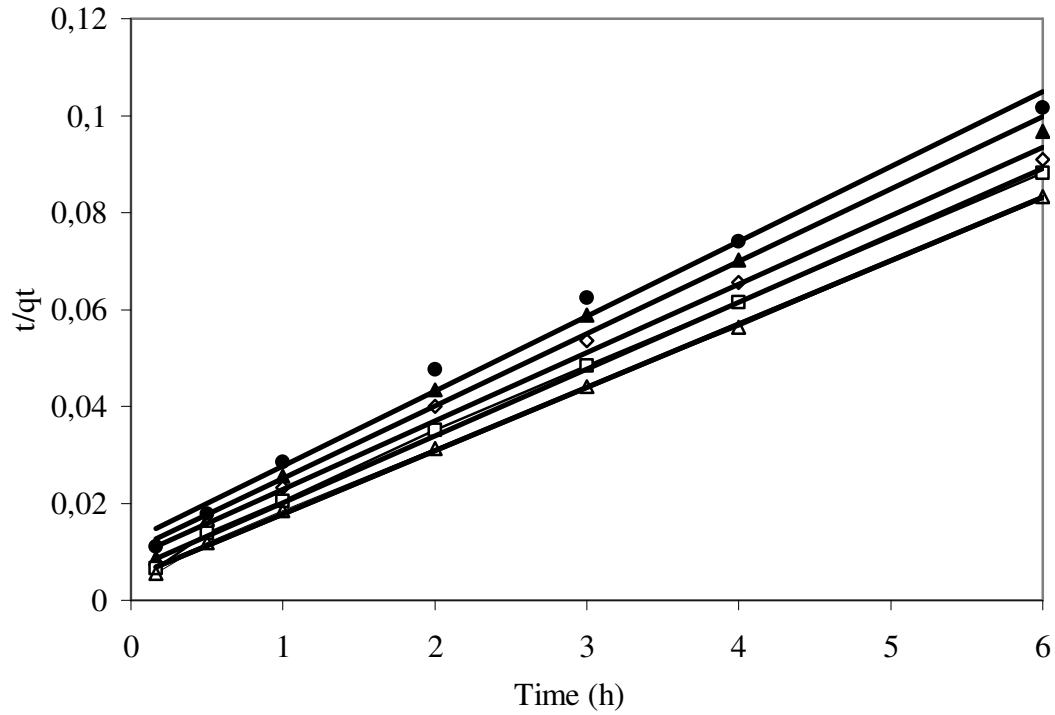

Figure 3.41 A plot of t / q_t versus time according to the pseudo- second order biosorption kinetics. Temperature (^{0}C): ● 30, ▲ 35, ○ 40, □ 45, Δ 50

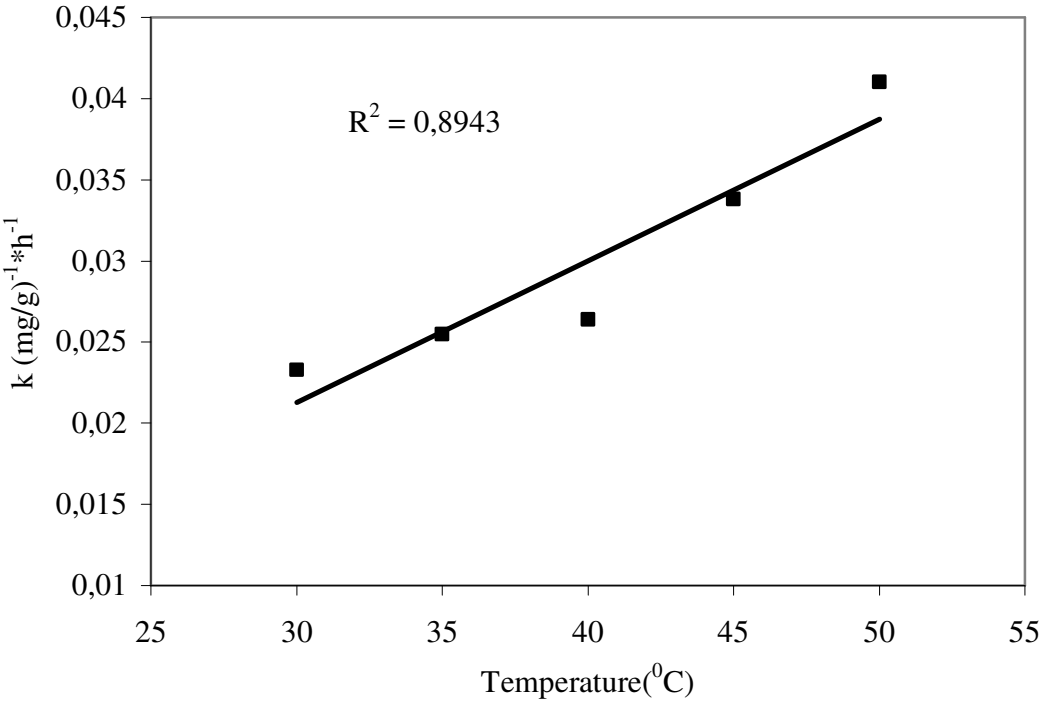

Figure 3.42 A plot of pseudo-second order biosorption rate constant (k) versus temperature

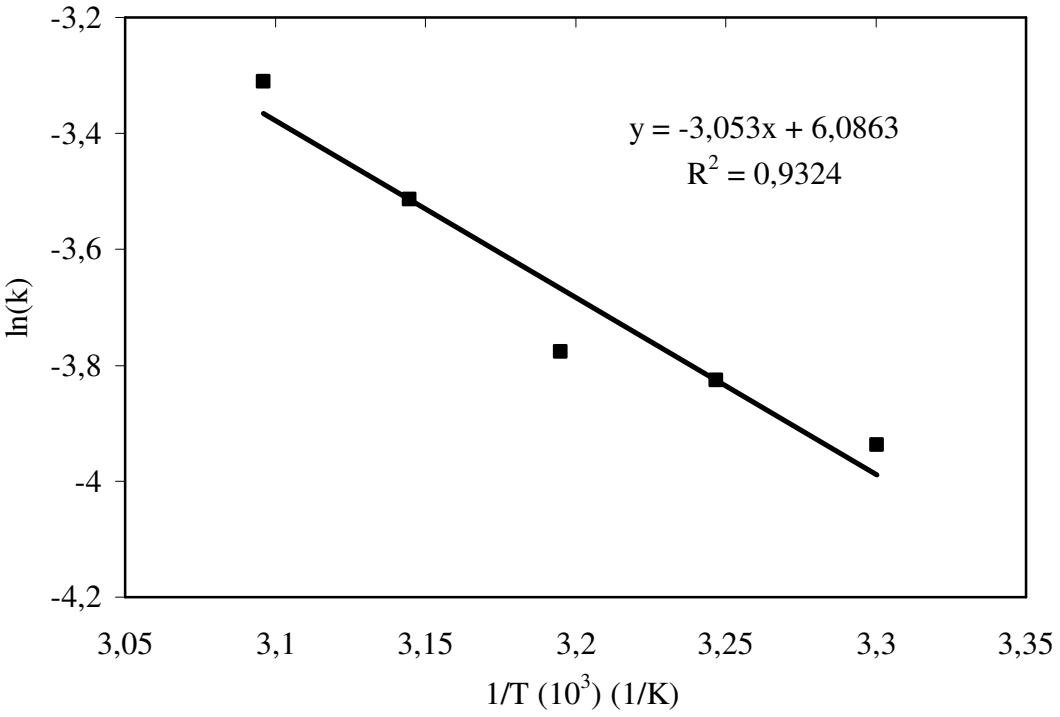

Figure 3.43 A plot of pseudo-second order biosorption rate constant (ln k) versus reciprocal absolute temperature (1/T).

3.4. Biosorption Isotherms

3.4.1. Variable Zn(II) Concentrations

The equilibrium isotherms were determined by mixing 0,2 g of pretreated PWS with the average particle size of 64 µm with 200 ml of zinc solution in 500 ml shake flask at 25 ^{0}C. In isotherm experiments, the zinc ion concentrations were varied between 50 and 350 mg l^{-1} in different flasks. The flasks containing zinc solution and PWS were placed in a shaker and agitated for 24 hours at a fixed agitation speed of 150 rpm.

Three different biosorption isotherms were used to correlate the equilibrium data. The biosorption isotherms used were the Langmuir, Freundlich and the generalized biosorption isotherms.

The plots of equilibrium concentrations of zinc ions in the solid and aqueous phases that is q versus C and also 1/q versus 1/C are presented in Figures 3.44 and 3.45, respectively. Figure 3.44 shows the relationship between the amount of zinc adsorbed per unit mass of PWS (q_e, mg g^{-1}) and its final concentration in the solution (C_e) using different zinc concentration. The increase in the curvature of the isotherm is possibly due to the less active sites being available at the end of the sorption process From the slope and intercept of the line in Figure 3.45, the Langmuir constants were found as q_m = 82,6 mg $g^{-1}$and K = 2,3 mg l^{-1} by using equation 4 with high correlation coefficient (R^2 = 0,94). Apparently, equilibrium biosorption data of zinc ions fit to the Langmuir isotherm reasonably well.

Freundlich isotherm was also used to correlate the equilibrium biosorption data at different zinc ion concentrations. Figure 3.46 depicts a plot of ln q versus ln C for zinc ion biosorption. From the slope and intercept of the line, Freundlich isotherm constants were found to be K= 42,2 mg g^{-1}, 1/n = 0,135 (n= 7,4) by using the equation 6. Apparently Freundlich isotherm represents the equilibrium data reasonably well. However, the fit is not as good as the Langmuir isotherm.

The third isotherm tested for correlation of the equilibrium data was the generalized biosorption isotherm equation which was calculated using equation 8. A plot of the equilibrium data in form of ln ((q_m / q) -1) versus ln C is depicted in Figure 3.47. The q_m value was taken as q_m = 82,6 mg g^{-1} as determined from the Langmuir isotherm. From the slope and intercept of the line presented in Figure 3.47, the following values were found for the constants of the generalized biosorption isotherm: K = 1,83 mg l^{-1} and n = 0,55. Apparently, the generalized adsorption isotherm represents the equilibrium data reasonably well with the correlation coefficient of 0,924 but the fit is not as good as the Langmuir isotherm.

Table3.1 summarizes the results of the isotherm constants for the three different equilibrium isotherms tested. On the basis of the correlation coefficients (R^2), Langmuir isotherm seemed to represent the equilibrium adsorption data with a much better fit as compared to the other isotherms.

Table 3.1. Summary of the isotherm constants and the correlation coefficients for different isotherms.

Parameter	Langmuir Isotherm	Freundlich Isotherm	Generalized Isotherm
q_m (mg g^{-1})	82,6		82,6
K (mg l^{-1})	2,3	42,2	1,83
n		7,4	0,55
R^2	0,94	0,92	0,924

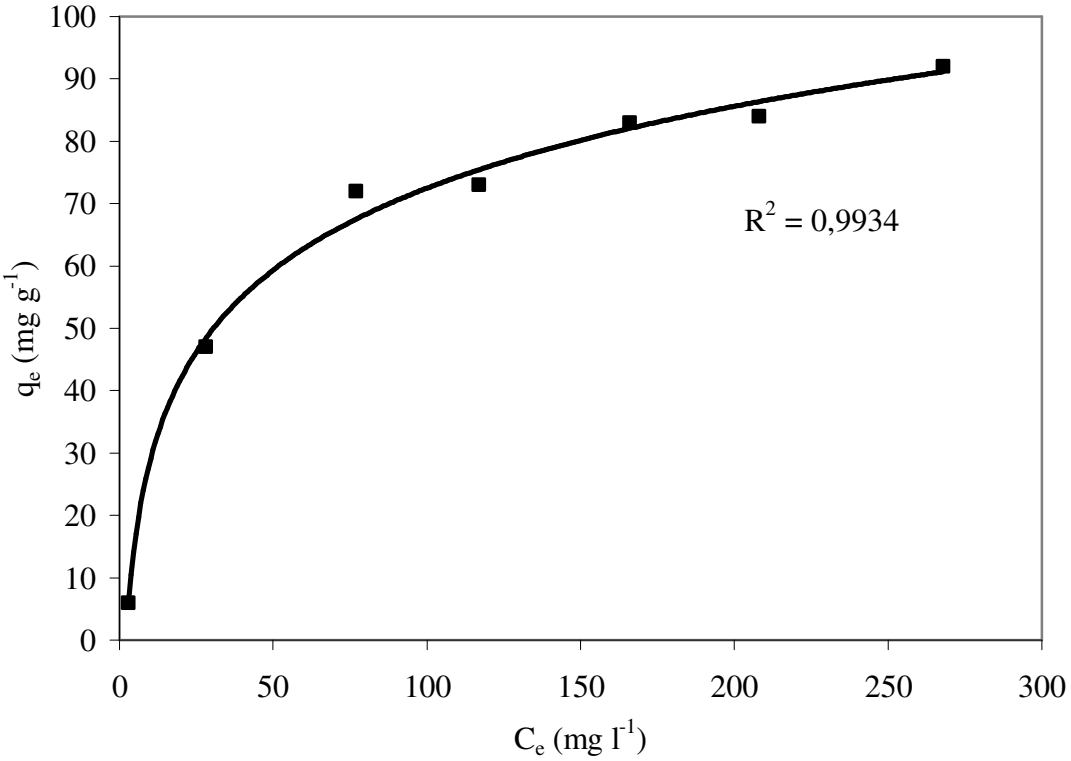

Figure 3.44. Variation of equilibrium solid phase (biosorbed) zinc ion concentration with the equilibrium zinc ion concentration.

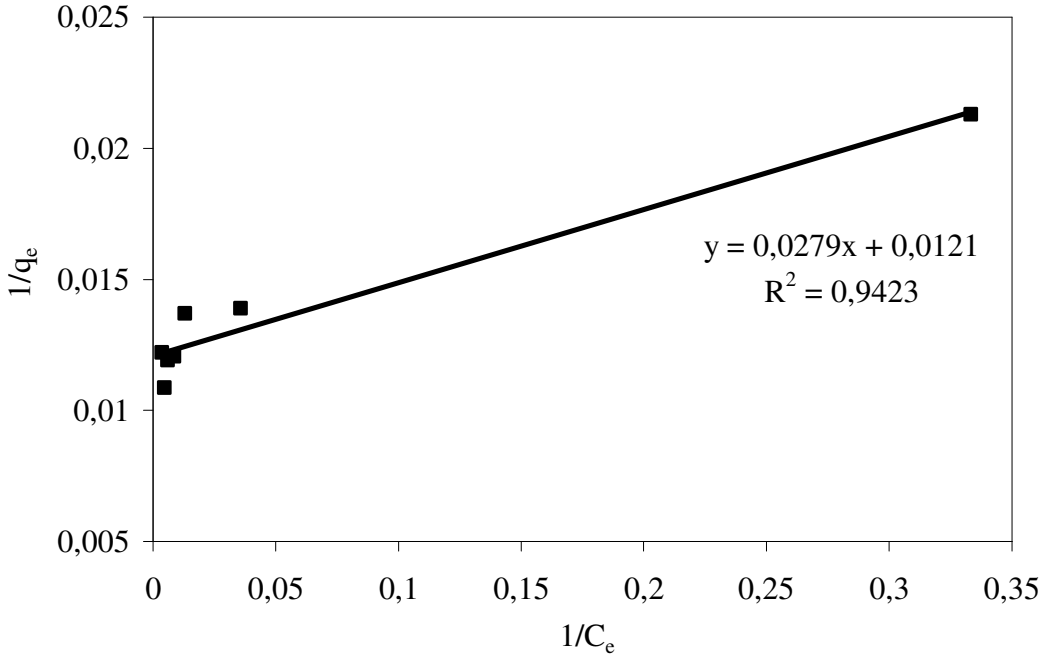

Figure 3.45. Langmuir isotherm plot of $1/q_e$ versus $1/C_e$ for biosorption of zinc ions onto pre-treated PWS. D_p = 64 µm.

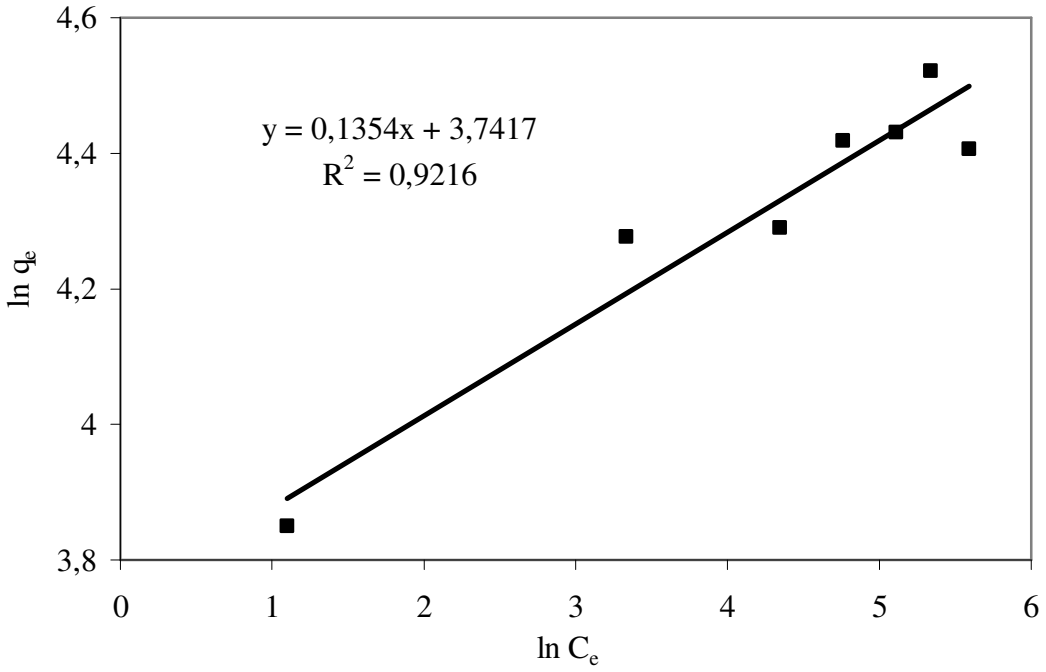

Figure 3.46. Freundlich isotherm plot of ln q_e versus ln C_e for biosorption of zinc ions onto pre-treated PWS. D_p = 64 µm.

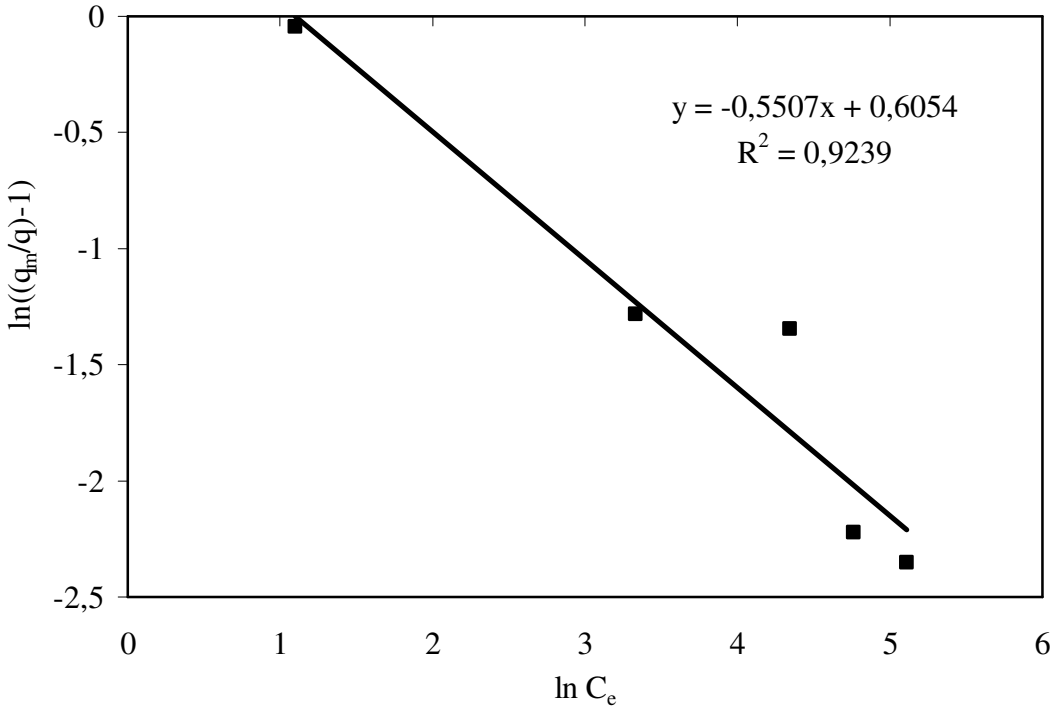

Figure 3.47. Generalized biosorption isotherm plot of ln((q_m/q))-1) versus ln C_e

3.4.2 Variable of PWS Concentrations

PWS concentrations of 0,25, 0,5, 1, 1,5, 2, 2,5 and 3 g l^{-1} were used along with the initial zinc ion concentration of 200 mg l^{-1}. Initial pH was set to 5; reaction time was 24 h and a mixing speed of 150 rpm was used.

The equilibrium distribution of zinc between the biosorbent and the solution is important in determining the maximum biosorption capacity of PWS for zinc. Figure 3.48 is a plot in the form of biosorbed zinc ions per unit mass of PWS (q_e), against the equilibrium concentration of zinc (II) ions remaining in solution (C_e). The curvature of experimental data did not fit to the theoretical predictions.

To investigate the biosorption isotherm, three equilibrium models, the Langmuir, Freundlich and the generalized isotherm equations were used. Langmuir isotherm in form of $1/q_e$ versus $1/C_e$ is shown in Figure 3.49. The Freundlich isotherm was used to correlate the experimental data as shown in Figure 3.40 which depicts a plot of ln q versus ln C for zinc ion biosorption. The isotherm constants were determined from the slope and intercept of the line. A plot of the equilibrium data in form of $\ln((q_m / q) -1)$ versus ln C_e is depicted in Figure 3.41 for the generalized isotherm. The q_m value was taken as q_m = 86,2 mg g^{-1} as determined from the Langmuir isotherm.

None of the adsorption isotherms was suitable for this set of experiments with different PWS concentrations. The generalized isotherm constant (n) was found to be negative indicating non-cooperative binding of zinc ions onto PWS surfaces. The correlation coefficients were very low and experimental data did not fit to the isotherm equations. Table 3.2 summarizes the results of the isotherm constants for the three different equilibrium isotherms tested. The results indicated that the isotherm constants should be determined by using variable zinc ion experiments but not the variable adsorbent (PWS) experiments.

Table 3.1. Summary of the isotherm constants and the correlation coefficients for different isotherms.

Parameter	Langmuir Isotherm	Freundlich Isotherm	Generalized Isotherm
q_m (mg g^{-1})	86,2		86,2
K (mg l^{-1})	29,16	5,4	2,97 10^{-6}
n		7,4	-2,51
R^2	0,182	0,332	0,293

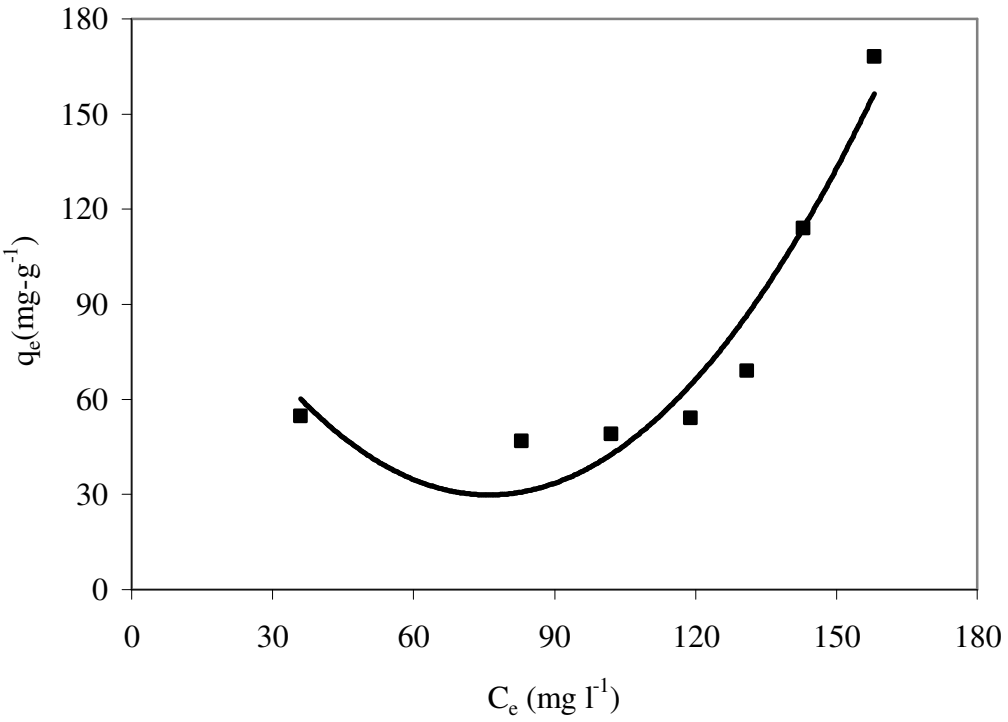

Figure 3.48. Variation of equilibrium solid phase (biosorbed) zinc ion concentration with liquid phase zinc ion concentration at different PWS concentrations

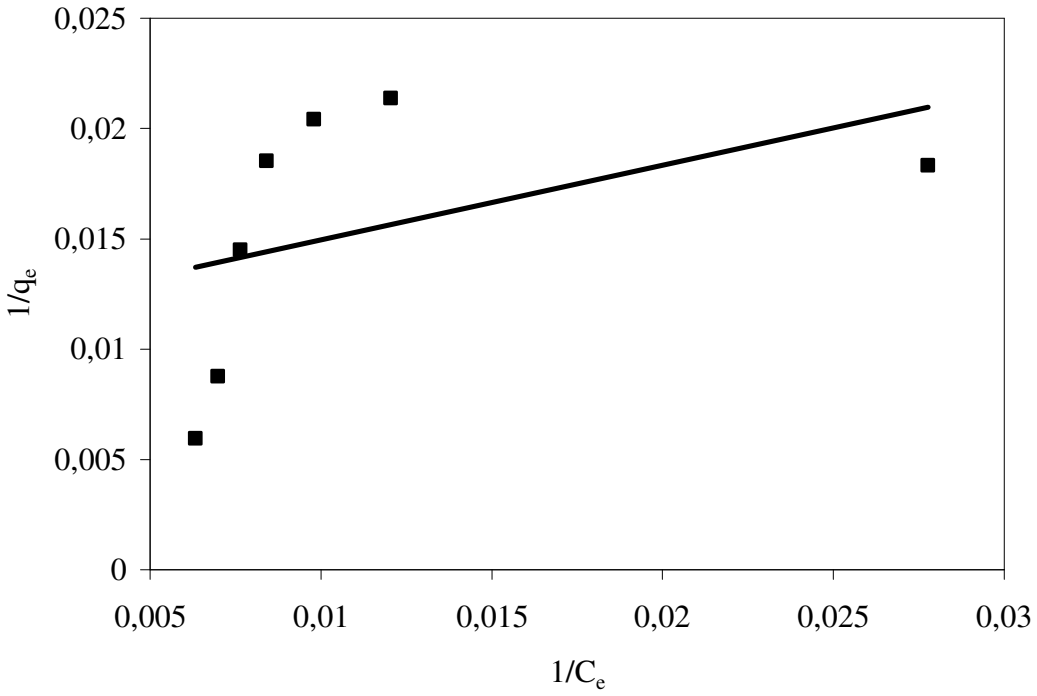

Figure 3.49. Langmuir isotherm plot of $1/q_e$ versus $1/C_e$ for biosorption of zinc ions onto pre-treated PWS at different PWS concwntrations. D_p = 64 µm

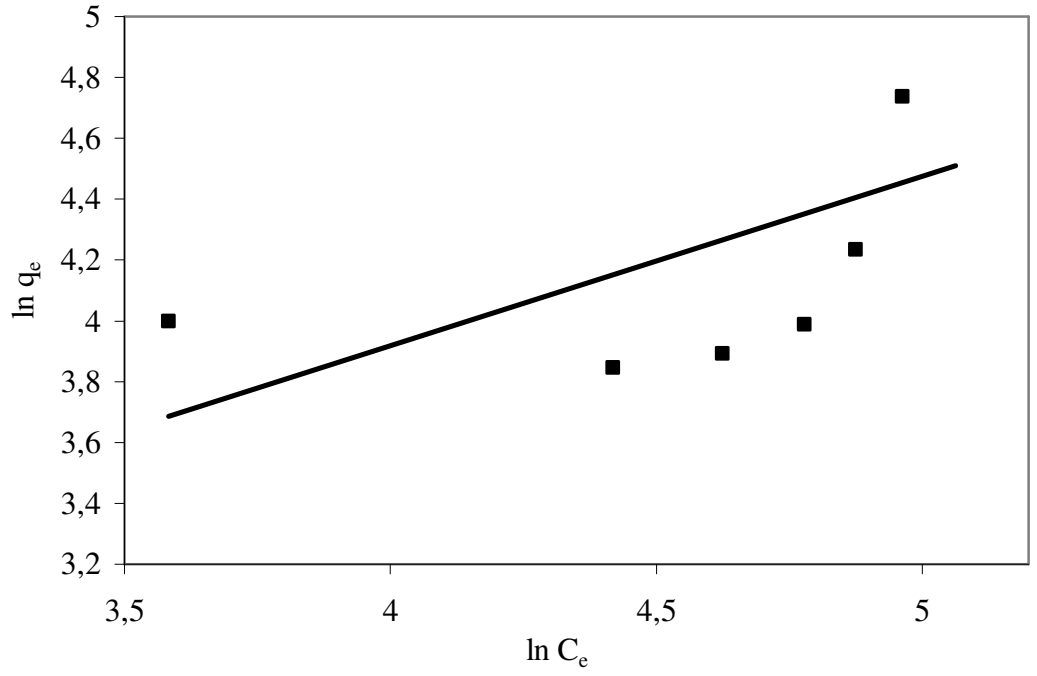

Figure 3.50. Freundlich isotherm plot of ln q_e versus ln C_e for biosorption of zinc ions onto pre-treated PWS at different PWS concentrations. D_p = 64 µm.

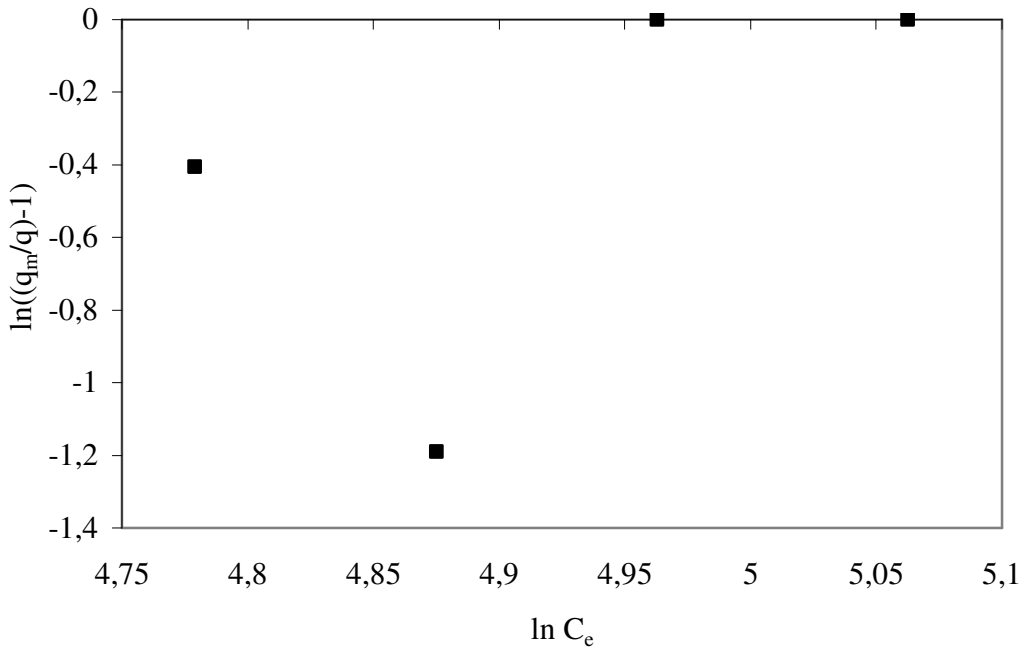

Figure 3.51. Generalized biosorption isotherm plot of $\ln((q_m/q))-1)$ versus $\ln C_e$ at different PWS concentrations.

3.5. Fed-batch Biosorption Studies

This set of experiments was used to provide an alternative to adsorption column operations. In fed-batch adsorption system the feed zinc ion solution is fed to a well mixed tank containing PWS with a constant flow rate and no effluents were removed until the tank is full. The PWS in the tank is allowed to settle for an hour or two at the end of the operation and zinc ion free solution (supernatant) was removed from the tank. The same operation may be repeated with a new PWS solution. The operation is similar to the adsorption column operation with the only advantage that the solid-liquid contact time is larger in fed-batch operation. Fed-batch adsorption contactors are more advantages than adsorption columns. Biosorbents like PWS are distributed more homogenously in the fed-batch adsorption contactor by a good mixing. Therefore, heavy metals can be adsorbed faster and more easily onto the surface of the biosorbent yielding high heavy metal removal efficiencies. In column reactors, mixing and mass transfer limitations may exist causing low biosorption performances. Well mixed fed-batch contactors eliminate mass transfer limitations in adsorption operations.

Effect of operating parameters such as flow rate and inlet zinc ion and PWS concentrations on biosorption of zinc ions were investigated in fed-batch operation. Initial pH was adjusted to 5 since the optimal pH was determined to be 5 in batch shake flask experiments. Fed-batch adsorption studies were performed using a glass tank with a diameter of 15 cm and a height of 30 cm. Initially, the adsorption tank was filled with 1 liter of pure water and desired amount of PWS was added to the tank. The tank was placed on a magnetic stirrer and mixed with a constant speed using a magnetic bar at the room temperature nearly 25 ^{0}C. A control tank containing only zinc solution with no PWS was used and zinc solution was fed to the control tank with the same flow rate as that of the experimental tank. The samples (5 ml) were withdrawn from the tank every hour and were centrifuged at 8000 rpm (7000 g) to remove solids. The clear supernatant was analyzed for zinc ion content.

3.5.1. Experiments with Different Flow Rates

In the first set of fed-batch adsorption experiments, the feed flow rate was changed from 0,05 L h^{-1} and 0,5 L h^{-1} while the inlet zinc concentration in the feed was constant at 100 mg l^{-1}. The adsorption tank was filled with 1 liter of pure water and 3 g of pretreated biosorbent (PWS) with the average particle size of 64 µm was added to the tank. Temperature and pH were nearly 25 ^{0}C (room temperature) and pH=5, throughout the experiments. The control tank was operated under the same conditions of the experimental tank in the absence of PWS. Percent zinc(II) removals in control experiments were considered to be zero and zinc(II) content of the control experiments were used as the base in calculation of zinc(II) removal efficiencies.

Variations of final zinc ion concentrations and percent zinc removals with time are depicted in Figure 3.52 for Q=0,05 L h^{-1}. Zinc ion concentration in the control tank increased with time due to accumulation of zinc ions. Zinc concentration in the control tank was 77,8 mg l^{-1} at the end of 70 hours of operation and started to reach equilibrium. Final Zn^{2+} concentration in the experimental tank was 36,3 mg l^{-1} at the end of 70 hours. Percent zinc ion removal decreased from 100% at the beginning of

the operation to 63,7% at the end of 70 hours fed-batch operation. The reason of this decrease was the saturation of limited number of active sites on the PWS surfaces.

Variation of solid phase zinc ion concentration (q_e, mg Zn $gPWS^{-1}$) with time is depicted in Figure 3.53. As expected the equilibrium solid phase zinc ion concentration increased with time. Equilibrium solid phase zinc ion concentration was 62 mg g^{-1} at the end of 70 hours. Solid phase zinc ion concentration increased rapidly at the beginning of the biosorption, and slowed down later on. No zinc ion removal was observed in the control tank.

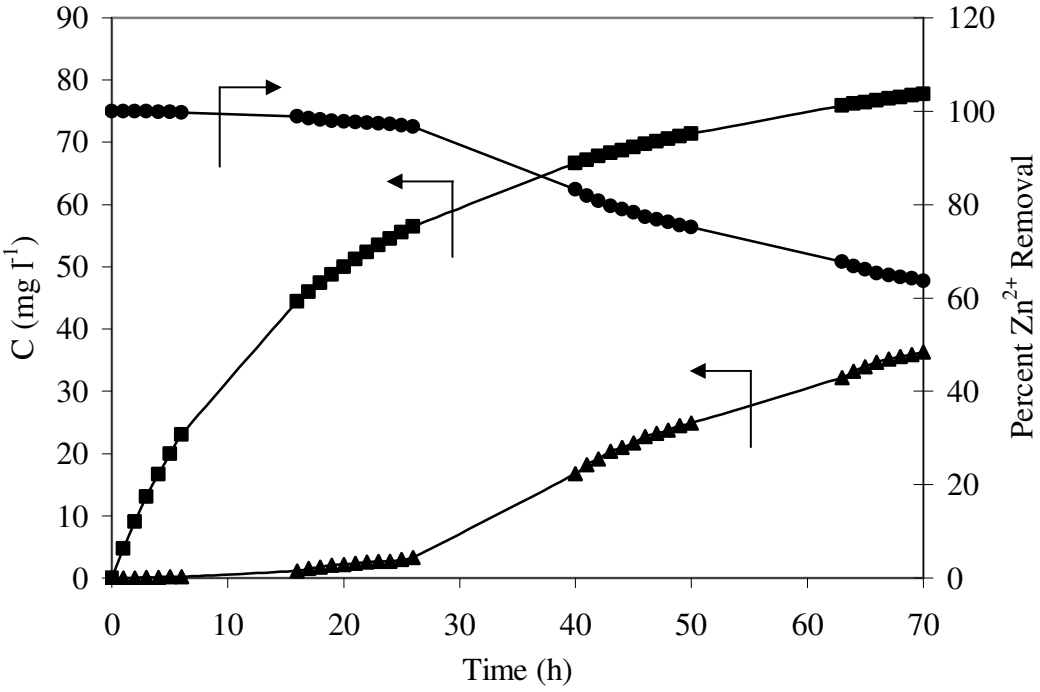

Figure 3.52 Variation of final zinc concentration and percent Zn^{2+} removal with time for Q=0,05 L h^{-1}
▲ Final Zn^{2+} concentration (mg l^{-1}), ● Percent Zn^{2+} removal , ■ Control Zn^{2+} concentration

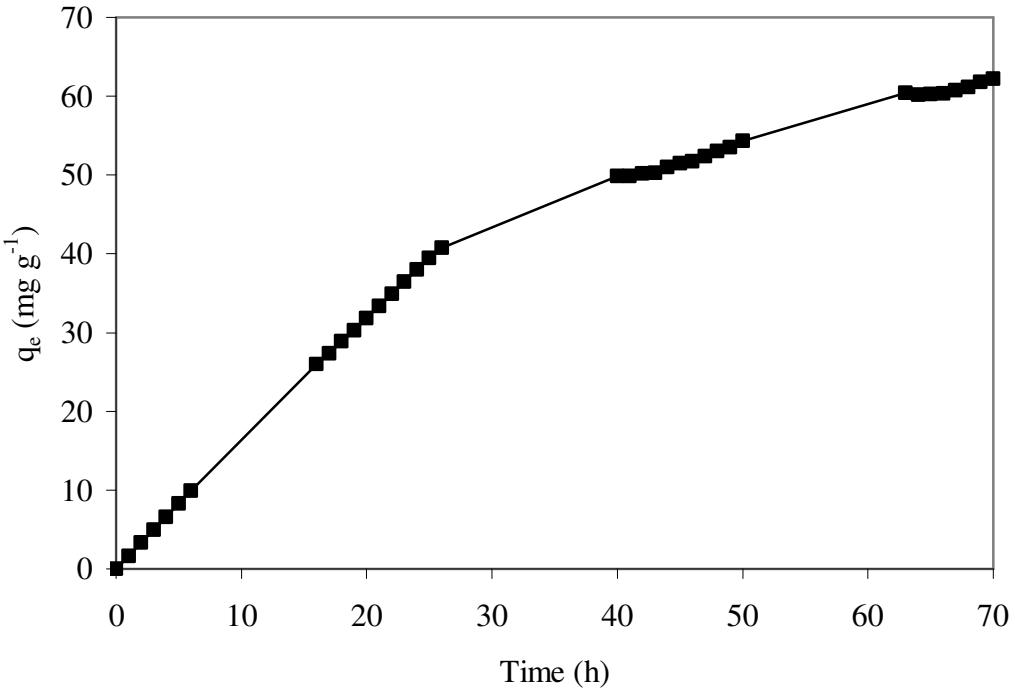

Figure 3.53 Variation of solid phase zinc ion concentration (q, mg Zn $gPWS^{-1}$) with time in a fed-batch experiment with Q=0,05 L h^{-1}

Figure 3.54 depicts variations of percent Zn^{2+} removal and the final zinc ion concentrations with time for Q=0,1 L h^{-1}. Final zinc ion concentration in the control tank increased with time due to the accumulation of zinc ions without any removal by biosorption. The time needed to reach equilibrium was 34 hours. Percent zinc ion removal decreased from 100% to 63,6% and the final Zn^{2+} concentration increased to 36,4 mg l^{-1} at the end of the 34 hours when the initial Zn^{2+} concentration was 100 mg l^{-1}.

Figure 3.55 depicts variation of solid phase (biosorbed) zinc ion concentrations with time for Q=0,1 L h^{-1}. Biosorbed Zn^{2+} concentration increased with time and equilibrium was reached after 34 hours of fed-batch operation. At the end of 1 hour fed-batch operation, biosorbed Zn^{2+} concentration was 3,6 mg g^{-1} which increased to 60 mg g^{-1} at the end of 34 hours.

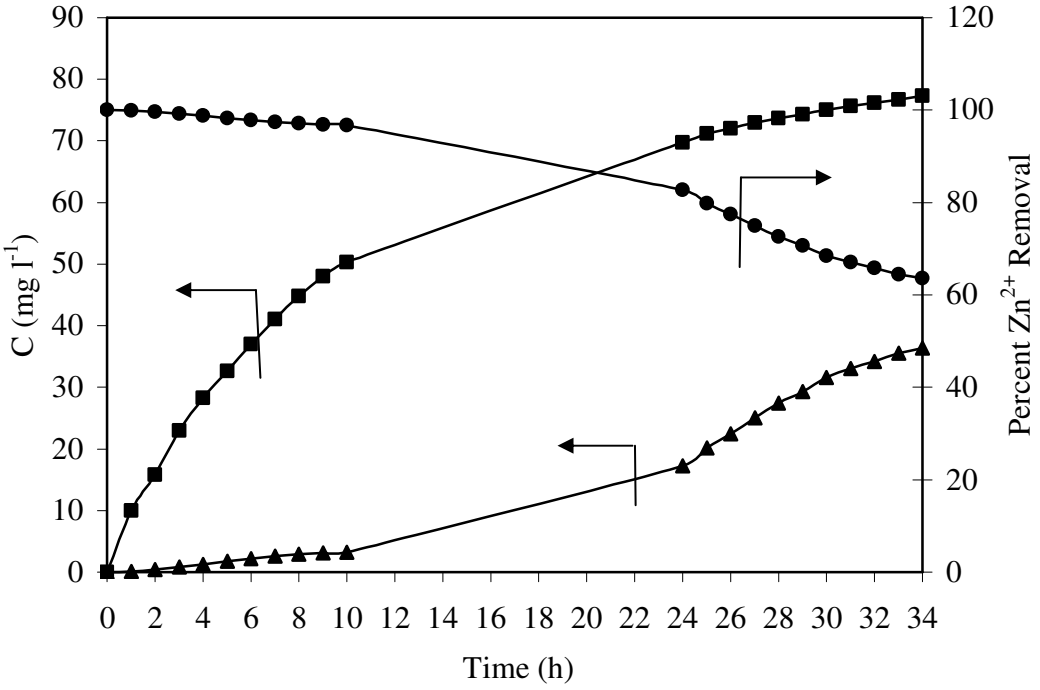

Figure 3.54 Variation of final zinc concentration and percent Zn^{2+} removal with time for Q=0,1 L h^{-1}
▲ Final Zn^{2+} concentration (mg l^{-1}), ● Percent Zn^{2+} removal , ■ Control Zn^{2+} concentration

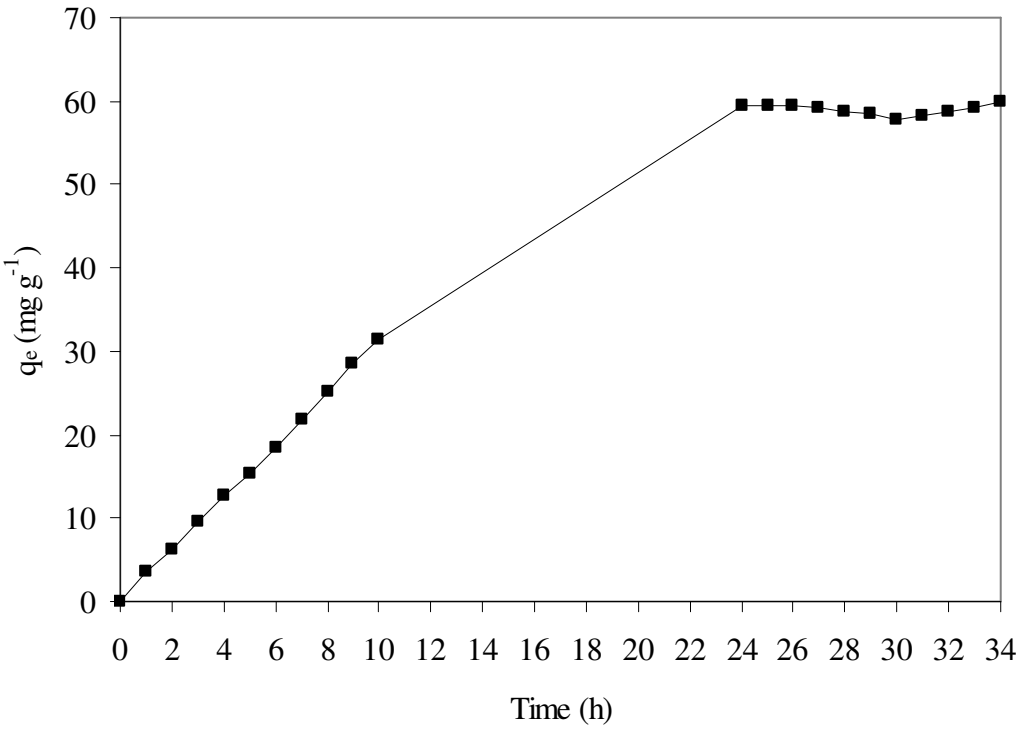

Figure 3.55 Variation of solid phase Zn^{2+} concentration (q, mg Zn $gPWS^{-1}$) with time in a fed-batch experiment with Q=0,1 L h^{-1}

Variations of percent Zn^{2+} removal and the final zinc ion concentrations with time for Q=0,2 L h^{-1} are depicted in Figure 3.56. Zinc(II) concentration in the control tank increased with time due to accumulation of zinc(II) in the absence of PWS. Final zinc ion concentration in the adsorption tank was nearly 36 mg l^{-1} at the end of 21 hours as compared to 82 mg l^{-1} in the control tank. Percent Zn^{2+} removal decreased from 99,7 % at the beginning to 63,7% at the end 21 hours.

In Figure 3.57, variation of solid phase (biosorbed) zinc ion concentrations with time for Q=0,2 L h^{-1} is presented. Biosorbed zinc concentration increased rapidly within seven hours and rose slowly for the last 5 hours of fed-batch operation. The highest biosorbed zinc concentration was 77 mg g^{-1} at the end of 21 hours. No zinc ion removal was observed in the control tank.

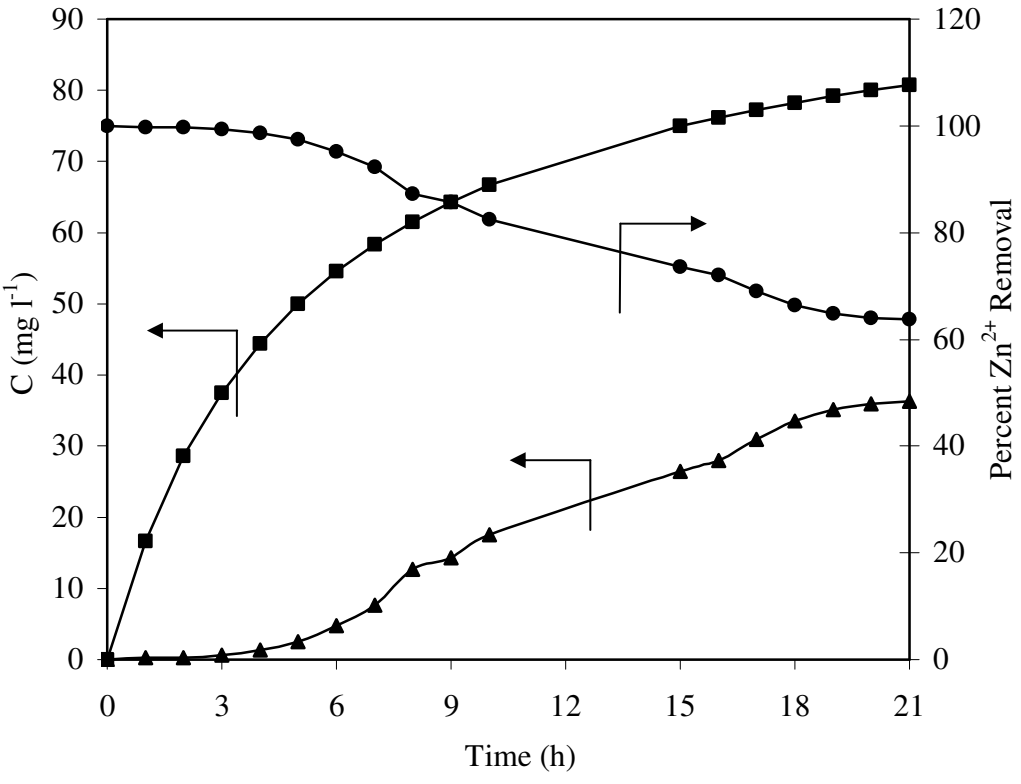

Figure 3.56 Variation of final zinc concentration and percent Zn^{2+} removal with time for Q=0,2 L h^{-1}
▲ Final Zn^{2+} concentration (mg l^{-1}), ● Percent Zn^{2+} removal , ■ Control Zn^{2+} concentration

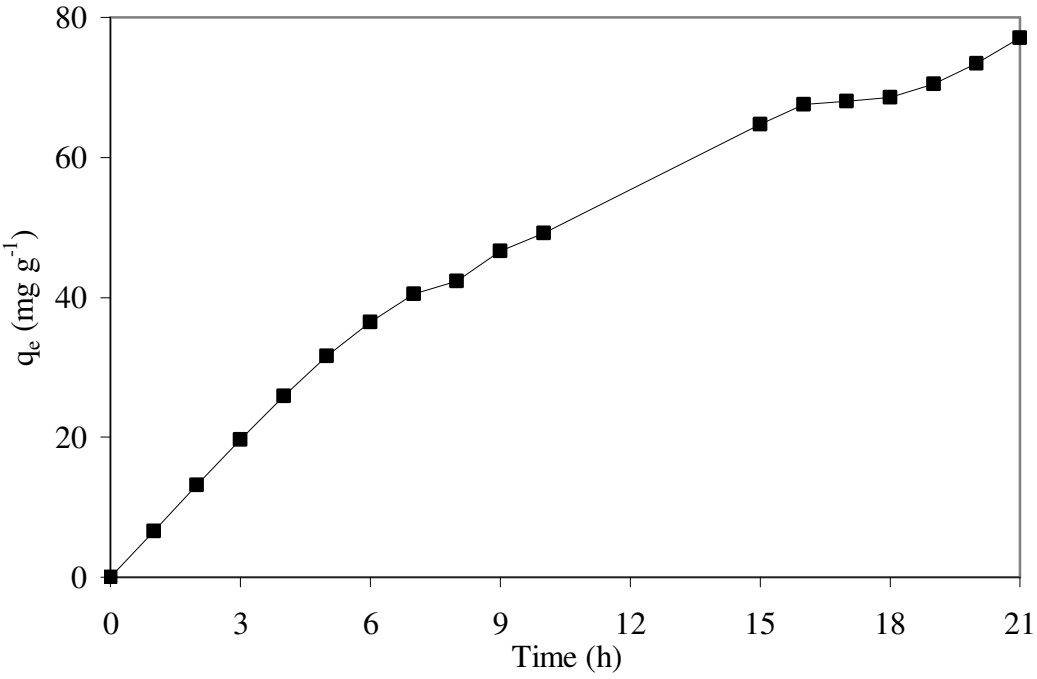

Figure 3.57 Variation of solid phase Zn^{2+} concentration (q, mg Zn $gPWS^{-1}$) with time in a fed-batch experiment with Q=0,2 L h^{-1}

Figure 3.58 depicts variations of percent zinc removal and the final zinc ion concentrations with time for Q=0,3 L h^{-1}. Percent zinc ion removal decreased from 96,4% to 67% and the final Zn^{2+} concentration increased from 3,7 mg l^{-1} to 33 mg l^{-1} at the end of 3 and 15 hours due to the limited binding sites on the surfaces of the PWS. No adsorption was observed in the control tank and the final zinc ion concentration increased with time reaching 82 mg l^{-1} at the end of 15 hours of fed-batch operation.

Variation of solid phase Zn^{2+} concentration (q, mg Zn $gPWS^{-1}$) with time is depicted in Figure 3.59. Biosorbed zinc concentration increased with time and reached 89 mg g^{-1} at the end of 15 hours.

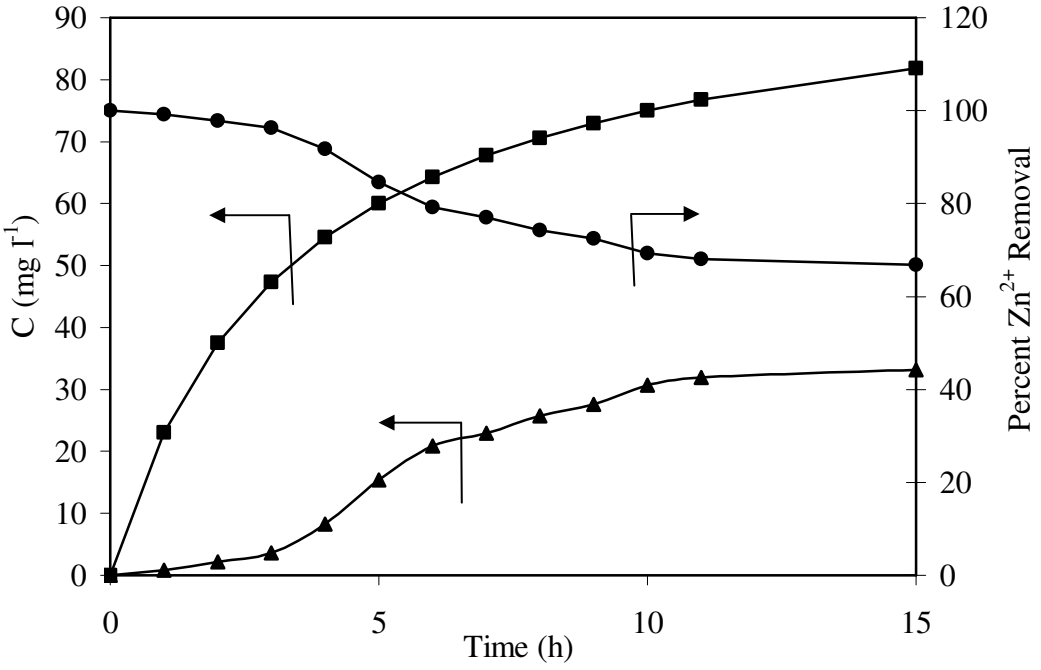

Figure 3.58 Variation of final zinc concentration and percent Zn^{2+} removal with time for Q=0,3 L h^{-1}
▲ Final Zn^{2+} concentration (mg l^{-1}), ● Percent Zn^{2+} removal , ■ Control Zn^{2+} concentration

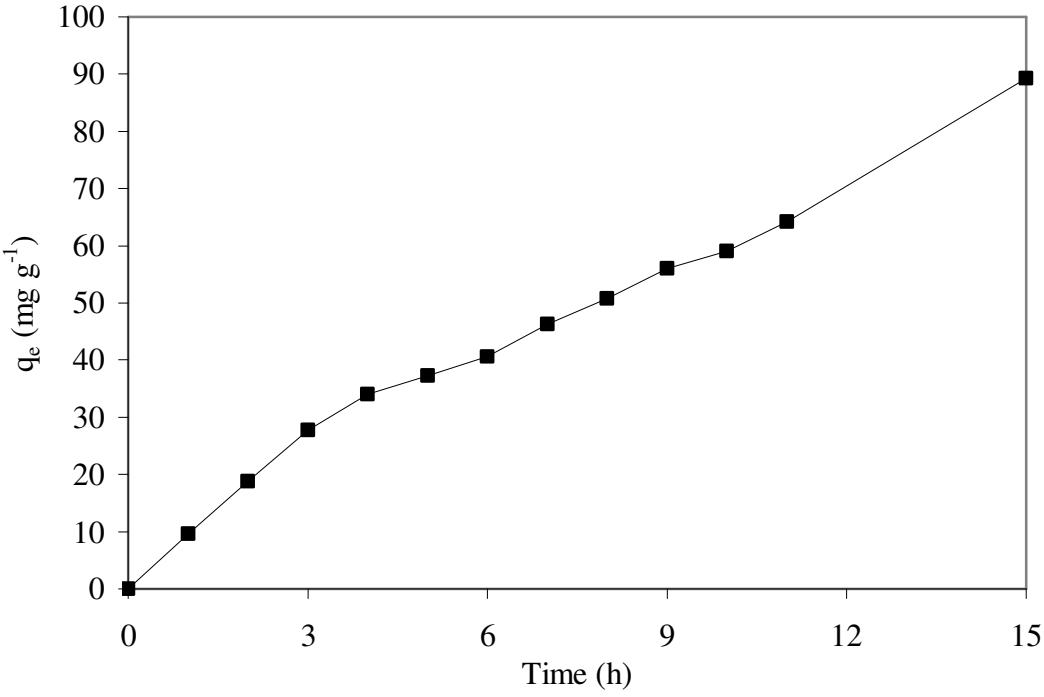

Figure 3.59 Variation of solid phase Zn^{2+} concentration (q, mg Zn $gPWS^{-1}$) with time in a fed-batch operation with Q=0,3 L h^{-1}

When feed flow rate was raised to 0,4 l h^{-1}, 0,5 liter pure water containing 3 g of PWS was used in the tank instead of 0,5 liter initial solution to allow more time for biosorption. Figure 3.60 depicts variations of percent Zn^{2+} removal and the final zinc ion concentrations with time for Q=0,4 L h^{-1}. The system reached equilibrium within 10 hours and percent Zn^{2+} removal decreased to 68,6% at the end of 10 hours from nearly 100% at the beginning. Zinc ion concentrations were 13,6 mg l^{-1} and 31,5 mg l^{-1} at the end of 4 and 10 hours. Final zinc ion concentrations increased to 89 mg l^{-1} at the end of 10 hours in the control tank.

In Figure 3.61, variation of solid phase (biosorbed) zinc ion concentrations with time is presented for Q=0,4 L h^{-1}. Biosorbed zinc ion concentration in the solid phase reached 13,2 mg g^{-1} within one hour and then increased to 86 mg g^{-1} at the end of 10 hours.

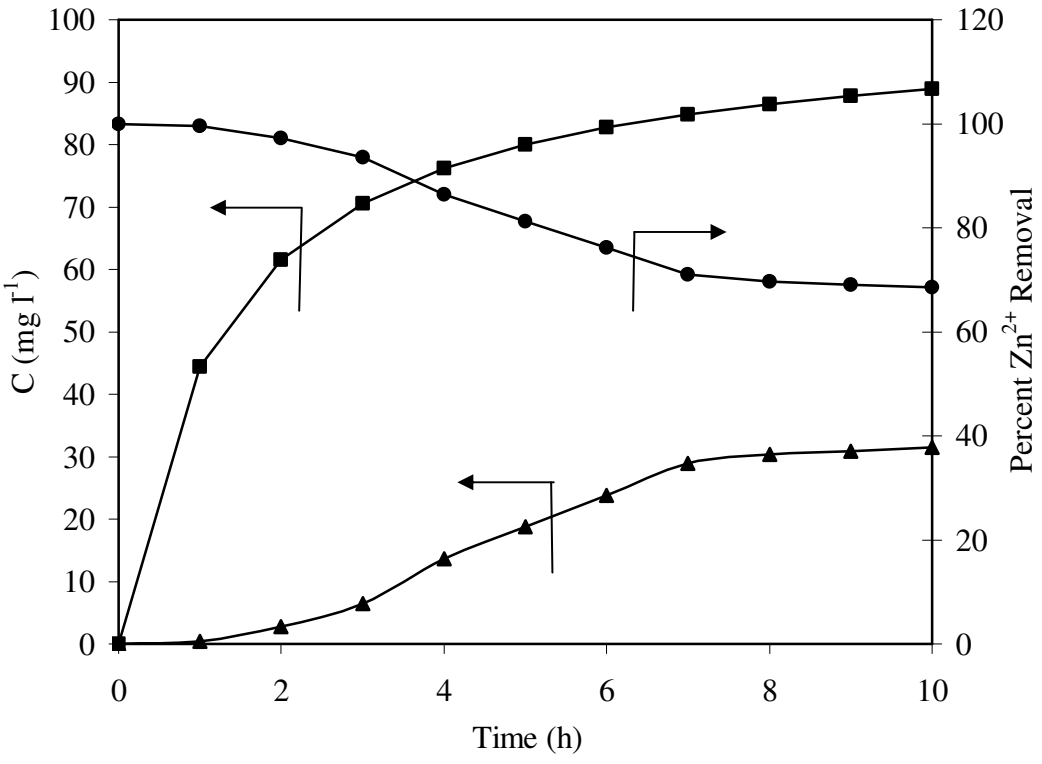

Figure 3.60 Variation of final zinc concentration and percent Zn^{2+} removal with time for Q=0,4 L h^{-1}

▲ Final Zn^{2+} concentration (mg l^{-1}), ● Percent Zn^{2+} removal , ■ Control Zn^{2+} concentration

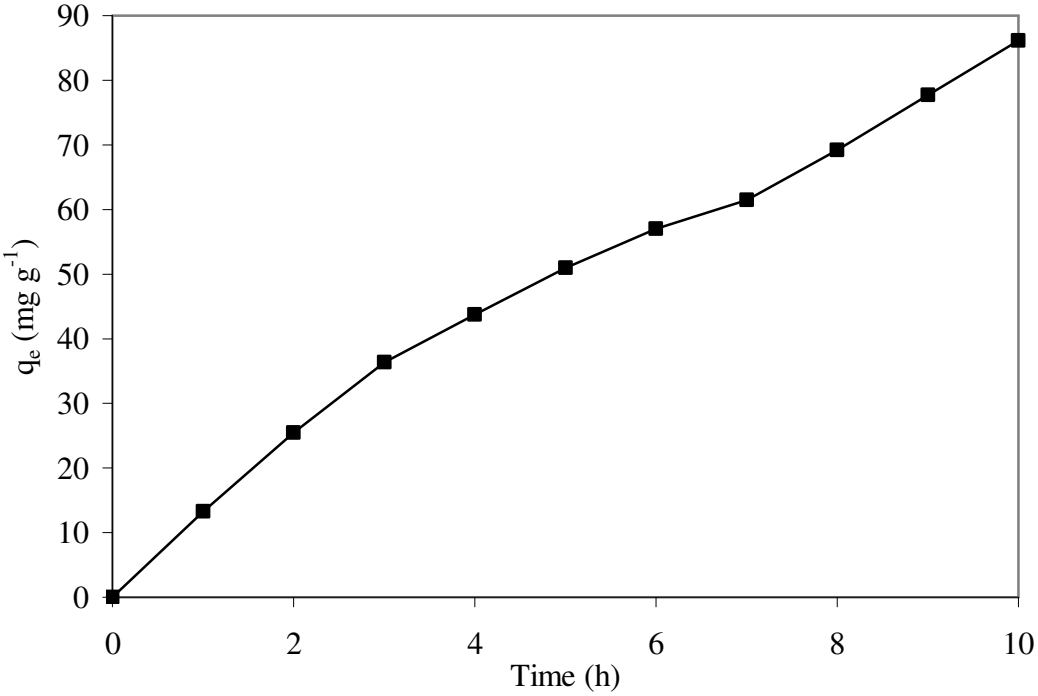

Figure 3.61 Variation of solid phase Zn^{2+} concentration (q, mg Zn $gPWS^{-1}$) with time for Q=0,4 L h^{-1}

Figure 3.62 depicts variations of percent zinc removal and the final zinc concentrations with time for Q=0,5 L h^{-1} (Vo = 0,5 L, PWSo = 3 g). Final zinc concentrations increased with time for both tanks. As can be seen from Figure 3.62, zinc ion removal from solution was almost completed within 6 hours; however the system was operated for 10 hours to reach equilibrium. Final zinc concentrations increased to 91 mg l^{-1} in the control tank and 31 mg l^{-1} in the adsorption tank at the end of 10 hours. Percent zinc removal decreased from 97,5% to 69 % at the end of 2 and 10 hours.

In figure 3.63, variation of solid phase (biosorbed) zinc ion concentrations with time is presented for Q=0,5 L h^{-1}. Biosorbed zinc ion concentration increased with time and reaching to 16,3 mg g^{-1} within one hour and to 110 mg g^{-1} at the end of 10 hours.

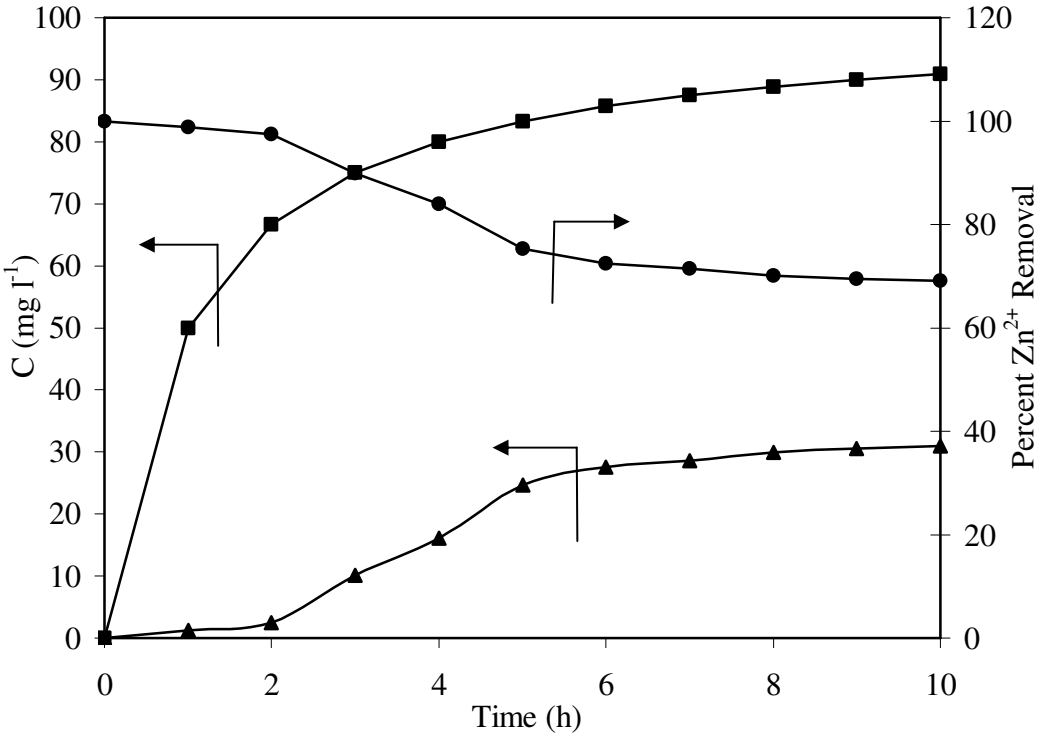

Figure 3.62 Variation of final zinc concentration and percent Zn^{2+} removal with time for Q=0,5 L h^{-1}

▲ Final Zn^{2+} concentration (mg l^{-1}), ● Percent Zn^{2+} removal , ■ Control Zn^{2+} concentration

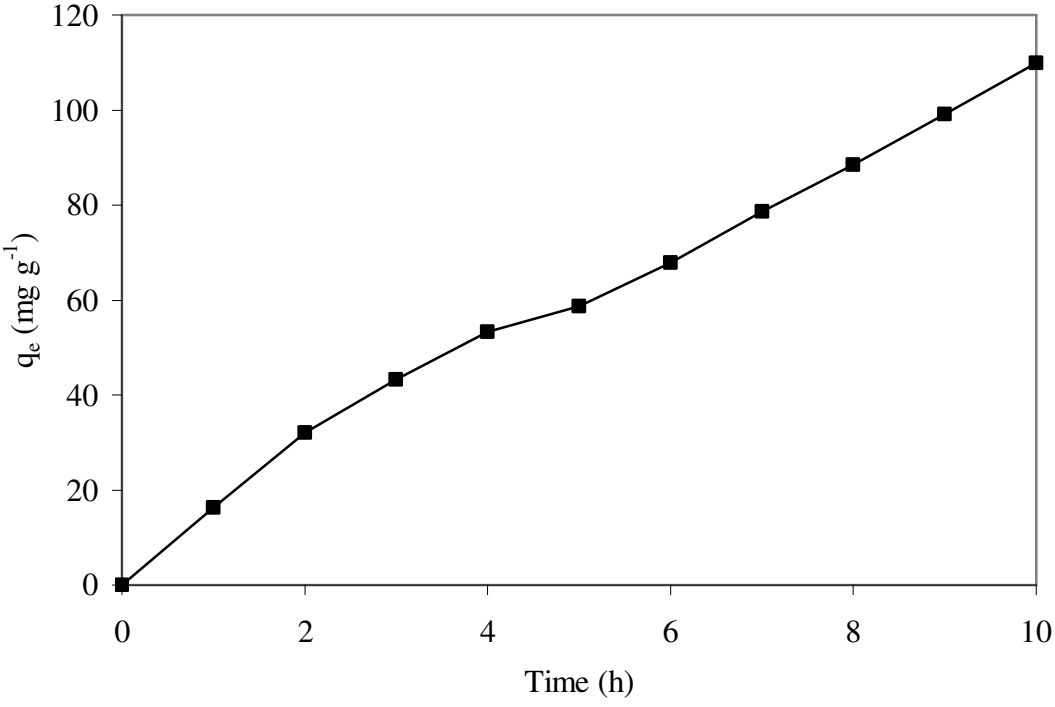

Figure 3.63 Variation of solid phase Zn^{2+} concentration (q, mg Zn $gPWS^{-1}$) with time for Q=0,5 L h^{-1}

Final percent Zn^{2+} removal increased a little with increasing flow rate and maximum value was obtained at 0,5 L h^{-1}. Final percent Zn^{2+} removal increased from 63,7% to 69% when the flow rate was increased from 0,05 L h^{-1} to 0,5 L h^{-1}. And also, biosorbed zinc concentration increased from 62 to 110 mg g^{-1} when the flow rate increased from 0,05 L h^{-1} to 0,5 L h^{-1}.

As may be seen from the figures, the lowest flow rate gave a more gentle breakthrough curve. Breakthrough curves became steeper and breakpoint time decreased with increasing flow rate. For all flow rate studies, after the breakpoint, zinc removal was maintained approximately constant zinc uptake was observed. Zinc adsorption reached saturation within 5-50 hours at different flow rates between 0,05 L h^{-1} and 0,5 L h^{-1}. At the lowest flow rate of 0,05 L h^{-1}, relatively higher zinc uptake values were observed by PWS at the beginning of fed-batch adsorption operation. This behavior can be explained by the fact that zinc biosorption by PWS was adversely affected by limited number of active sites when the flow rate was high. However, equilibrium percent zinc removal increased a little with increasing flow rate.

3.5.2. Experiments with Different Zn(II) Concentrations

In the second set of fed-batch adsorption studies, the flow rate was kept constant at 0,2 L h^{-1} and the system was operated by changing the feed zinc ion concentrations from 37,5 to 275 mg l^{-1}. The adsorption tank was filled with 1 liter of pure water and 3 g of pretreated biosorbent (PWS) with the average particle size of 64 µm was added to the tank. Temperature and pH were 25°C (room temperature) and pH=5, throughout the experiments. Control experiments were carried out under the same conditions in the absence of PWS. The samples (5 ml) withdrawn from the control and adsorption tanks every hour were centrifuged at 8000 rpm (7000 g) to remove solids. The clear supernatants were analyzed for zinc ion contents using an Atomic Absorption Spectrometer (ATI Unicam 929 AA Spectrometer) at 213,9 nm wavelength. Percent zinc(II) removals in control experiments were considered to be

zero and zinc(II) content of the control tanks were used as the base in calculation of zinc(II) removal efficiencies.

Variations of percent zinc removal and the final zinc ion concentrations with time are shown in Figure 3.64 for 37,5 mg l^{-1} feed zinc ion concentration. Zinc(II) ion concentration in the adsorption tank increased while percent zinc removal decreased with time. Final zinc concentrations in the control tank reached higher levels than the adsorption tank because of no zinc uptake in the control tank. The system operated for 20 hours and final zinc ion concentrations were determined to be 30 mg l^{-1} and 11 mg l^{-1} in the control and the experimental tanks respectively. Percent zinc removals were 99,9% and 70,7% at the end of 1 and 20 hours, respectively.

Variation of solid phase Zn^{2+} concentration (q, mg Zn $gPWS^{-1}$) with time is depicted in Figure 3.65 for a feed zinc concentration of 37,5 mg l^{-1}. Solid phase zinc ion concentration increased with time. Biosorbed zinc ion concentration was 32 mg g^{-1} at the end of 20 hours.

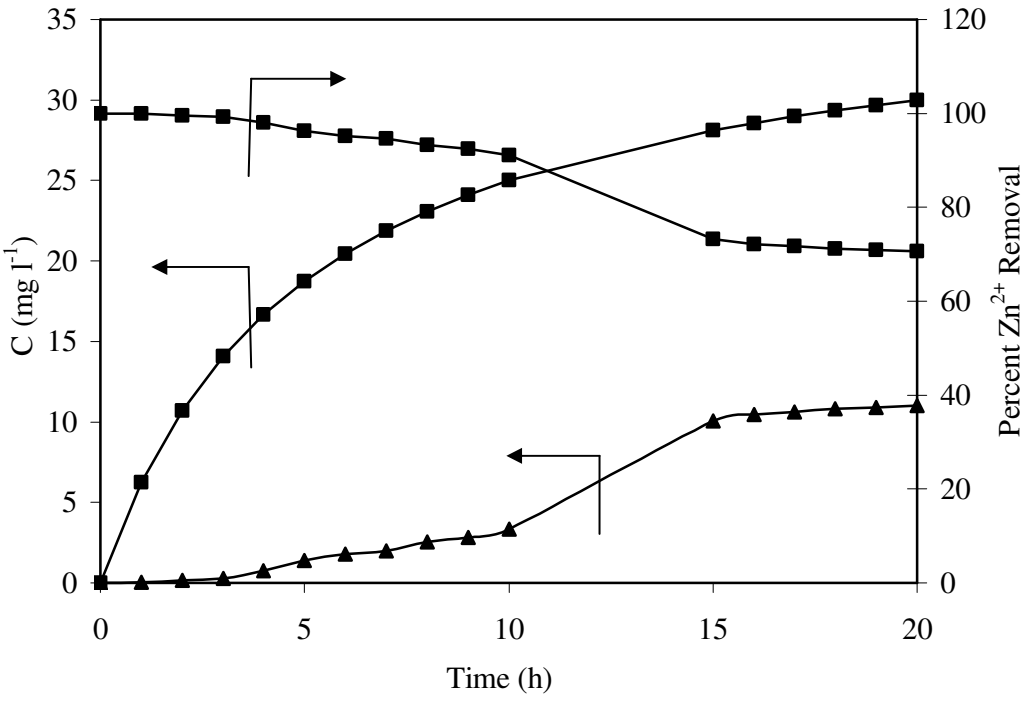

Figure 3.64 Variation of final zinc concentration and percent Zn^{2+} removal with time for 37,5 mg l^{-1} feed zinc concentration. ▲ Final Zn^{2+} concentration (mg l^{-1}), ● Percent Zn^{2+} removal, ■ Control Zn^{2+} concentration

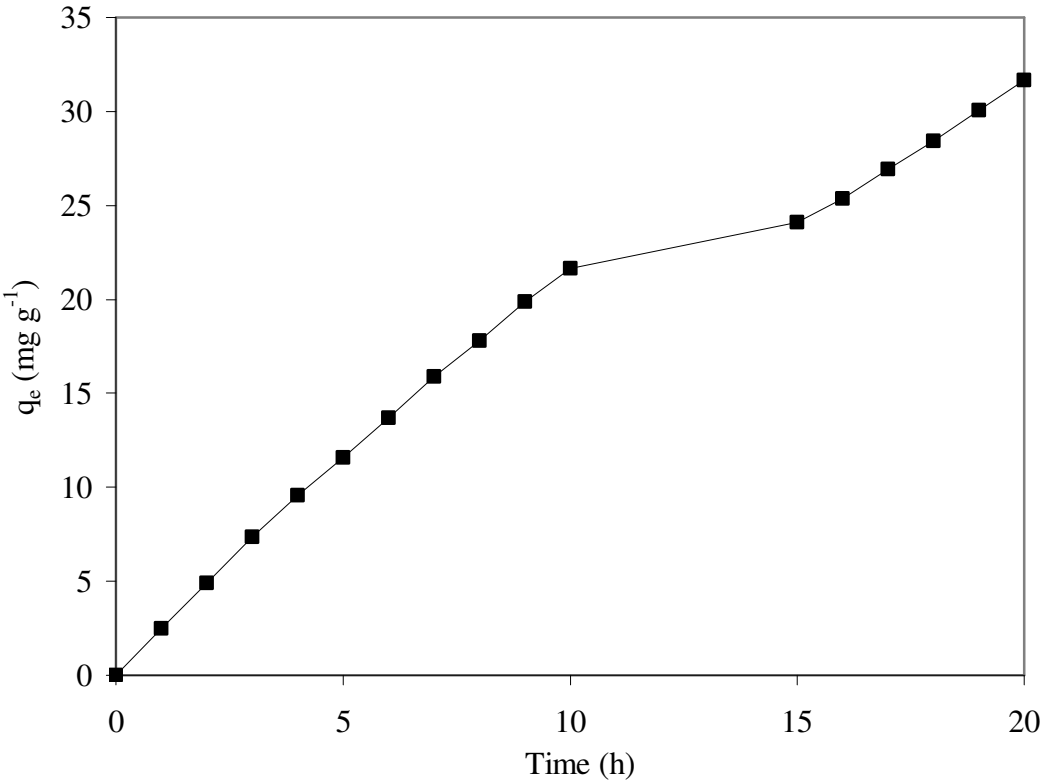

Figure 3.65 Variation of solid phase Zn^{2+} concentration (q, mg Zn $gPWS^{-1}$) with time for 37,5 mg l^{-1} feed zinc concentration

Figure 3.66 depicts variations of percent zinc removal and the final zinc ion concentrations with time for 75 mg l^{-1} feed zinc concentration. Percent zinc removal decreased from 99% to 62% and the final Zn^{2+} concentration increased from 0,459 mg l^{-1} to 28,7 mg l^{-1} at the end of 1 and 20 hours. The percent of zinc removal decreased from nearly 100% at the beginning to only 62% because of low feed zinc concentration. Zinc concentration in the control tank increased with time and reached to 60 mg l^{-1} at the end of 20 hours.

Variation of solid phase Zn^{2+} concentration (q, mg Zn $gPWS^{-1}$) with time is depicted in Figure 3.67. Solid phase zinc ion concentration increased with time and reached to 52 mg g^{-1} at the end of 20 hours.

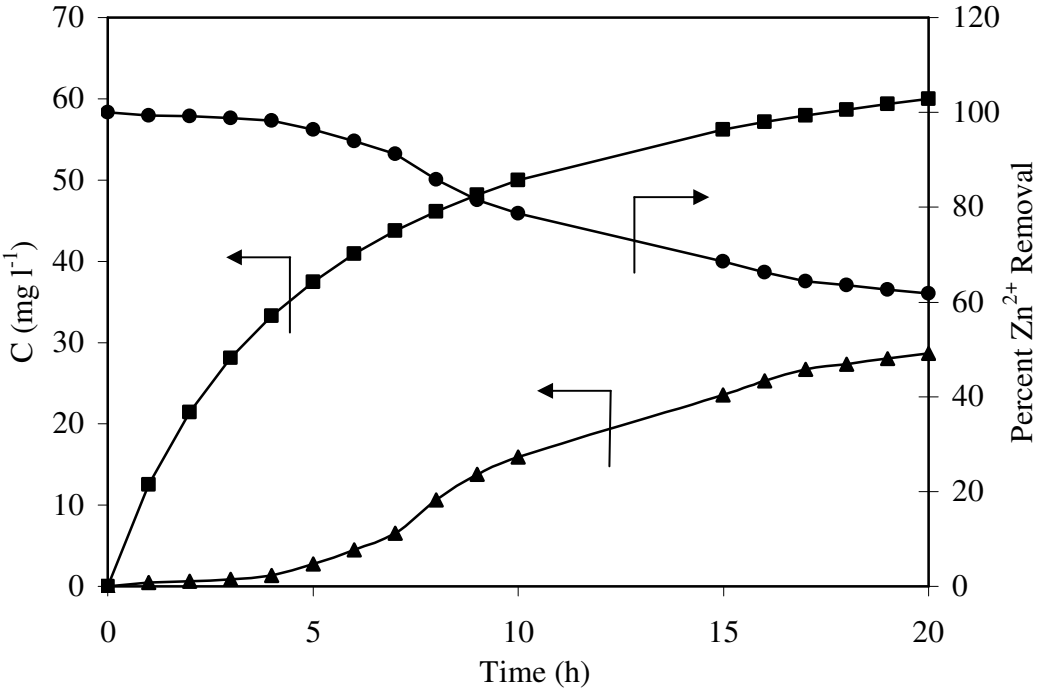

Figure 3.66 Variation of final zinc concentration and percent Zn^{2+} removal with time for 75 mg l^{-1} zinc concentration. ▲ Final Zn^{2+} concentration (mg l^{-1}), ● Percent Zn^{2+} removal, ■ Control Zn^{2+} concentration

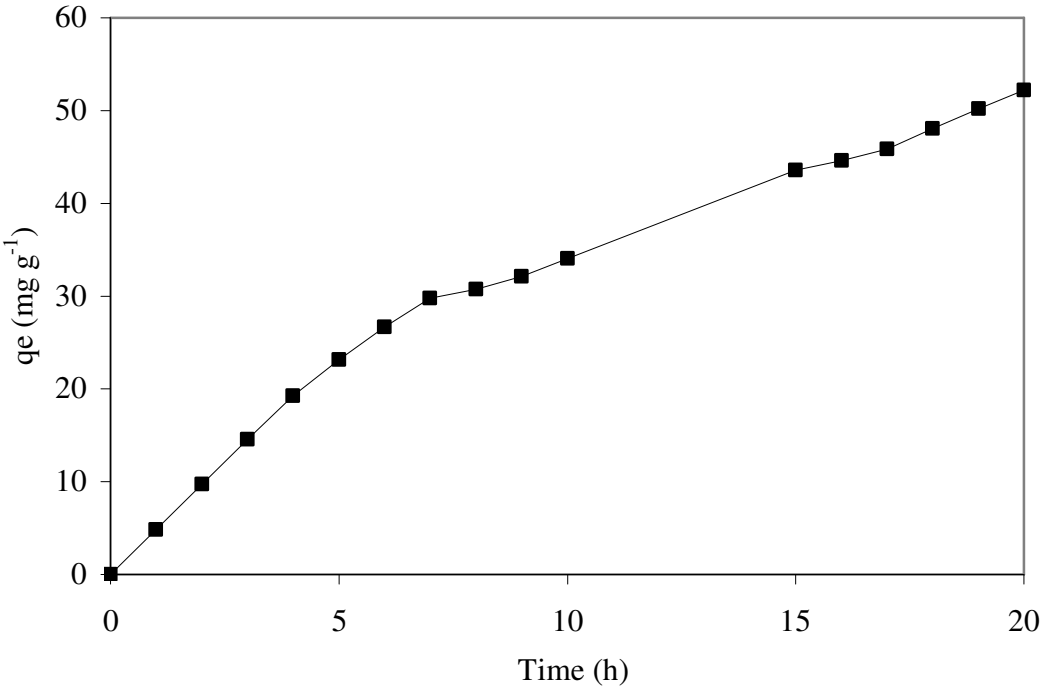

Figure 3.67 Variation of solid phase Zn^{2+} concentration (q, mg Zn $gPWS^{-1}$) with time for 75 mg l^{-1} feed zinc concentration.

Figure 3.68 depicts variations of percent Zn^{2+} removal and the final zinc ion concentrations with time for 125 mg l^{-1} feed zinc ion concentration. Final zinc ion concentration in the control tank increased with time due to the accumulation of zinc ions. The time needed to reach equilibrium was 20 hours. Percent zinc ion removal decreased to 58% and the final Zn^{2+} concentration increased to 52 mg l^{-1} at the end of the 20 hours when the initial Zn^{2+} concentration was 125 mg l^{-1}.

In Figure 3.69, variation of solid phase (biosorbed) zinc ion concentrations with time is presented for 125 mg l^{-1} feed zinc ion concentration. As seen from the Figure 3.69, biosorbed zinc concentration increased with time. The highest biosorbed zinc concentration was 80 mg g^{-1} at the end of 20 hours.

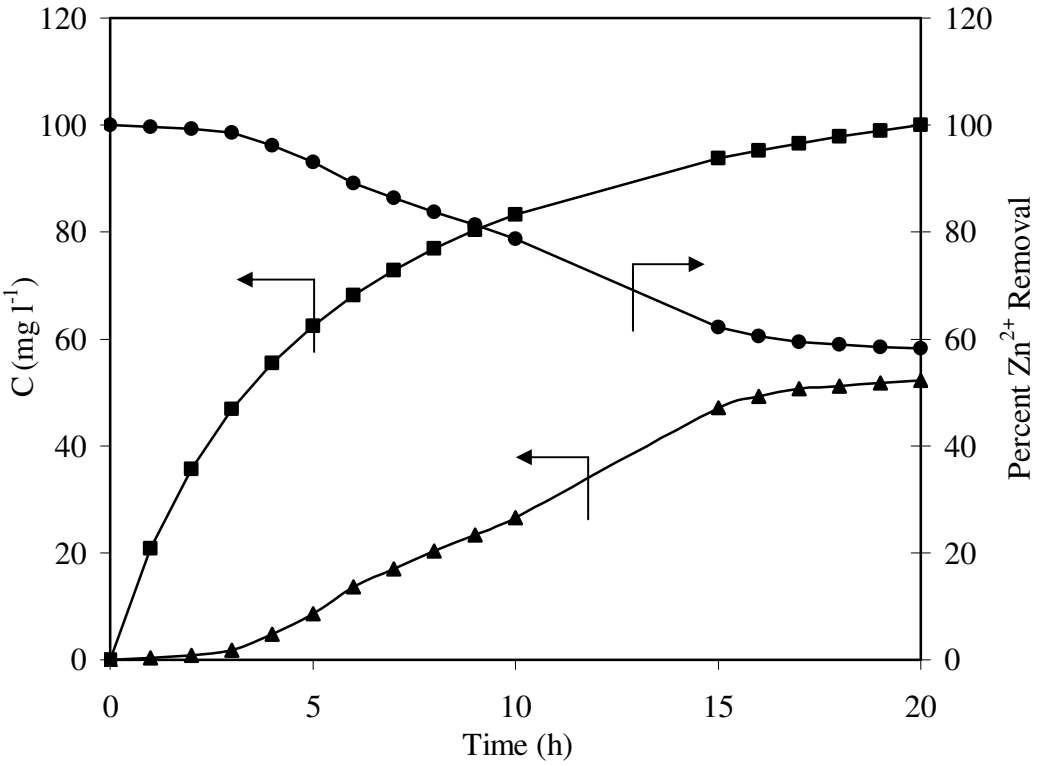

Figure 3.68 Variation of final zinc concentration and percent Zn^{2+} removal with time for 125 mg l^{-1} zinc concentration. ▲ Final Zn^{2+} concentration (mg l^{-1}), ● Percent Zn^{2+} removal, ■ Control Zn^{2+} concentration

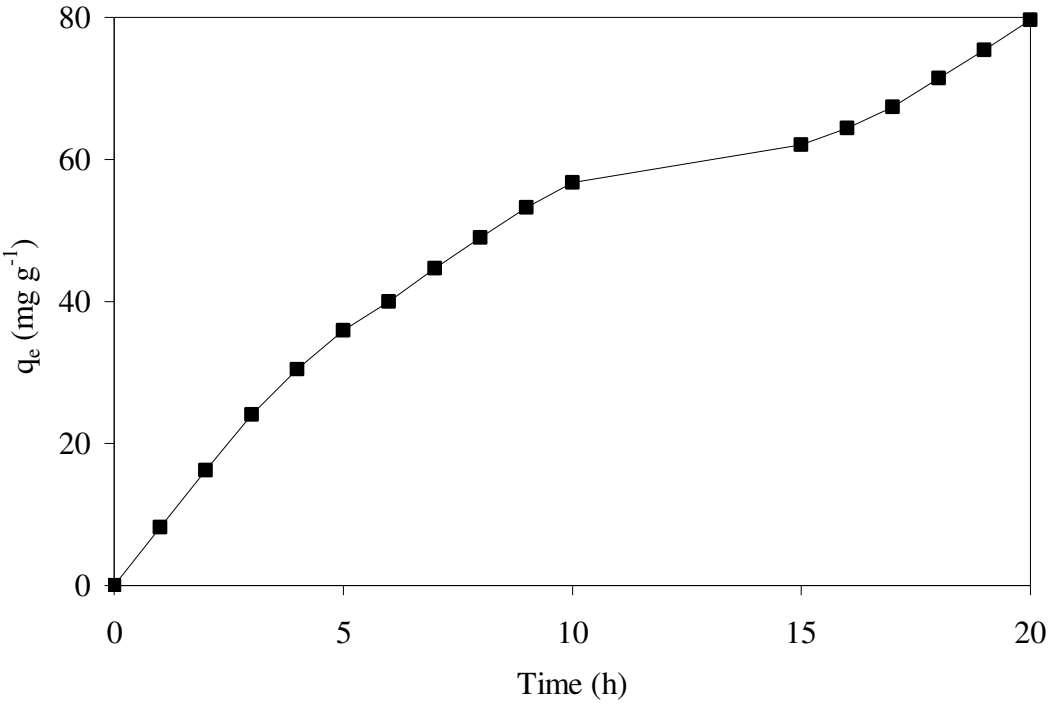

Figure 3.69 Variation of solid phase Zn^{2+} concentration (q_e, mg Zn $gPWS^{-1}$) with time for 125 mg l^{-1} feed zinc concentration

Figure 3.70 depicts variations of percent Zn^{2+} removal and the final zinc ion concentrations with time for 175 mg l^{-1} feed zinc ion concentration. Final zinc ion concentration in the control tank increased with time and no zinc adsorption was observed due to lack of adsorbent (PWS). The time needed to reach equilibrium was 20 hours in the adsorption tank. Percent zinc ion removal decreased to 48% and the final Zn^{2+} concentration increased to 91 mg l^{-1} at the end of the 20 hours when the initial Zn^{2+} concentration was 175 mg l^{-1}. The final zinc concentration in the control tank was nearly 139 mg l^{-1} at the end of 20 hours.

Figure 3.71 depicts variation of solid phase (biosorbed) zinc ion concentrations with time for 175 mg l^{-1} feed zinc ion concentration. Biosorbed Zn^{2+} concentration increased with time and reached equilibrium after 20 hours of fed-batch operation. At the end of 1 hour of operation, biosorbed Zn^{2+} concentration was 11,3 mg g^{-1} which increased to 81 mg g^{-1} at the end of 20 hours operation.

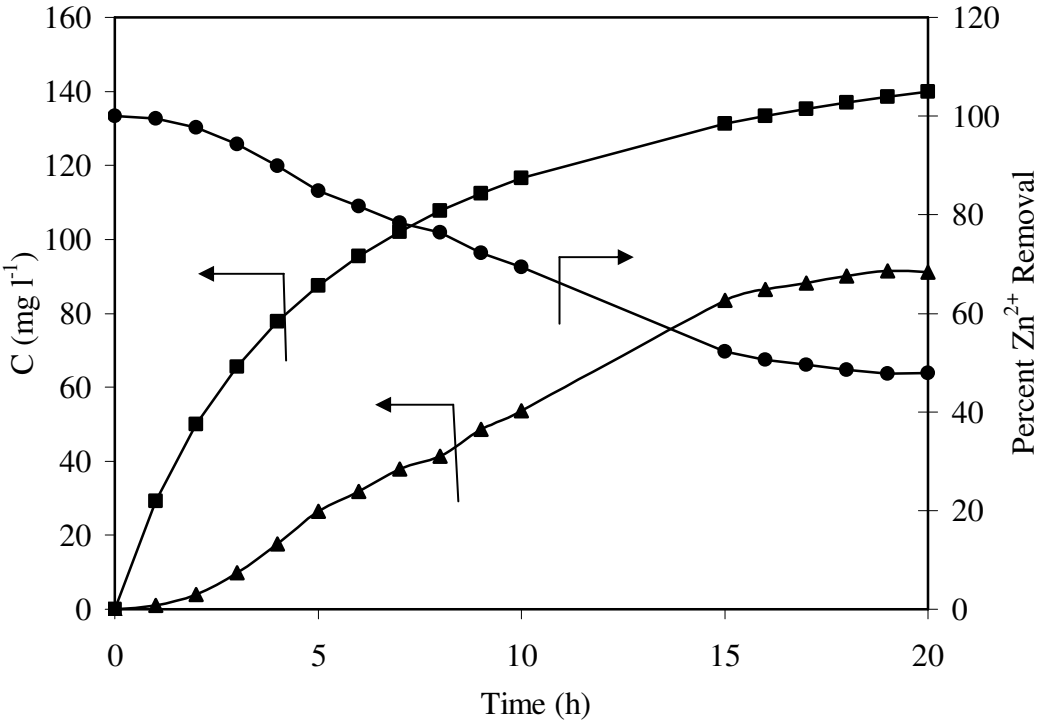

Figure 3.70 Variation of final zinc concentration and percent Zn^{2+} removal with time for 175 mg l^{-1} zinc concentration. ▲ Final Zn^{2+} concentration (mg l^{-1}), ● Percent Zn^{2+} removal, ■ Control Zn^{2+} ion

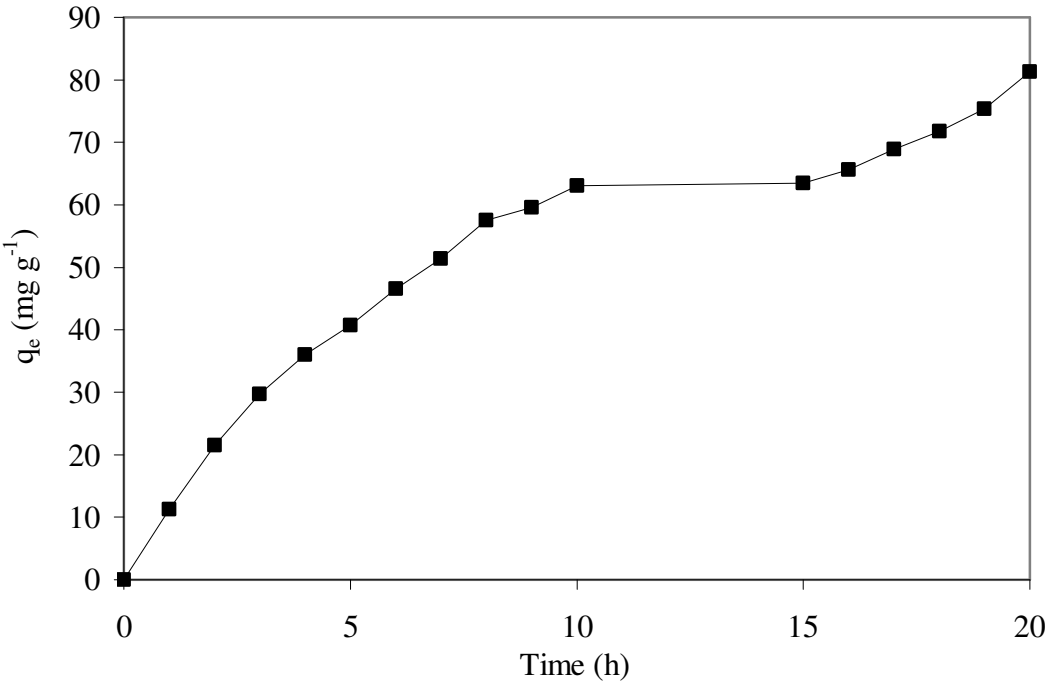

Figure 3.71 Variation of solid phase Zn^{2+} concentration (q, mg Zn $gPWS^{-1}$) with time for 175 mg l^{-1} feed zinc concentration

Figure 3.72 depicts variations of percent removal and the final zinc ion concentrations with time for 225 mg l^{-1} feed zinc ion concentration. Percent zinc ion removal decreased from 87,5% to 45% and the final Zn^{2+} concentration increased from 28 mg l^{-1} to 123 mg l^{-1} at the end of 3 and 20 hours due to the limited binding sites on the surface of the PWS and high inlet zinc concentration. No adsorption was observed in the control tank and the zinc ion concentration increased with time and reached 180 mg l^{-1} at the end of 20 hours.

Variation of solid phase Zn^{2+} concentration (q, mg Zn $gPWS^{-1}$) with time is depicted in Figure 3.73. Biosorbed zinc concentration increased with time and reached 94,5 mg g^{-1} at the end of 20 hours.

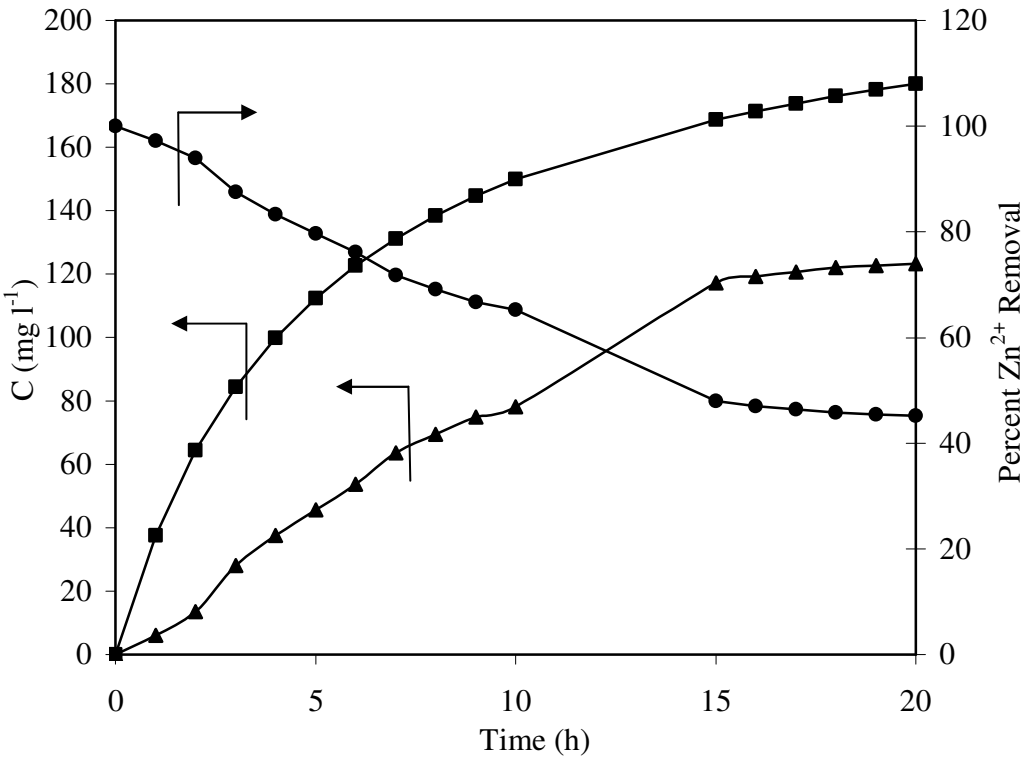

Figure 3.72 Variation of final zinc concentration and percent Zn^{2+} removal with time for 225 mg l^{-1} zinc concentration. ▲ Final Zn^{2+} concentration (mg l^{-1}), ● Percent Zn^{2+} removal, ■ Control Zn^{2+} concentration

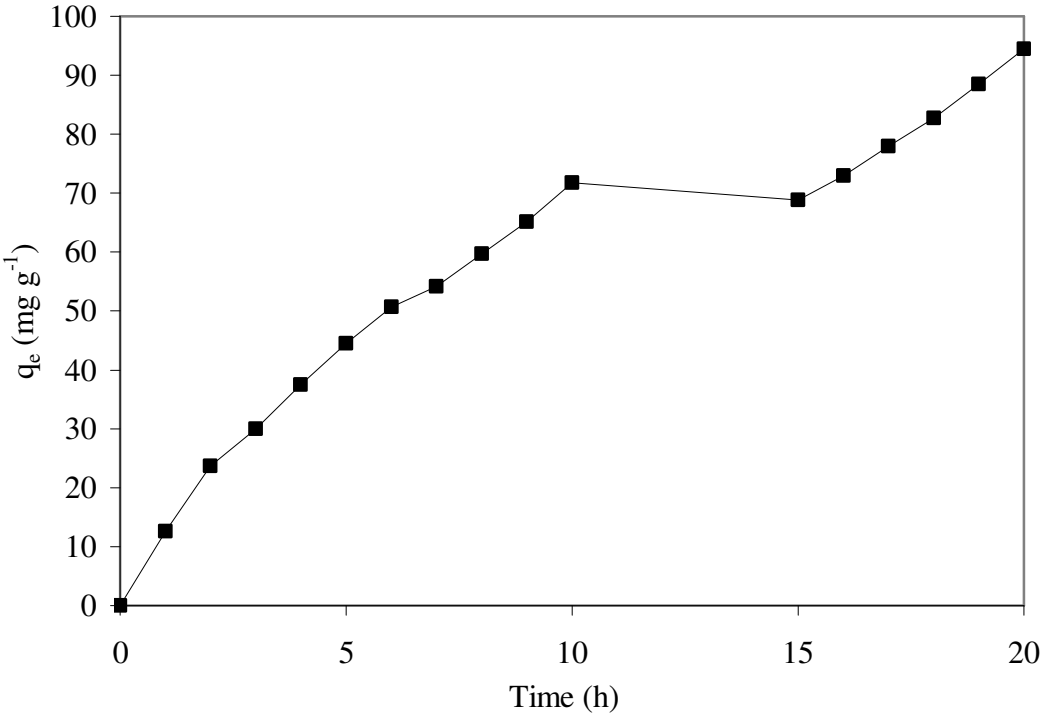

Figure 3.73 Variation of solid phase Zn^{2+} concentration (q, mg Zn $gPWS^{-1}$) with time for 225 mg l^{-1} feed zinc concentration

Figure 3.74 depicts variations of percent zinc removal and the final zinc concentrations with time for 275 mg l^{-1} feed zinc ion concentration. Final zinc concentrations increased with time for both tanks. As can be seen from Figure 3.74, zinc ion removal from solution was almost completed within 15 hours; however the system was operated for 20 hours to reach equilibrium. Final zinc ion concentration increased to 220 mg l^{-1} in the control tank and 160 mg l^{-1} in the adsorption tank at the end of 20 hours. Percent zinc removal decreased from 92,5% to 42 % at the end of 2 and 20 hours.

In Figure 3.75, variation of solid phase (biosorbed) zinc ion concentrations with time is presented for 275 mg l^{-1} feed zinc concentration. Biosorbed zinc ion concentration increased with time and reached to 100 mg g^{-1} at the end of 20 hours while it was 14,5 mg g^{-1} after one hour operation.

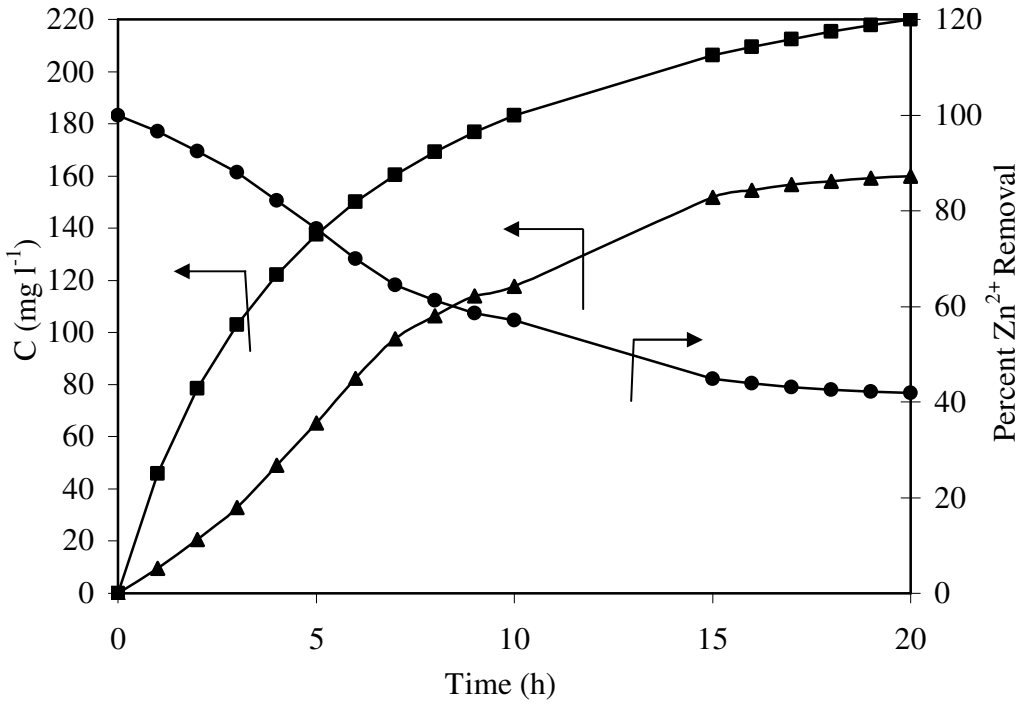

Figure 3.74 Variation of final zinc concentration and percent Zn^{2+} removal with time for 275 mg l^{-1} zinc concentration. ▲ Final Zn^{2+} concentration (mg l^{-1}), ● Percent Zn^{2+} removal, ■ Control Zn^{2+} concentration

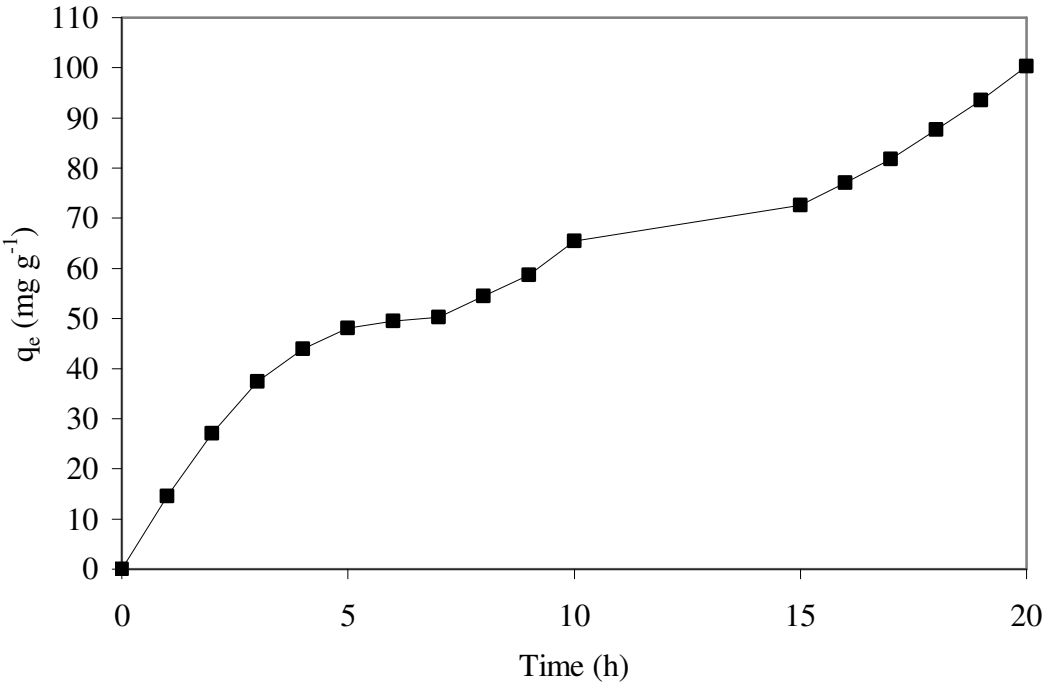

Figure 3.75 Variation of solid phase Zn^{2+} concentration (q, mg Zn $gPWS^{-1}$) with time for 275 mg l^{-1} feed zinc concentration

Although the solid phase zinc concentrations increased with increasing feed zinc concentrations from 37,5 mg l^{-1} to 275 mg l^{-1}, percent zinc removals showed an opposite trend. The removal efficiency was higher at low inlet zinc concentrations. 71% and 62% zinc removals by adsorption was observed at equilibrium when the inlet zinc concentrations were 37,5 mg l^{-1} and 75 mg l^{-1}. And also, the breakpoint time decreased with increasing inlet zinc concentration as the binding sites became more quickly saturated in the system. Even after the breakthrough occurred, the biosorbent was still capable of accumulating zinc ions, although at a progressively lower efficiency. Biosorbed zinc ion concentrations increased from 32 mg g^{-1} to 100 mg g^{-1} with an increase of feed zinc concentration from 37,5 to 275 mg l^{-1}.

Figure 3.76 depicts variations of zinc ion concentrations in solution with time for different feed zinc concentrations. Final zinc concentration increased from 11 mg l^{-1} to 160 mg l^{-1} when initial zinc concentration increased from 37,5 mg l^{-1} to 275 mg l^{-1}. At low initial Zn^{2+} concentrations, all zinc ions were biosorbed onto binding sites on PWS surfaces since binding sites were in excess of zinc ions yielding low zinc ions in solution. However, at high initial zinc ion concentrations, a large fraction of binding sites on PWS surfaces were occupied by zinc ions since zinc ions were in excess of the binding sites yielding high Zn^{2+} concentrations in the solution at equilibrium.

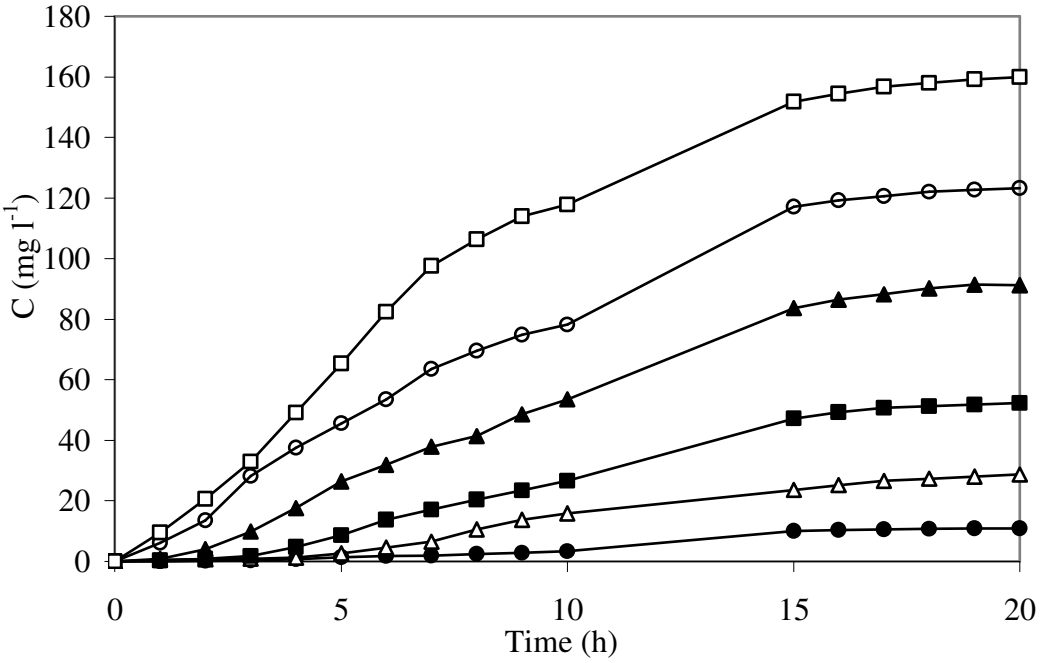

Figure 3.76 Variations of zinc ion concentrations with time for different feed zinc concentrations.
● 37,5 mg l^{-1}, Δ 75 mg l^{-1}, ■ 125 mg l^{-1}, ▲ 175 mg l^{-1}, ○ 225 mg l^{-1}, □ 275 mg l^{-1}

3.5.3. Experiments with Different PWS Concentrations

The biosorbent (PWS) concentration was varied between 1 and 6 g l^{-1} in the last stage of fed-batch adsorption studies while the initial zinc ion concentration, PWS particle size and pH were constant at 200 mg l^{-1}, 64 μm and pH = 5, respectively. The flow rate was adjusted to 0,25 L h^{-1} throughout this set of experiments. The control tank was operated under the same conditions of adsorption tank in the absence of PWS. Percent zinc(II) removals in control experiments were considered to be zero and zinc(II) content of the control experiments were used as the base in calculation of percent zinc(II) removals. The samples (5 ml) withdrawn from the control and adsorption tank every hour were centrifuged at 8000 rpm (7000 g) to remove solids before analysis.

Variations of percent Zn^{2+} removal and the final zinc ion concentrations with time for the biosorbent (PWS) content of 1 g are depicted in Figure 3.77. Zinc concentrations in the control tank increased steadily because of accumulation of zinc ions in the absence of PWS, resulting in a Zn^{2+} concentration of nearly 158 mg l^{-1} at

the end of 15 h operation period. Similar trend was observed in the adsorption tank where Zn^{2+} concentrations in the adsorption tank increased steadily with time. However, Zn^{2+} concentrations in adsorption tank were lower than those of the control experiments because of Zn^{2+} removal by adsorption resulting in a Zn^{2+} concentration of nearly 144 mg l^{-1} at the end of 15 h of operation. Percent zinc removal decreased from 78% to 28 % at the end of 2 and 15 hours. Zinc removals in the control tank were assumed to be zero by definition.

Variation of solid phase Zn^{2+} concentration (q, mg Zn $gPWS^{-1}$) with time is depicted in Figure 3.78 for 1 g PWS content. Equilibrium solid phase zinc ion concentration increased rapidly with time. Very high biosorbed zinc concentrations were obtained during the operation, resulting in a biosorbed zinc concentration of 64 mg g^{-1} at the end of 15 hours.

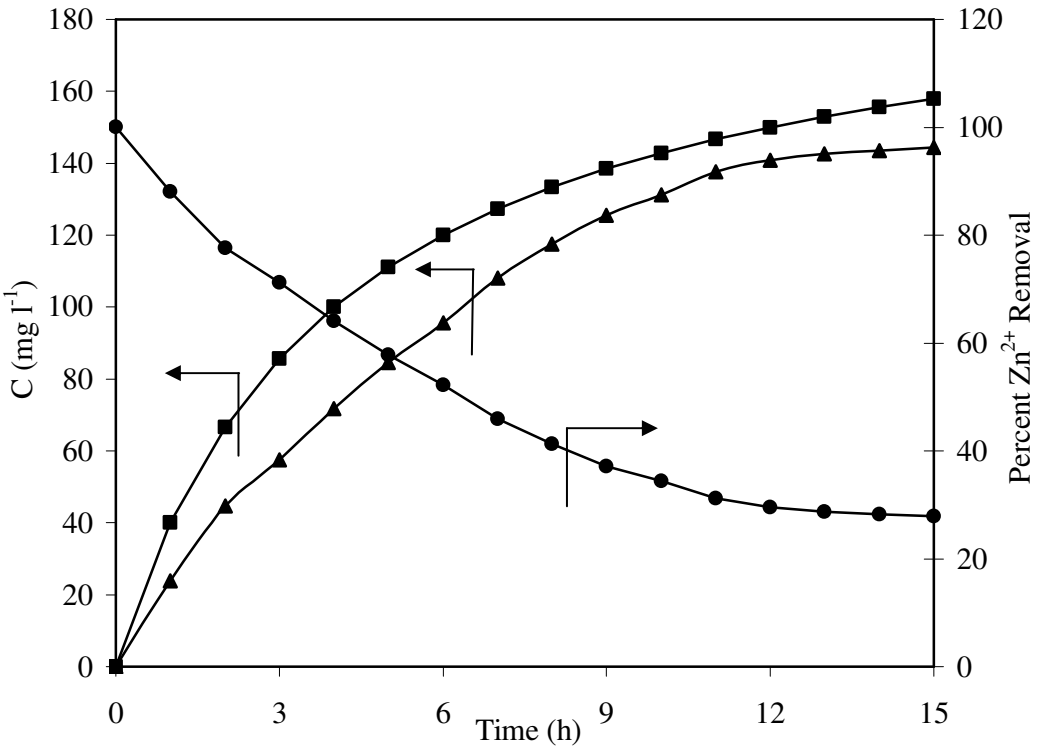

Figure 3.77 Variation of percent Zn^{2+} removal and the final zinc ion concentrations with time for 1 g PWS. ▲ Final Zn^{2+} concentration (mg l^{-1}), ● Percent Zn^{2+} removal, ■ Control Zn^{2+} concentration

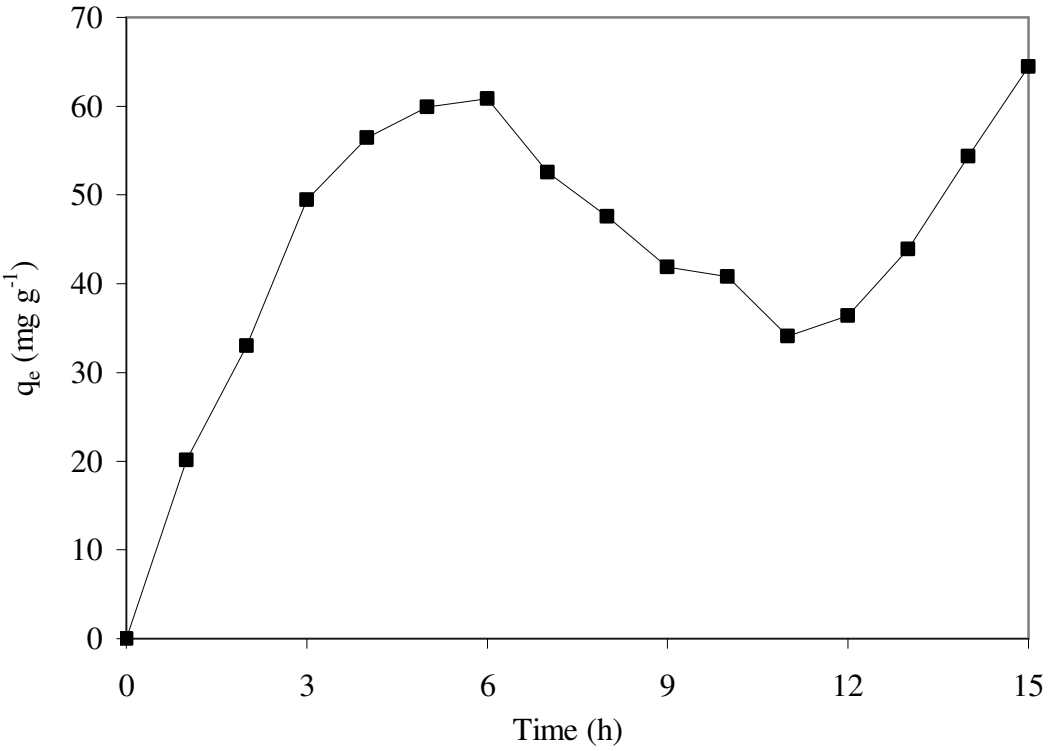

Figure 3.78 Variation of solid phase Zn^{2+} concentration (q, mg Zn $gPWS^{-1}$) with time for 1 g PWS

Figure 3.79 depicts variations of percent Zn^{2+} removal and the final zinc ion concentrations with time for the biosorbent (PWS) concentration of 2 g l^{-1}. The time needed to reach equilibrium was 15 hours Final zinc concentrations in the control and adsorption tank increased steadily with time. Zinc adsorption was not observed in control tank due to the absence of PWS yielding high final Zn^{2+} concentration such as 158 mg l^{-1} at the end of 15 hours. The adsorption of Zn^{2+} at low PWS concentrations was low because of the limited binding sites on the biosorbent (PWS). Percent zinc ion removal decreased to 37% at the end of the 15 hours of operation when the initial Zn^{2+} concentration was 200 mg l^{-1}.

Figure 3.80 depicts variation of solid phase (biosorbed) zinc ion concentrations with time for the biosorbent (PWS) content of 2 g. Biosorbed Zn^{2+} concentration increased with time and equilibrium was reached after 15 hours of fed-batch operation. At the end of 1 hour operation, biosorbed Zn^{2+} concentration was found 15 mg g^{-1} which increased to 77 mg g^{-1} at the end of 15 hours of operation..

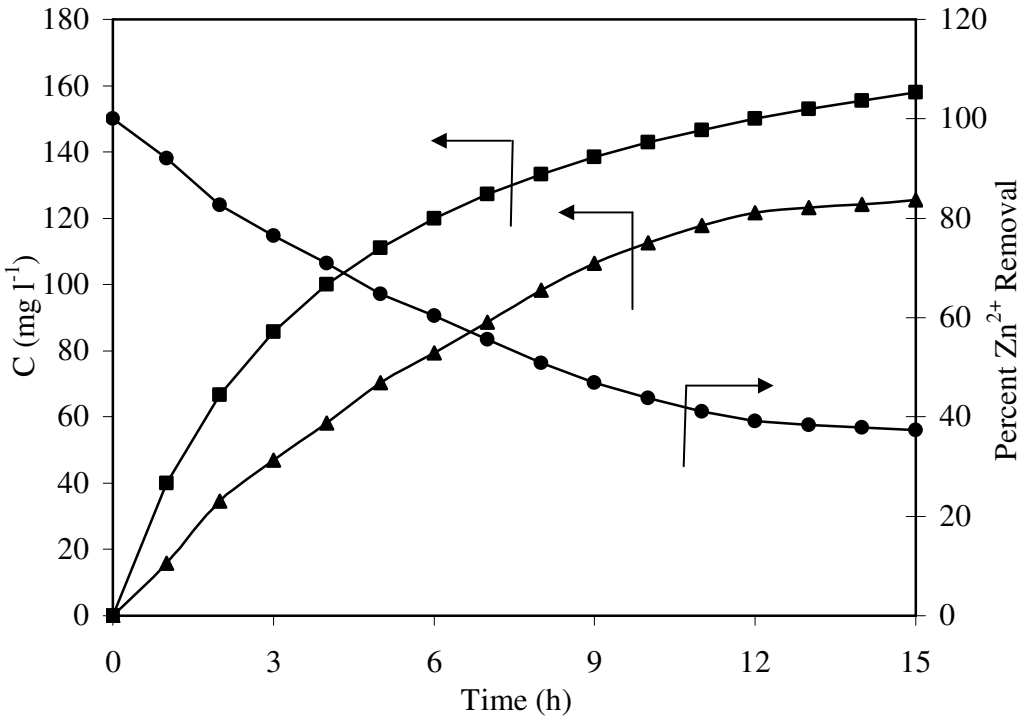

Figure 3.79 Variation of percent Zn^{2+} removal and the final zinc ion concentrations with time for 2 g of PWS. ▲ Final Zn^{2+} concentration (mg l^{-1}), ● Percent Zn^{2+} removal, ■ Control Zn^{2+} concentration

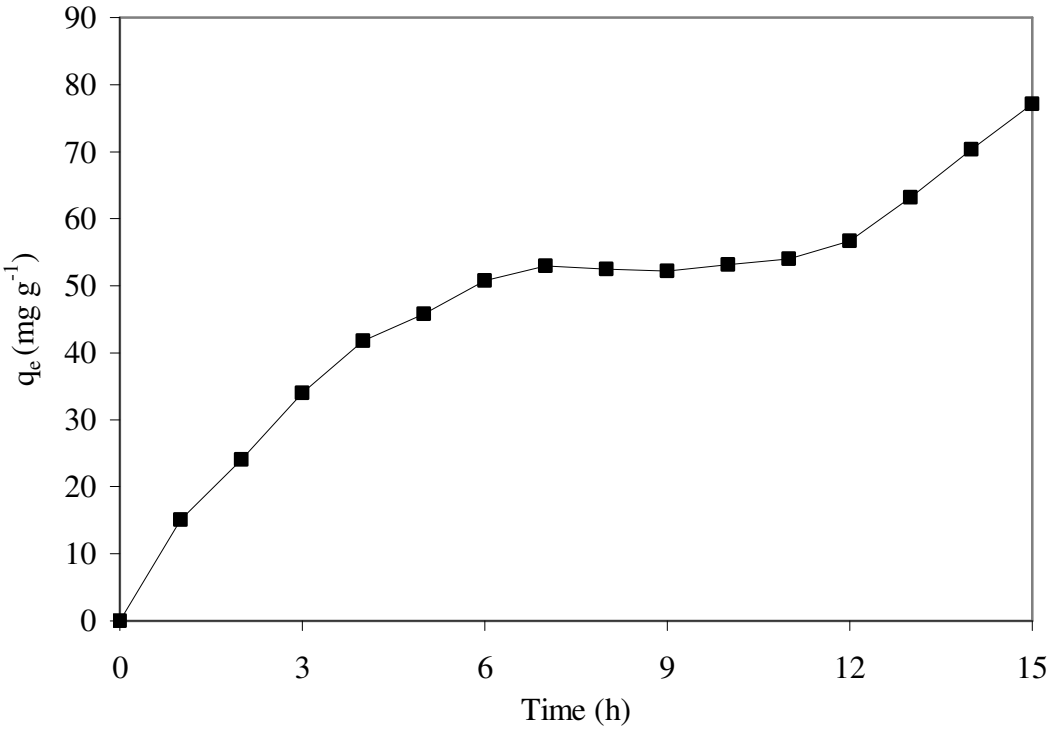

Figure 3.80 Variation of solid phase Zn^{2+} concentration (q, mg Zn $gPWS^{-1}$) with time for 2 g PWS

Figure 3.81 depicts variations of percent removal and the final zinc ion concentrations with time for the biosorbent (PWS) content of 3 g. Percent zinc ion removal decreased from 83% to 50% and final Zn^{2+} concentration increased from 33,5 mg l^{-1} to 99 mg l^{-1} at the end of 3 and 15 hours when initial zinc concentration and flow rate were 200 mg l^{-1} and 0,25 L h^{-1}. No adsorption was observed in the control tank and zinc ion concentration increased with time reaching 160 mg l^{-1} at the end of 15 hours.

Variation of solid phase Zn^{2+} concentration (q, mg Zn $gPWS^{-1}$) with time is depicted in Figure 3.82 for the fed-batch operation with 3 g PWS. Biosorbed zinc concentration increased with time and reached 93 mg g^{-1} at the end of 15 hours.

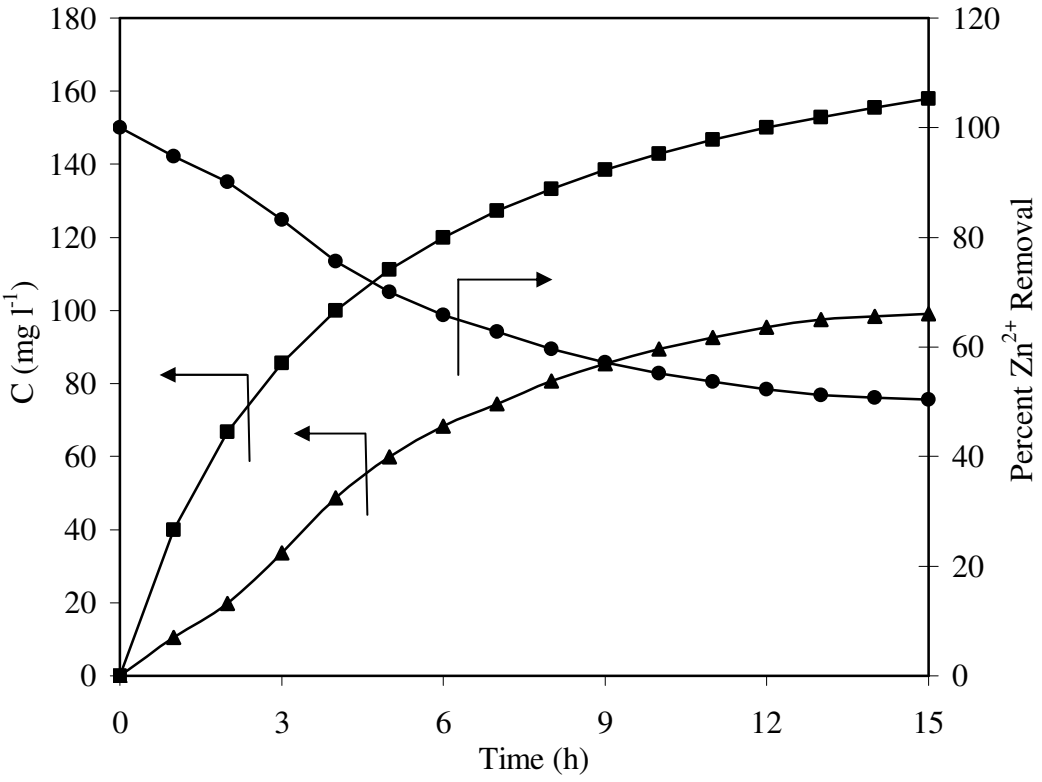

Figure 3.81 Variation of percent Zn^{2+} removal and the final zinc ion concentrations with time for 3 g PWS. ▲ Final Zn^{2+} concentration (mg l^{-1}), ● Percent Zn^{2+} removal, ■ Control Zn^{2+} concentration

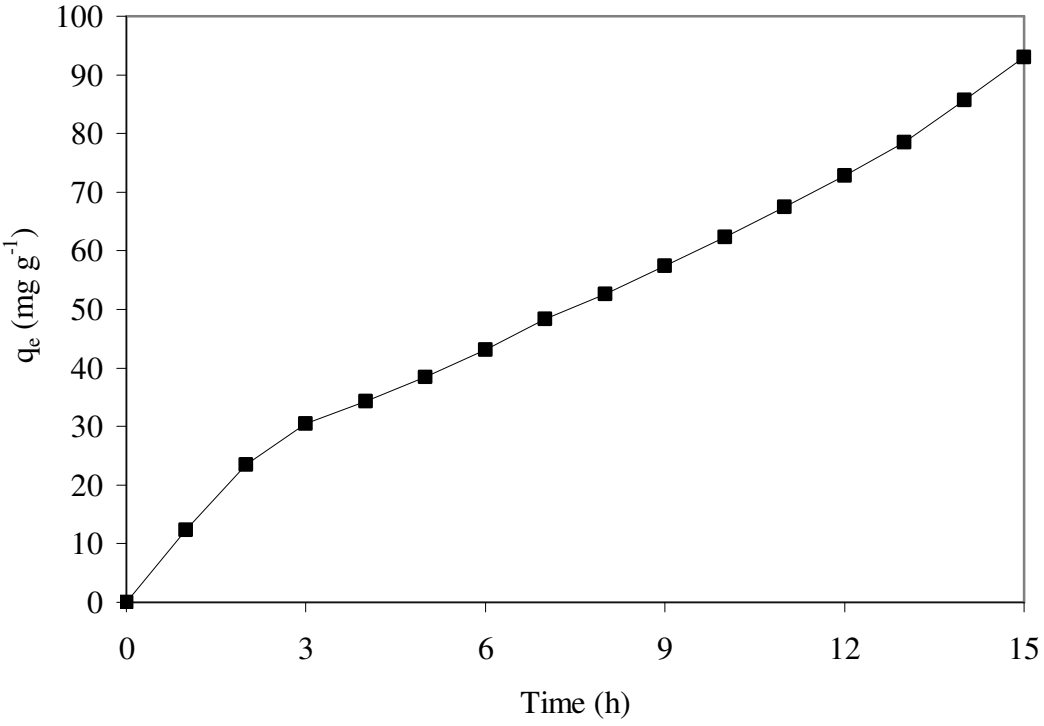

Figure 3.82 Variation of equilibrium solid phase Zn^{2+} concentration (q_e, mg Zn $gPWS^{-1}$) with time for 3 g PWS

Increased PWS concentrations resulted in more efficient Zn^{2+} removals. Variation of percent zinc removal and the final zinc ion concentrations with time are shown in Figure 3.83 for the biosorbent (PWS) content of 4 g. Zinc(II) concentration in the fed-batch adsorption tank increased while percent zinc removal decreased with time. Zinc concentrations in the control tank were higher than those in the adsorption tank because of no zinc uptake in the control tank. The system reached equilibrium within 15 hours and percent Zn^{2+} removals decreased to 58%. Zinc ion concentrations were 37 mg l^{-1} and 84 mg l^{-1} at the end of 4 and 15 hours.

In Figure 3.84, variation of solid phase (biosorbed) zinc ion concentrations with time is presented. Biosorbed zinc ion concentration was 10 mg g^{-1} at the end of one hour which increased to 88 mg g^{-1} at the end of 15 hours.

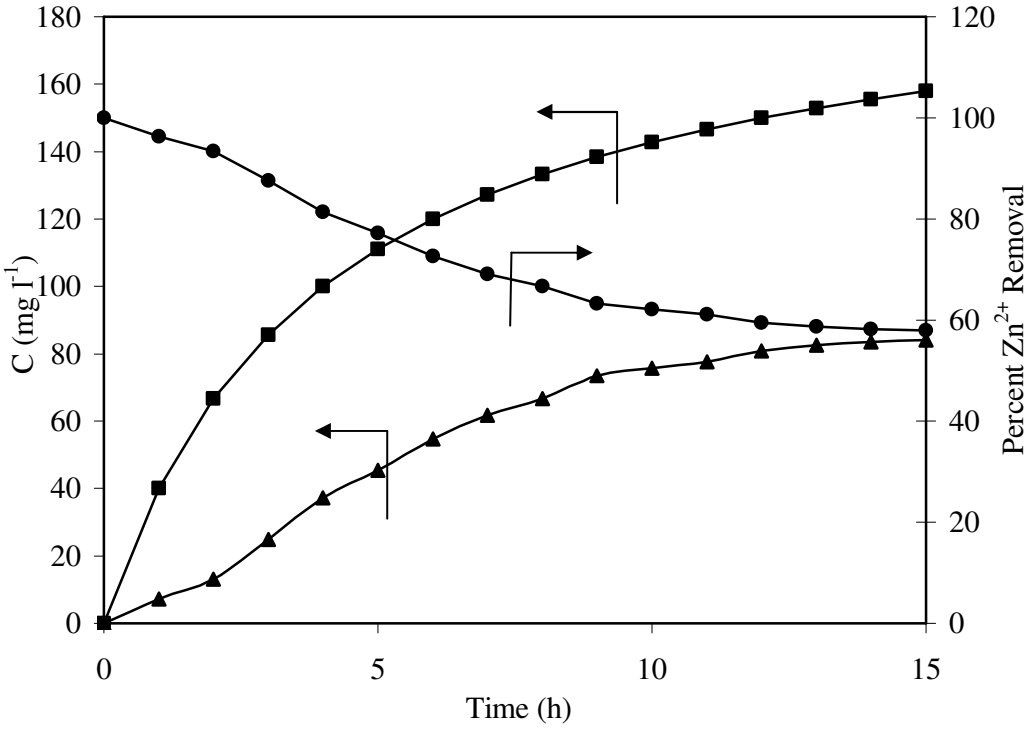

Figure 3.83 Variation of percent Zn^{2+} removal and the final zinc ion concentrations with time for 4 g PWS. ▲ Final Zn^{2+} concentration (mg l^{-1}), ● Percent Zn^{2+} removal, ■ Control Zn^{2+} concentration

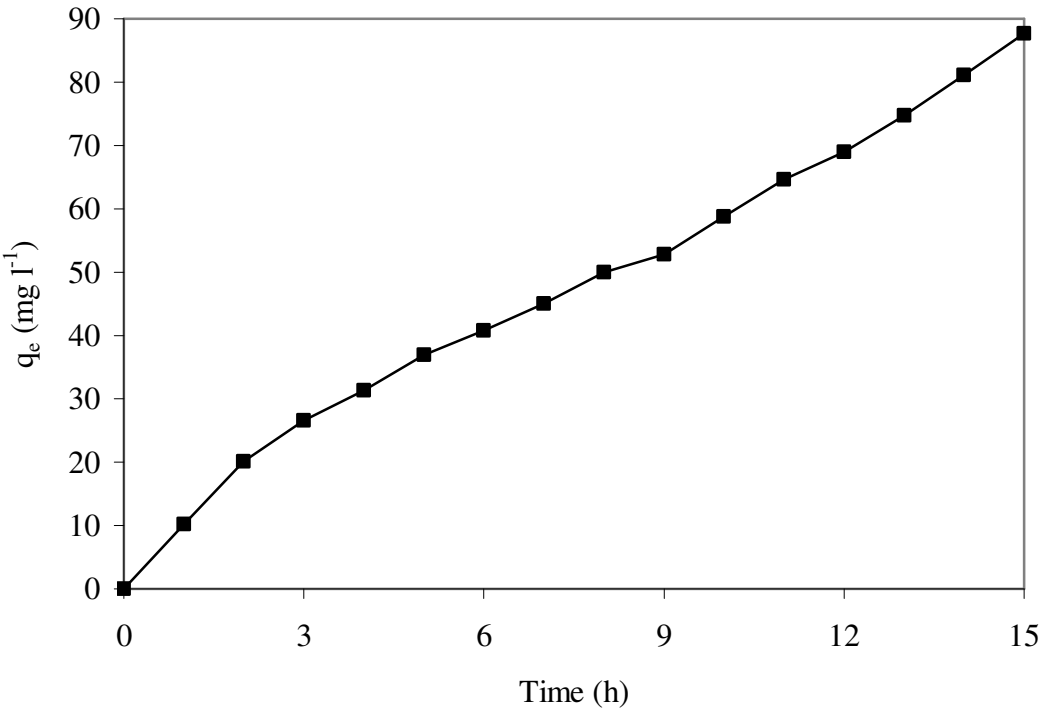

Figure 3.84 Variation of solid phase Zn^{2+} concentration (q, mg Zn $gPWS^{-1}$) with time for 4 g PWS

Figure 3.85 depicts variations of percent zinc removal and the final zinc concentrations with time for the biosorbent (PWS) content of 5 g. Final zinc concentrations increased with time for both tanks. As can be seen from Figure 3.85, zinc ion removal from solution was almost completed within 10 hours; however the system was operated for 15 hours to reach equilibrium. Zinc concentrations increased to 158 mg l^{-1} in the control tank and 69 mg l^{-1} in the adsorption tank at the end of 15 hours. Percent zinc removal decreased from 95 % to 65 % at the end of 2 and 15 hours.

In Figure 3.86, variation of solid phase (biosorbed) zinc ion concentrations with time is presented for the biosorbent (PWS) content of 5 g. Biosorbed zinc ion concentration increased rapidly with time. Biosorbed zinc concentration at the end of 15 hours of fed-batch operation was 84 mg g^{-1}.

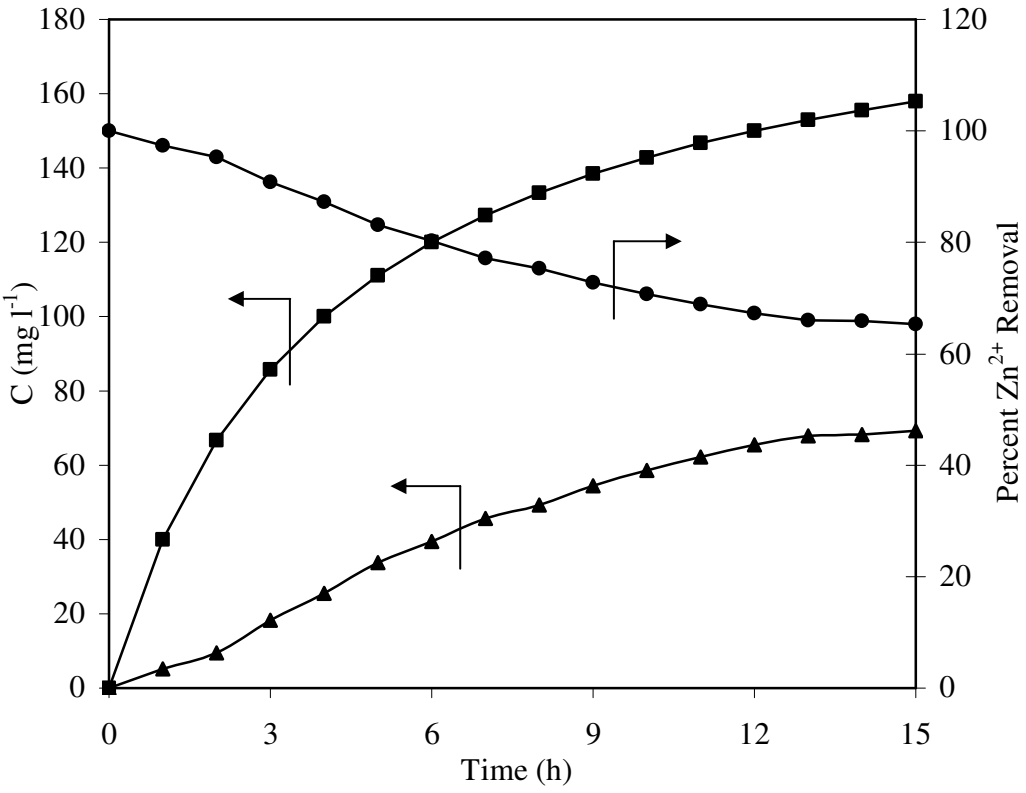

Figure 3.85 Variation of percent Zn^{2+} removal and the final zinc ion concentrations with time for 5 g PWS. ▲ Final Zn^{2+} concentration (mg l^{-1}), ● Percent Zn^{2+} removal, ■ Control Zn^{2+} concentration

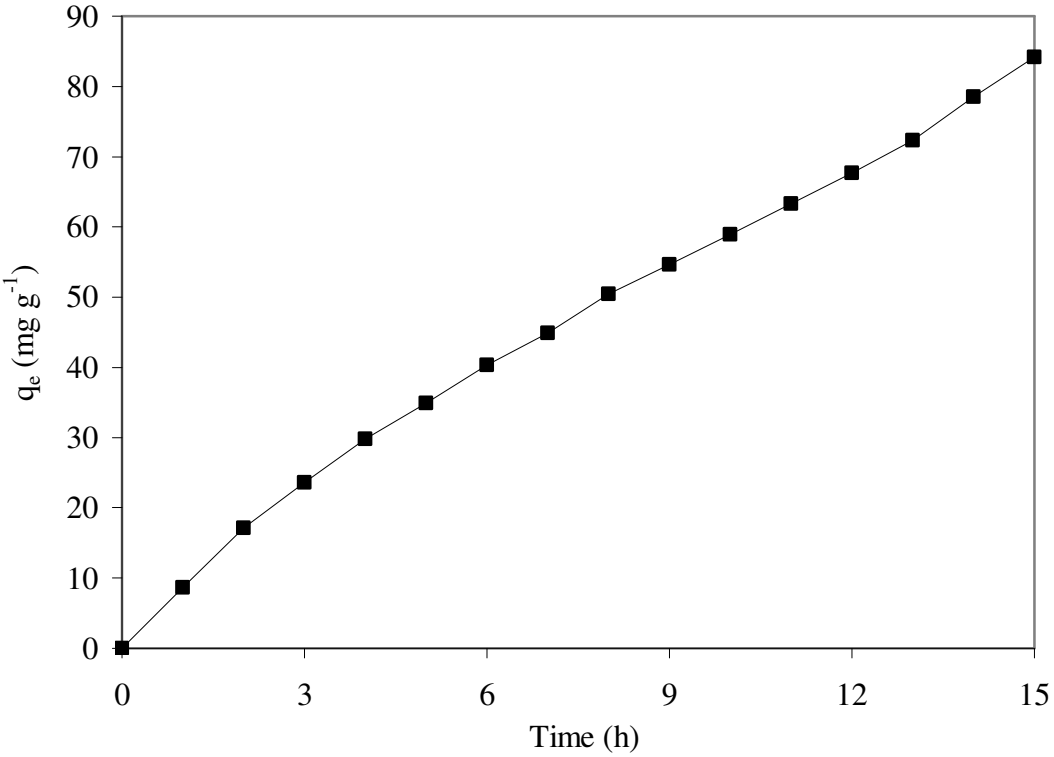

Figure 3.86 Variation of solid phase Zn^{2+} concentration (q, mg Zn $gPWS^{-1}$) with time for 5 g PWS

Figure 3.87 depicts variations of percent removal and the final zinc ion concentrations with time for the biosorbent (PWS) content of 6 g. Percent Zn^{2+} removals decreased from 94% to 70% which was very high removal efficiencies. The final Zn^{2+} concentration increased from 12,5 mg l^{-1} to 60 mg l^{-1} at the end of 3 and 15 hours. No adsorption was observed in the control tank and the final zinc ion concentration reached to 158 mg l^{-1} at the end of hours.

Figure 3.88 depicts variation of solid phase (biosorbed) zinc ion concentrations with time for 6 g PWS. Biosorbed Zn^{2+} concentration increased with time and reached equilibrium after 15 hours of fed-batch operation. At the end of 1 hour of operation, biosorbed Zn^{2+} concentration was 8,2 mg g^{-1} which increased to 77,5 mg g^{-1} at the end of 15 hours.

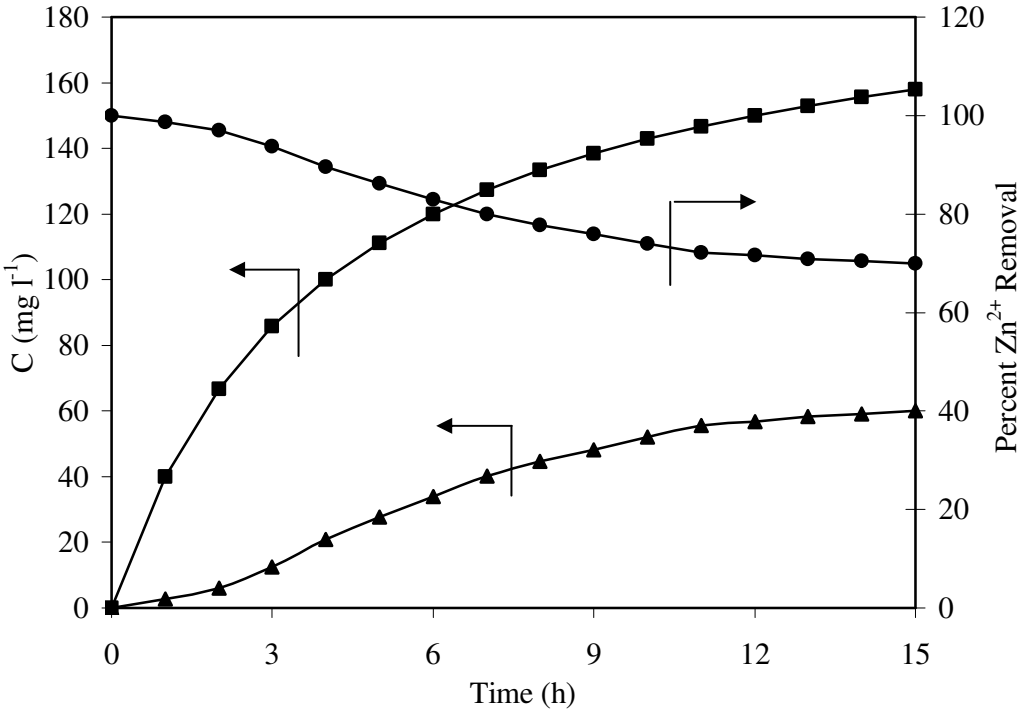

Figure 3.87 Variation of percent Zn^{2+} removal and the final zinc ion concentrations with time for 6 g PWS. ▲ Final Zn^{2+} concentration (mg l^{-1}), ● Percent Zn^{2+} removal, ■ Control Zn^{2+} concentration

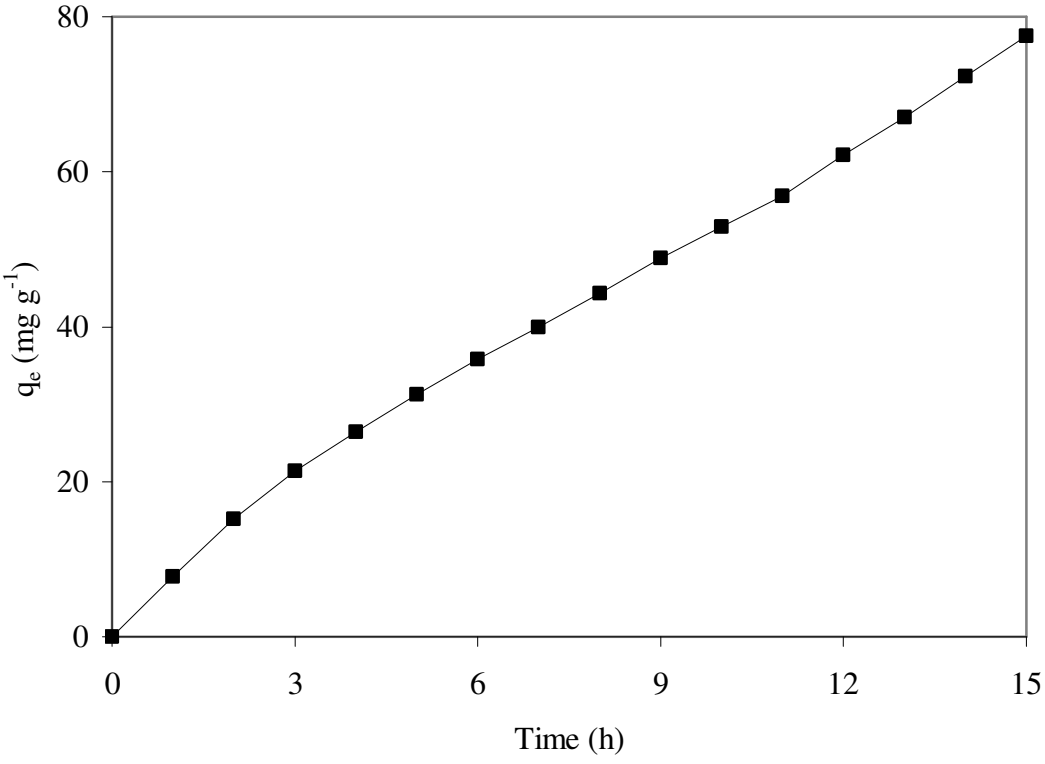

Figure 3.88 Variation of solid phase Zn^{2+} concentration (q, mg Zn $gPWS^{-1}$) with time for 6 g PWS

Percent zinc removals increased with increasing adsorbent (PWS) concentrations. Percent Zn^{2+} removals at equilibrium increased from 28% to 70% when PWS content increased from 1 to 6 g. Biosorbed zinc concentrations increased with increasing PWS concentration. At low PWS content such as 1 and 2 g, the available binding sites on biosorbent surfaces were occupied by zinc ions since zinc ion concentrations exceeded the binding sites yielding low equilibrium biosorbent zinc ion concentrations such as 64 and 77 mg g^{-1}, respectively. However, at high biosorbent (PWS) content such as 5 and 6 g large binding sites were available on PWS surfaces and only a fraction of those binding sites were occupied by Zn^{2+} ions yielding high solid phase Zn^{2+} concentrations such as 84 and 77,5 mg g^{-1}. The extent of biosorption was limited by Zn^{2+} ion concentration at high PWS concentrations.

Figure 3.89 depicts variations of final zinc concentrations with time for different PWS concentrations. Final zinc concentration decreased from 144 mg l^{-1} to 60 mg l^{-1} when PWS content increased from 1 to 6 g. At low biosorbent contents such as 1 and 2 g, the extent of zinc biosorption was limited by the availability of the binding sites on the biosorbent (PWS) yielding high residual zinc ions in solution at equilibrium. However, at high biosorbent contents such as 5 and 6 g, the binding sites on the biosorbent surfaces exceeded zinc ions in solution and large fractions of zinc ions were biosorbed onto the binding sites resulting in low residual zinc ions of 65 and 70 mg l^{-1} in solution, respectively.

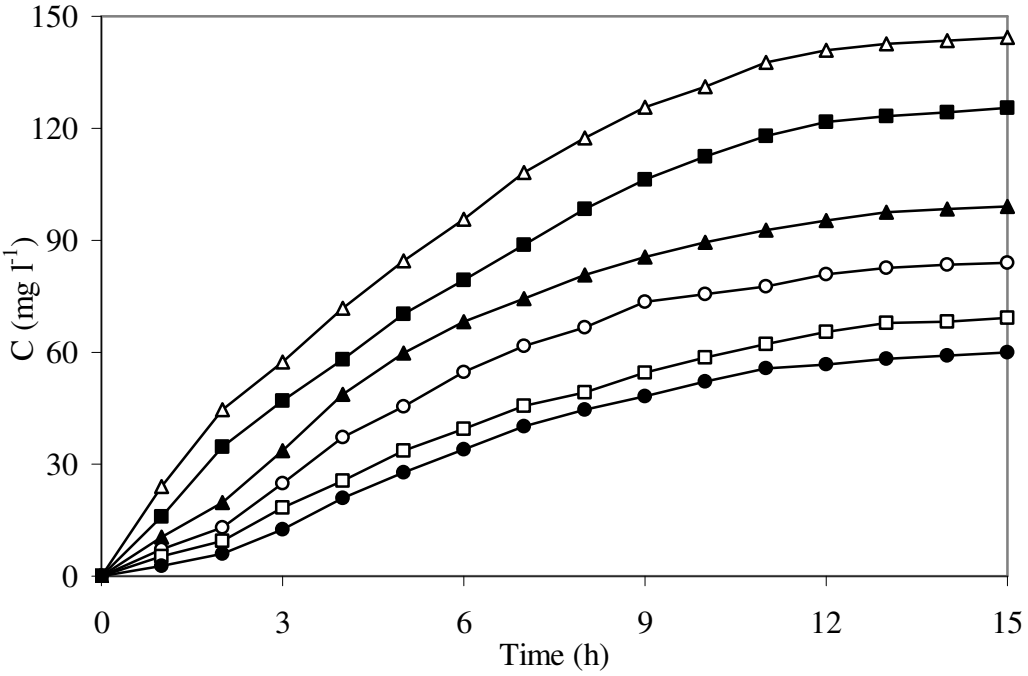

Figure 3.89 Variations of zinc concentrations with time for different PWS concentrations in fed-batch operation. PWS (g): Δ 1, ■ 2, ▲ 3, ○ 4, □ 5, ● 6

3.5.4. Determination of Biosorption Constants

Bohart and Adams equation was modified for fed-batch adsorption contactor to determine the biosorption constants using the experimental data. The modified Bohart and Adams equation was presented in equation 16. A plot of time required to reach desired effluent concentration (e.g, 10 mg l^{-1}) versus $m/(Q*C_0)$ would yield a line with a slope of (q'_s) and an intercept of $1/(KC_0)$. From the slope and intercept of the respective lines the adsorption capacity of the adsorbent (q'_s) and the rate constant of adsorption (K) were calculated for different fed-batch operations such as variable flow rate, initial Zn^{2+} concentration and PWS concentrations.

The time needed for 10 mg l^{-1} final Zn^{2+} concentrations (breakthrough time) was obtained from the experimental graphs (C versus time) for different flow rates with 3 g PWS and 100 mg l^{-1} zinc concentration. A plot of breakthrough time versus $m/(Q*C_0)$ is depicted in Figure 3.90. From the slope and the intercept of the best-fit line the following values were obtained for q'_s and K.

q'_s = 0,0574 kg Zn/kg PWS= 57,4 gZn/ kgPWS, K = 0,0236 m^3/kg.h, (R^2= 0,999)

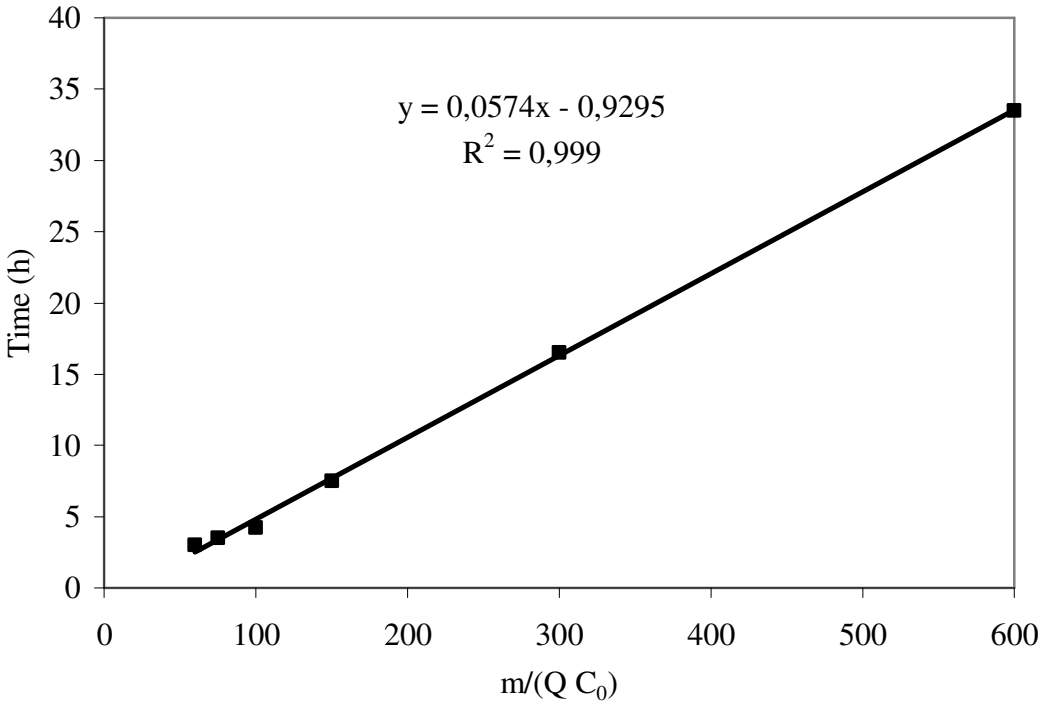

Figure 3.90 A plot of break through time versus m/(Q*C_0) for determination of the constants of modified Bohart and Adams equation for different flow rates

The time needed for 10 mg l^{-1} final Zn^{2+} concentrations was obtained from the experimental graphs of C versus time obtained for different feed zinc concentrations while the feed flow rate was 0,2 L h^{-1} with 3 g PWS. A plot of breakthrough time versus m/(Q C_0) is depicted in Figure 3.91. Different rate constants (K) were calculated for each of the feed zinc concentrations when the desired final zinc concentration was 10 mg l^{-1}. However, the adsorption capacity of the adsorbent (q'_s) was the same for all the initial zinc concentrations. From the slope and the intercept of the best-fit line the following values were obtained for q'_s.

q'_s = 0,0484 kg Zn/kg PWS = 48,4 g Zn/ kg PWS (R^2 = 0,996)

The rate of constant of biosorption (K) for different zinc concentrations were found to be 0,0199 m^3/kg.h for 37,5 mg l^{-1}, 0,0184 m^3/kg.h for 75 mg l^{-1}, 0,0144 m^3/kg.h for 125 mg l^{-1}, 0,0118 m^3/kg.h for 175 mg l^{-1}, 0,0101 m^3/kg.h for 225 mg l^{-1} and 0,0088 m^3/kg.h for 275 mg l^{-1} zinc ion concentrations, respectively.

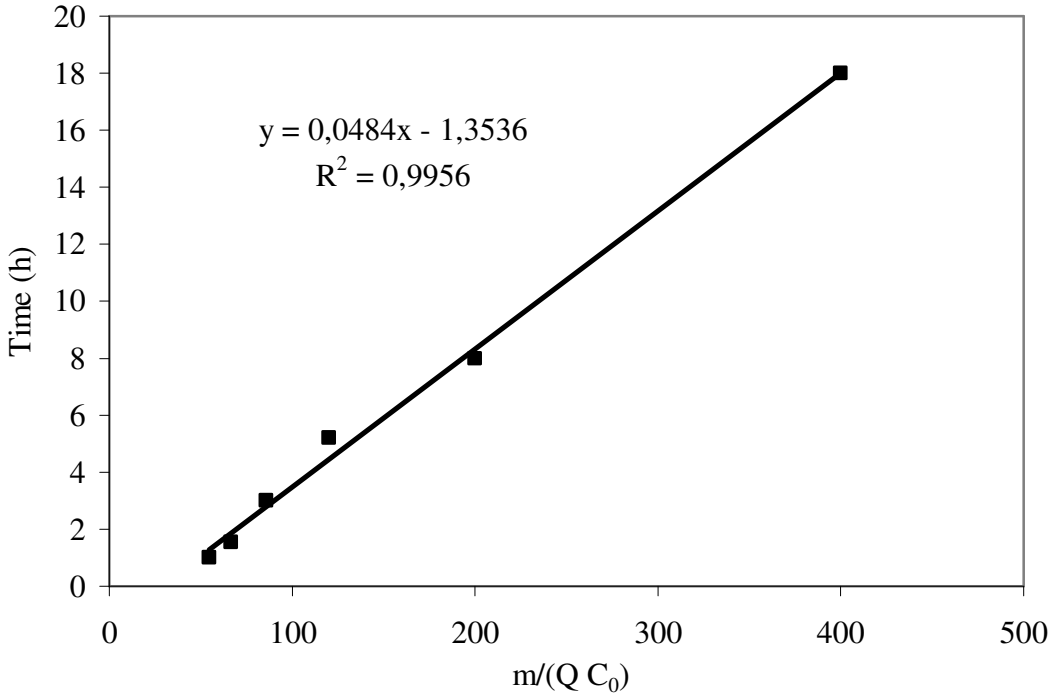

Figure 3.91 A plot of breakthrough time versus m/(Q C_0) for determination of the constants of modified Bohart and Adams equation for different feed zinc concentrations

Similar experiments were performed with variable PWS concentrations while the feed flow rate and feed zinc concentrations were 0,25 L h^{-1} and 200 mg l^{-1}, respectively. The experimental data was plotted in form of C versus time and the breakthrough times needed to obtain 10 mg l^{-1} Zn^{2+} concentrations were obtained those graphs. The breakthrough times were plotted versus m/(Q C_0) as depicted in Figure 3.92. From the slope and the intercept of the best-fit line the following values were obtained for q'_s and K.

q'_s = 0,0241 kg Zn/kg PWS= 24,1 g Zn/ kg PWS, K = 0,0502 m^3/kg.h, (R^2 = 0,968)

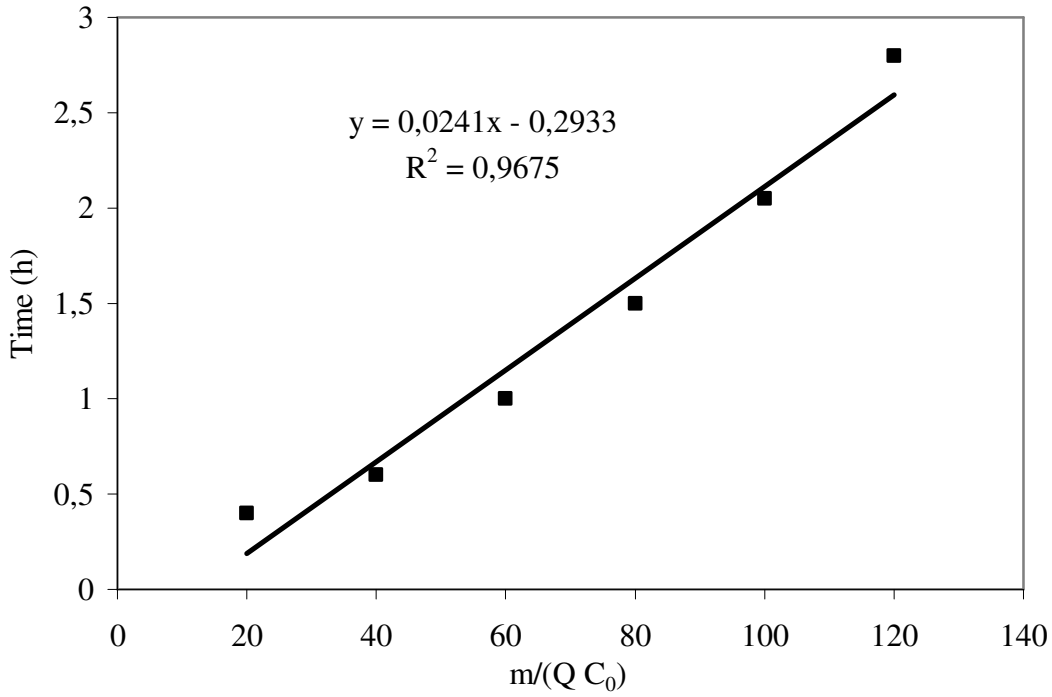

Figure 3.92 A plot of breakthrough time versus m/(QC_0) for determination of the constants of modified Bohart and Adams equation for different PWS concentrations

Good correlation coefficients were obtained in determining the rate constants from fed-batch experimental results. Therefore the modified model and the determined constants can be used for the design of fed-batch adsorption contactors over a range of feasible flow rates and concentrations.

CHAPTER FOUR
CONCLUSIONS

The potential use of powdered activated sludge (PWS) for removal of zinc ions from solutions by biosorption was evaluated using batch and fed-batch experiments. The experimental results showed that activated sludge from a paint industry wastewater treatment plant (DYO, Izmir) had a high biosorption capacity to remove zinc ions. The waste sludge was pre-treated with 1% hydrogen peroxide to improve the biosorption capacity. Pre-treated sludge was dried, ground and sieved to different mesh sizes. The fraction of the PWS with a particle size of 64 µm was used in part of the experimental studies. Biosorption of zinc(II) ions onto PWS is influenced by various parameters such as pH, initial Zn^{2+} concentration, PWS concentration, agitation speed and temperature. The first part of the experiments was carried out using batch shake flasks to investigate the effects of the operating parameters on zinc biosorption onto PWS.

Performance of biosorption of zinc ions onto pre-treated PWS samples were investigated for five different particle sizes between 53 and 231µm. The extent of biosorption of zinc ions increased and the final Zn^{2+} concentration in solution decreased with decreasing particle size (D_p) because of larger external surface area of PWS at small particle sizes. It was determined that 6 hours of incubation was sufficient to reach the biosorption equilibrium. Percent biosorption increased from 54% to 68% when particle size decreased from 231 µm to smaller than 53 µm yielding effluent Zn^{2+} concentrations as 46 and 32 mg l^{-1}, respectively at the end of 6 hours incubation.

Medium pH affected the surface charges of PWS and also the solubility of the zinc ions. At low pH values, or high (H^+) ion concentrations, the surfaces of PWS particles (which would be negatively charged at neutral pH) were neutralized yielding lower attraction forces between the PWS surfaces and Zn^{2+} ions. Therefore, the extent of biosorption was negligible at low pH levels which increased with

increasing pH as a result of more negative charges on PWS surfaces attracting Zn^{2+} ions. Zinc ions precipitated in form of $Zn(OH)_2$ at pH levels at and above 6 resulting in high removal efficiency of Zn^{2+} ions from solution. Therefore, the optimal pH yielding maximum extent of biosorption without any zinc ion precipitation was pH= 5 which yielded a solid phase Zn^{2+} concentration of nearly 60 mg g^{-1}.

Initial zinc ion concentration also affected the extent of biosorption at constant PWS concentration and the particle size. As the zinc ion concentration increased more and more binding sites on PWS surfaces were occupied by Zn^{2+} ions yielding larger solid phase Zn^{2+} concentrations (q_e, mg g^{-1}) at equilibrium. The maximum biosorbed Zn^{2+} concentration was found to be 86 mg g^{-1} with initial Zn^{2+} and PWS concentrations of 350 mg l^{-1} and 1 g l^{-1}, respectively.

Increases in PWS concentrations resulted in increased binding sites on the biosorbent when initial zinc ion concantration was constant at 100 mg l^{-1}. Therefore, lower fractions of PWS surfaces were occupied by Zn^{2+} ions as the PWS concentration increased which yielded lower solid phase Zn^{2+} concentrations (q_e). The equilibrium biosorbed Zn^{2+} concentration (q_e) decreased from 200 to 55 mg g^{-1} when the PWS concentration was increased from 0,25 to 3 g l^{-1}.

Biosorption of zinc ions increased with increasing agitation speed because of better contact between the solid and liquid phases. At low agitation speed such as 50 rpm, some of the biosorbent precipitated at the bottom of the shake flask yielding low solid phase Zn^{2+} concentrations such as 47 mg g^{-1}. When the agitation speed increased at 200 rpm, high solid phase Zn^{2+} concentration and percent zinc removals were obtained such as 69 mg g^{-1} and 69 % removal.

One other parameter affecting zinc removal by adsorption was temperature. Again, biosorbed Zn^{2+} concentration and percent Zn^{2+} removals increased with increasing temperature. The highest equilibrium solid phase zinc concentration was obtained as 73 mg g^{-1} at 50 ^{0}C at the end of 24 hours of incubation. The difference in

percent zinc removal between the lowest and the highest temperatures (30 and 50 ^{0}C) was only 13% at the end of equilibrium time.

Pseudo-first order and second order kinetic models were used to correlate the pre-equilibrium biosorption data for the different experimental conditions and the kinetic constants were determined for both models. Variable pH and agitation speed experimental data fitted to the first-order adsorption kinetics. The highest rate constants for the pseudo-first order kinetic were 1,027 h^{-1} for pH=8 and 0,68 h^{-1} for 200 rpm, respectively. The pseudo-second order model was found to be more suitable for the experimental data obtained with variable particle size, initial zinc and PWS concentrations. The highest rate constants for the pseudo-second order kinetic were 0,024 $(mg/g)^{-1}.h^{-1}$ for the smallest particle size of 53 µm; 0,082 $(mg/g)^{-1}.h^{-1}$ for 50 mg l^{-1} initial Zn^{2+} concentration; 0,033 $(mg/g)^{-1}.h^{-1}$ for 2,5 g l^{-1} PWS concentration and 0,041 $(mg/g)^{-1}.h^{-1}$ for 50 ^{0}C, respectively.

The Freundlich, Langmuir and Generalized adsorption isotherm models were used for the mathematical description of the biosorption equilibrium.The constants of each isotherm were determined by using the equilibrium biosorption data obtained with varaiable initial Zn^{+2} and PWS concentrations. The Langmuir isotherm was found to fit the experimental data better than the other isotherms tested although the other isotherms also represented the data reasonably well. The maximum biosorption capacity of pre-treated PWS for the zinc ions was found to be nearly 82 mgZn. $gPWS^{-1}$.

Fed-batch adsorption contactor was used to enhance the removal of zinc from aqueous solution by biosorption. The experimental results showed that the biosorption of zinc is dependent on the flow rate, the inlet zinc and PWS concentration and time. These parameters affect percent zinc removal and the saturation capacity of biosorbent (PWS) directly. The breakpoint time decreased with increasing flow rate. However, biosorbed (solid phase) Zn^{2+} concentration and percent zinc removal increased with increasing flow rate. The equilibrium zinc uptakes increased with increasing inlet zinc concentration from 37,5 mg l^{-1} to 275

mg l^{-1}, however, percent zinc removals showed an opposite trend. Biosorbed zinc ion concentrations increased from 32 mg g^{-1} to 100 mg g^{-1} with an increase of inlet zinc concentration from 37,5 mg l^{-1} to 275 mg l^{-1}. When initial PWS concentration increased, Zn^{2+} ions were removed more efficiently. When the quantity of biosorbent per unit volume increased, zinc uptake was higher in the adsorption tank because of the high adsorption sites. Percent Zn^{2+} removal at the end of 20 hours of operation increased from 28% to 70% when initial PWS contents increased from 1 g to 6 g. Biosorbed zinc concentrations increased with increasing PWS concentration resulting in 64 mg g^{-1} for 1 g PWS and 77,5 mg g^{-1} for 6 g PWS. Consequently, it can be said that the saturation capacity of PWS is greater under conditions of lower concentrations of zinc, higher flow rates and PWS concentrations. Fed-batch adsorption experimental results were correlated with the modified Bohart and Adams equation to find the adsorption capacity of the adsorbent (q'_s) and the rate of constant of adsorption (K) for different operating conditions.

CHAPTER FIVE
RECOMMENDATIONS

Following recommendations can be made for future studies on removal of heavy metals by biosorption.

1. Adsorption capacities of other low-cost adsorbents may be evaluated. New adsorbents with better adsorption capacities need to be developed and used.

2. Different types of reactors can be used. Performances continuous packed bed columns may be investigated.

3. The combined effects of powdered waste sludge and different biosorbents may be investigated.

4. Multi-component adsorption of different metal ions may be investigated which is important for actual industrial applications.

4. A comparison can be made on the biosorption performances of viable and non viable biosorbents.

REFERENCES

Al-Asheh, S. (1997). Sorption of heavy metals by biological materials. Chemical Engineering Department thesis, *University of Ottawa*, Ottawa, pp. 1-42.

Aksu, Z. (2000). Biosorption of reactive dyes by dried activated sludge: equilibrium and kinetic modelling. *Biochemical Engineering Journal*, 7, 79–84.

Aksu, Z., & Akpinar, D. (2001). Competitive biosorption of phenol and chromium(VI) from binary mixtures onto dried anaerobic activated sludge. *Biochemical Engineering Journal* , 7, 183-193.

Aksu, Z., Açıkel, U., Kabasakal, E., Tezer, S. (2002). Equilibrium modelling of individual and simultaneous biosorption of chromium(VI) and nickel(II) onto dried activated sludge. *Water Research,* 36, 3063-3073.

Arican, B., Gokcay, C.F., & Yetis, U. (2002). Mechanistics models of nickel sorption by activated sludge. *Process Biochemistry*, 37, 1307-1315.

Aksu, Z., (2005). Application of biosorption for the removal of organic pollutants: a review. *Process Biochemistry*, 40, 997-1026.

Bux, F., Atkinson, B., & Kasan, H.C. (1999). Zinc biosorption by waste activated and digested sludges. *Water Science Technology*, 39, 127-130.

Byerley, JJ., & Scharer, JM. (1987). Uranium (VI) biosorption from process solutions. *Chemical Engineering Journal*, 36 (3), 49-59.

Bektas, N., & Kara, S. (2003). Removal of lead from aqueous solutions by natural clinoptilolite: equilibrium and kinetic studies. *Seperation Purification Tecnology*, 39, 189-200.

Batzias, F.A., & Sidiras, D.K. (2004). Dye adsorption by calcium chloride treated beech sawdust in batch and fixed-bed systems. *Journal of Hazardous Materials*, 114, 167–174.

Cooney, D.O. (2000). *Adsorption design for wastewater treatment* (1st ed.). Boca Raton: CRC Press.

Davisa, T.A., Voleskya, B.B., & Mucci, A. (2003). A review of the biochemistry of heavy metal biosorption by brown algae. *Water Research*, 37, 4311–4330.

Eckenfelder, W.W. (1989). *Industrial water pollution control* (2nd ed.). Newyork: Mc Graw-Hill.

Fourest, E., & Roux, J.C. (1992). Heavy metal biosorption by fungal mycelial by-products: mechanisms and influence of pH.. *Applied Microbiology and Biotechnology,* 37, 399–403.

Gabriel J, Baldrian P, Hladíková K, & Háková M. (2001). Copper sorption by native and modified pellets of wood-rotting basidiomycetes. *Applied Microbiologi and Letters*, 32 (3), 194-197.

Galli E, Di Mario F, Rapanà P, Lorenzoni P, & Angelini R. (2003). Copper biosorption by *Auricularia polytricha***.** *Applied Microbiologi and Letters*, 37 (2), 133-137.

Goel, J., Kadirvelu, K., Rajagopal, C., & Garg, V.K. (2005). Removal of lead(II) by adsorption using treated granular activated carbon: Batch and column studies. *Journal of Hazardous Materials*, Article in press.

Ho, Y.S., & McKay, G. (1998). Kinetic models for the sorption of dye from aqueous solution by wood. *Transactions of the Institution of the Chemical Engineers*, 76B, 183-191.

Ho, Y.S., & McKay, G. (1999). Batch lead (II) removal from aqueous solution by peat: Equilibrium and kinetics. *Transactions of the Institution of the Chemical Engineers,* 77B, 165-173.

Hamadi, N. K., Chen, X.D., Farid, M.M., & Lu, M.G.Q. (2001). Adsorption kinetics for the removal of chromium(VI) from aqueous solution by adsorbents derived from used tyres and sawdust. *Chemical Engineering Journal*, 84, 95–105.

Hammaini, A., Ballester, A., Blázquez, M.L., González, F., & Muñoz, J. (2002). Effect of the presence of lead on the biosorption of copper, cadmium and zinc by activated sludge. *Hydrometallurgy*, 67, 109-116.

Kratochvil, D., & Volesky, B. (1998). Advances in the biosorption of heavy metals. *Tıbtech*, 16, 291-299.

Liu, Y., Yang, S.F., Xu, H., Woon, K.H., Lin, Y.M., & Tay, J.H. (2003). Biosorption kinetics of cadmium(II) on aerobic granular sludge. *Process Biochemistry,* 38, 997-1001.

Norton, L., Baskaran, K., & McKenzie, T. (2004). Biosorption of zinc from aqueous solutions using biosolids. *Advances in Environmental Research*, 8, 629–635.

Ozdemir, G., Ozturk, T., Ceyhan, N., Isler, R., & Cosar, T. (2003). Heavy metal biosorption by biomass of *Ochrobactrum anthropi* producing exopolysaccharide in activated sludge. *Bioresource Technology*, 90, 71-74.

Schiewer, S. (1996). Multi- metal ion exchange in biosorption. Chemical Engineering Department of thesis, *University of McGill*, Montreal, pp. 1-27.

Sag, Y. & Kutsal, T. (2000). Determination of the biosorption heats of heavy metal ions on *Zoogloea ramigera* and *Rhizopus arrhizus. Biochemical Engineering Journal***,** 6, 145-151.

Sag, Y., Tatar, B., & Kutsal, T. (2003). Biosorption of Pb(II) and Cu(II) by activated sludge in batch and continuous-flow stirred reactors. *Bioresource Technology*, 87, 27-33.

Selatnia, A., Boukazoula, A., Kechide, N., Bakhti, M.Z. & Chergui, A. (2003). Biosorption of Fe^{3+} from aqueous solution by a bacterial dead *Streptomyces rimosus* biomass. *Process Biochemistry*, Article in pres.

Singh, K.K., Rastogi, R., & Hasan, S.H. (2005). Removal of cadmium from wastewater using agricultural waste 'rice polish'. *Journal of Hazardous Materials,* 121, 51-58.

Utkiger, V., Bor-Yann, C., Tabak, H., Bishop, D.F., & Govind, R. (2000). Treatment of acid mine drainage: I. Equilibrium biosorption of zinc and copper on non-viable activated sludge. *International Biodetorioration & Biodegradation*, 46, 19-28

Xu, Y. (2002). Biosorption of heavy metals by *Laminaria japonica*. Engineering Faculty of thesis, *University of Texas*, Arlington, pp. 1-32.

Yetis, U., Ozcengiz, G., Dilek, F.B., Ergen, N., Erbay, A., & Dolek, A. (1998). Heavy metal biosorption by white-rot fungi. *Water Science Technology*, 38, 323-330.

Yan, G. (2001). Heavy metal biosorption by the fungus, *Mucor Rouxii,* Engineering Faculty of thesis, *University of Regina*, Regina. pp. 1-49.

APPENDICES

RAW DATA OF EXPERIMENTAL STUDES

Table A.1 Raw data for selection of biosorbents (1 g l^{-1} PWS, 100 mg l^{-1} Zn^{2+}, pH=5, 150 rpm, T=25 ^{0}C, 109 µm)

Biosorbed zinc ion concentrations (mg g^{-1})									
Time (h)	0	0,166	0,5	1	2	3	4	6	24
1. Pakmaya	0	15	17	20	25	31	35	37	39
2. DYO	0	21	23	26	32	40	48	49	49
3. Güzelbahçe	0	20	23	28	33	38	40	41	42
4. Çiğli	0	14	17	23	29	33	37	38	38

Table A.2 Raw data for selection of biosorbent (1 g l^{-1} PWS, 100 mg l^{-1} Zn^{2+}, pH=5, 150 rpm, T=25 ^{0}C, 109 µm)

% Zn^{2+} removals									
Time (h)	0	0,166	0,5	1	2	3	4	6	24
1. Pakmaya	0	0,15	0,17	0,2	0,25	0,31	0,35	0,37	0,39
2. DYO	0	0,21	0,23	0,26	0,32	0,4	0,48	0,49	0,49
3. G.bahçe	0	0,2	0,23	0,28	0,33	0,38	0,4	0,41	0,42
4. Çiğli	0	0,14	0,17	0,23	0,29	0,33	0,37	0,38	0,38

Table A.3 Raw data for pretreatment of PWS (1 g l^{-1} PWS, 100 mg l^{-1} Zn^{2+} , pH=5, 150 rpm, T=25 ^{0}C, 109 µm)

	Biosorbed zinc ion concentrations (mg g^{-1})			**% Zn^{2+} removals**		
Time(h)	**H_2O_2**	**NaOH**	**H_2SO_4**	**H_2O_2**	**NaOH**	**H_2SO_4**
0	0	0	0	0	0	0
0,166	23	21	15	0,23	0,21	0,15
0,5	32	28	23	0,32	0,28	0,23
1	42	36	30	0,42	0,36	0,3
2	47	41	35	0,47	0,41	0,35
3	51	47	39	0,51	0,47	0,39
4	59	54	44	0,59	0,54	0,44
6	63	58	48	0,63	0,58	0,48
24	64	60	48	0,64	0,6	0,48

Table A.4 Raw data for variable pH (1 g l^{-1} PWS , 100 mg l^{-1} Zn^{2+} , 150 rpm, T=25 ^{0}C, 109 µm)

Biosorbed zinc ion concentrations (mg g^{-1})									
Time (h)	**0**	**0,166**	**0,5**	**1**	**2**	**3**	**4**	**6**	**24**
pH=3	0	9	12	17	21	28	32	36	37
pH=4	0	11	17	20	25	32	40	46	48
pH=5	0	21	28	35	42	48	54	60	59
pH=6	0	25	36	41	47	52	56	61	62
pH=7	0	29	42	56	64	68	70	72	72
pH=8	0	68	75	78	81	84	88	90	90

Table A.5 Raw data for variable pH (1 g l^{-1} PWS concentration, 100 mg l^{-1} Zn^{2+} concentration, 150 rpm, T=25 ^{0}C, 109 µm)

Zn^{2+} removals									
Time (h)	**0**	**0,166**	**0,5**	**1**	**2**	**3**	**4**	**6**	**24**
pH=3	0	0,09	0,12	0,17	0,21	0,28	0,32	0,36	0,37
pH=4	0	0,11	0,17	0,2	0,25	0,32	0,4	0,46	0,48
pH=5	0	0,21	0,28	0,35	0,42	0,48	0,54	0,6	0,59
pH=6	0	0,25	0,36	0,41	0,47	0,52	0,56	0,61	0,62
pH=7	0	0,29	0,42	0,56	0,64	0,68	0,7	0,72	0,72
pH=8	0	0,68	0,75	0,78	0,81	0,84	0,88	0,9	0,9

Table A.6 Raw data of pseudo-first order biosorption kinetics at different pH (1 g l^{-1} PWS concentration, 100 mg l^{-1} Zn^{2+} concentration, 150 rpm, T=25 ^{0}C, 109 µm)

Time (h)	**$\ln(1-q_t/q_e)$**					
	pH=3	**pH=4**	**pH=5**	**pH=6**	**pH=7**	**pH=8**
0	0	0	0	0	0	0
0,166	-0,28768	-0,27329	-0,43078	-0,52735	-0,51547	-1,40877
0,5	-0,40547	-0,46135	-0,62861	-0,892	-0,87547	-1,79176
1	-0,63908	-0,57054	-0,87547	-1,11514	-1,50408	-2,0149
2	-0,87547	-0,78412	-1,20397	-1,47182	-2,19722	-2,30259
3	-1,50408	-1,18958	-1,60944	-1,91365	-2,89037	-2,70805
4	-2,19722	-2,03688	-2,30259	-2,50144	-3,58352	-3,80666

Table A.7 Raw data of kinetic constants of pseudo-first order biosorption kinetic studies for different pH

pH	3	4	5	6	7	8
k (h^{-1})	0,5265	0,4667	0,5849	0,8718	0,9719	1,0272

Table A.8 Raw data of pseudo-second order biosorption kinetic studies for different pH (1 g l^{-1} PWS , 100 mg l^{-1} Zn^{2+}, 150 rpm, T=25 ^{0}C, 109 µm)

Time (h)	**t/q_t**					
	pH=3	**pH=4**	**pH=5**	**pH=6**	**pH=7**	**pH=8**
0,166	0,018444	0,015091	0,007905	0,00664	0,005724	0,002441
0,5	0,041667	0,029412	0,017857	0,013889	0,011905	0,006667
1	0,058824	0,05	0,028571	0,02439	0,017857	0,012821
2	0,095238	0,08	0,047619	0,042553	0,03125	0,024691
3	0,107143	0,09375	0,0625	0,057692	0,044118	0,035714
4	0,125	0,1	0,074074	0,071429	0,057143	0,045455
6	0,166667	0,130435	0,1	0,098361	0,083333	0,066667

Table A.9 Raw data of kinetic constants of pseudo-second order biosorption kinetic studies for different pH

pH	3	4	5	6	7	8
k $(mg/g)^{-1}*h^{-1}$	0,0251	0,0181	0,0241	0,0349	0,0419	0,0772

Table A.10 Raw data of biosorbed zinc ion concentrations for different mesh size experiments (1 g l^{-1} PWS , 100 mg l^{-1} Zn^{2+} , pH=5, 150 rpm, T=25 ^{0}C)

Time (h)	**Biosorbed zinc ion concentrations (mg g^{-1})**				
	231 µm	**178 µm**	**109 µm**	**64 µm**	**53 µm**
0	0	0	0	0	0
0,167	8	10	12	15	18
0,5	15	18	23	26	29
1	23	26	31	35	40
2	32	36	40	46	51
3	41	45	49	54	59
4	49	51	56	60	64
6	54	56	61	64	68
24	56	58	63	66	70

Table A.11 Raw data of % Zn^{+2} removals for different mesh size experiments (1 g l^{-1} PWS, 100 mg l^{-1} Zn^{+2} , pH=5, 150 rpm, T=25 ^{0}C)

Time (h)	**Zn^{2+} removals**				
	231 µm	**178 µm**	**109 µm**	**64 µm**	**53 µm**
0	0	0	0	0	0
0,167	0,08	0,1	0,12	0,15	0,18
0,5	0,15	0,18	0,23	0,26	0,29
1	0,23	0,26	0,31	0,35	0,4
2	0,32	0,36	0,4	0,46	0,51
3	0,41	0,45	0,49	0,54	0,59
4	0,49	0,51	0,56	0,6	0,64
6	0,54	0,56	0,61	0,64	0,68
24	0,56	0,58	0,63	0,66	0,7

Table A.12 Raw data of pseudo-first order biosorption kinetic studies for different mesh size (1 g l^{-1} PWS, 100 mg l^{-1} Zn^{2+}, pH=5, 150 rpm, T=25 ^{0}C)

Time (h)	**$\ln(1-q_t/q_e)$**				
	231 µm	**178 µm**	**109 µm**	**64 µm**	**53 µm**
0	0	0	0	0	0
0,166	-0,1603	-0,1967	-0,2191	-0,2671	-0,3075
0,5	-0,3254	-0,3878	-0,4733	-0,5213	-0,5559
1	-0,555	-0,6242	-0,7097	-0,7916	-0,8873
2	-0,8979	-1,0296	-1,0664	-1,2685	-1,3863
3	-1,424	-1,6275	-1,626	-1,8563	-2,0223
4	-2,3795	-2,4159	-2,5014	-2,7726	-2,8332

Table A.13 Raw data of kinetic constants of pseudo-first order biosorption kinetic studies for different PWS particle sizes.

Dp (µm)	53	64	109	178	231
k (h^{-1})	0,7064	0,6702	0,5945	0,5765	0,5394

Table A.14 Raw data of pseudo-second order biosorption kinetic studies for different mesh size (1 g l^{-1} PWS , 100 mg l^{-1} Zn^{2+}, pH=5, 150 rpm, T=25 ^{0}C)

Time (h)	**t/q_t**				
	231 µm	**178 µm**	**109 µm**	**64 µm**	**53 µm**
0,166	0,010375	0,0083	0,006917	0,005533	0,004611
0,5	0,033333	0,027778	0,021739	0,019231	0,017241
1	0,043478	0,038462	0,032258	0,028571	0,025
2	0,0625	0,055556	0,05	0,043478	0,039216
3	0,073171	0,066667	0,061224	0,055556	0,050847
4	0,081633	0,078431	0,071429	0,066667	0,0625
6	0,111111	0,107143	0,098361	0,09375	0,088235

Table A.15 Raw data for kinetic constants of pseudo-second order biosorption kinetics for different PWS particle sizes.

D_p (µm)	53	64	109	178	231
k $(mg/g)^{-1}*h^{-1}$	0,0243	0,0224	0,0192	0,0179	0,0151

Table A.16 Raw data of biosorbed zinc ion concentrations for different agitation speed experiments 1 g l^{-1} PWS , 100 mg l^{-1} Zn^{2+} , pH=5, T=25 ^{0}C, 64 µm)

Time (h)	**Biosorbed zinc ion concentrations (mg g^{-1})**				
	50 rpm	**75 rpm**	**100 rpm**	**150 rpm**	**200 rpm**
0	0	0	0	0	0
0,166	5	6	8	10	17
0,5	13	14	15	18	25
1	21	23	26	30	37
2	27	33	37	42	49
3	33	39	44	51	57
4	39	44	51	60	63
6	45	49	56	63	67
24	47	51	57	64	69

Table A.17 Raw data of % Zn^{2+} removals for different agitation speed experiments (1 g l^{-1} PWS , 100 mg l^{-1} Zn^{2+} , pH=5, T=25 ^{0}C, 64 µm)

Time (h)	**Zn^{2+} removals**				
	50 rpm	**75 rpm**	**100 rpm**	**150 rpm**	**200 rpm**
0	0	0	0	0	0
0,166	0,05	0,06	0,08	0,1	0,17
0,5	0,13	0,14	0,15	0,18	0,25
1	0,21	0,23	0,26	0,3	0,37
2	0,27	0,33	0,37	0,42	0,49
3	0,33	0,39	0,44	0,51	0,57
4	0,39	0,44	0,51	0,6	0,63
6	0,45	0,49	0,56	0,63	0,67
24	0,47	0,51	0,57	0,64	0,69

Table A.18 Raw data of pseudo-first order biosorption kinetic studies for different agitation speed (1 g l^{-1} PWS , 100 mg l^{-1} Zn^{2+} , pH=5, T=25 ^{0}C, 64 µm)

Time (h)	**$\ln(1-q_t/q_e)$**				
	50 rpm	**75 rpm**	**100 rpm**	**150 rpm**	**200 rpm**
0	0	0	0	0	0
0,166	-0,1178	-0,1306	-0,1542	-0,1728	-0,2927
0,5	-0,3409	-0,3365	-0,3118	-0,3365	-0,467
1	-0,6286	-0,6337	-0,6242	-0,6466	-0,8035
2	-0,9163	-1,1192	-1,0809	-1,0986	-1,3143
3	-1,3218	-1,5892	-1,5404	-1,6582	-1,9021
4	-2,0149	-2,2824	-2,4159	-3,0445	-2,8184

Table A.19 Raw data of kinetic constants of pseudo-first order biosorption kinetic studies for different agitation speeds.

Agitation speed (rpm)	50	75	100	150	200
k (h^{-1})	0,485	0,56	0,57	0,667	0,6835

Table A.20 Raw data of pseudo-second order biosorption kinetic studies for different agitation speed (1 g l^{-1} PWS concentration, 100 mg l^{-1} Zn^{2+} concentration, pH=5, T=25 ^{0}C, 64 µm)

Time (h)	**t/q_t**				
	50 rpm	**75 rpm**	**100 rpm**	**150 rpm**	**200 rpm**
0,166	0,0332	0,02767	0,02075	0,0166	0,00976
0,5	0,03846	0,03571	0,03333	0,02778	0,02
1	0,04762	0,04348	0,03846	0,03333	0,02703
2	0,07407	0,06061	0,05405	0,04762	0,04082
3	0,09091	0,07692	0,06818	0,05882	0,05263
4	0,10256	0,09091	0,07843	0,06667	0,06349
6	0,13333	0,12245	0,10714	0,09524	0,08955

Table A.21 Raw data of kinetic constants of pseudo-second order biosorption kinetic studies for different agitation speed

Agitation speed (rpm)	50	75	100	150	200
k $(mg/g)^{-1}*h^{-1}$	0,0151	0,0153	0,0134	0,013	0,0182

Table A.22 Raw data of biosorbed zinc ion concentrations for different initial zinc ion concentrations (1 g l^{-1} PWS concentration, pH=5, 150 rpm, T=25 ^{0}C, 64 µm)

Time(h)	**Biosorbed zinc ion concentrations (mg g^{-1})**						
	50 mg/L	**100 mg/L**	**150 mg/L**	**200 mg/L**	**250 mg/L**	**300 mg/L**	**350 mg/L**
0	0	0	0	0	0	0	0
0,166	27	22	12	21	16	19	18
0,5	32	35	25	36	32	33	31
1	35	45	38	50	45	49	47
2	39	54	49	61	59	62	60
3	42	60	56	70	70	75	69
4	45	67	64	77	78	84	76
6	47	72	73	83	84	92	82
24	50	72	73	86	85	94	86

Table A.23 Raw data of % Zn^{2+} removals for different initial zinc ion concentrations (1 g l^{-1} PWS concentration, pH=5, 150 rpm, T=25 ^{0}C, 64 µm)

Time(h)	**Zn^{2+} removals**						
	50 mg/L	**100 mg/L**	**150 mg/L**	**200 mg/L**	**250 mg/L**	**300 mg/L**	**350 mg/L**
0	0	0	0	0	0	0	0
0,166	0,54	0,22	0,08	0,1	0,06	0,06	0,05
0,5	0,64	0,35	0,17	0,18	0,13	0,11	0,09
1	0,7	0,45	0,25	0,25	0,18	0,16	0,13
2	0,78	0,54	0,33	0,31	0,24	0,21	0,17
3	0,84	0,6	0,37	0,35	0,28	0,25	0,2
4	0,9	0,67	0,43	0,39	0,31	0,28	0,22
6	0,94	0,72	0,49	0,42	0,33	0,31	0,23
24	1	0,72	0,49	0,43	0,34	0,31	0,25

Table A.24 Raw data of pseudo-first order biosorption kinetic studies for different initial zinc ion concentrations

Time(h)	**$\ln(1-q_t/q_e)$**						
	50 mg/L	**100 mg/L**	**150 mg/L**	**200 mg/L**	**250 mg/L**	**300 mg/L**	**350 mg/L**
0	0	0	0	0	0	0	0
0,166	-0,85442	-0,36464	-0,17959	-0,29171	-0,21131	-0,23133	-0,24784
0,5	-1,1421	-0,66575	-0,41926	-0,56869	-0,47957	-0,44425	-0,47489
1	-1,36524	-0,98083	-0,73511	-0,92233	-0,76726	-0,76059	-0,85137
2	-1,77071	-1,38629	-1,11241	-1,3278	-1,21194	-1,12059	-1,31568
3	-2,24071	-1,79176	-1,45725	-1,85389	-1,79176	-1,68858	-1,84177
4	-3,157	-2,66723	-2,09323	-2,62708	-2,63906	-2,44235	-2,61496

Table A.25 Raw data of kinetic constants of pseudo-first order biosorption kinetic studies for different initial zinc ion concentrations

C_o (mg/L)	100	200	250	300	350
k (h^{-1})	0,6669	0,6599	0,6407	0,5977	0,6522

Table A.26 Raw data of pseudo-second order biosorption kinetic studies for initial zinc ion concentrations (1 g l^{-1} PWS concentration, pH=5, 150 rpm, T=25 ^{0}C, 64 µm)

Time (h)	**t/q_t**						
	50 mg/L	**100 mg/L**	**150 mg/L**	**200 mg/L**	**250 mg/L**	**300 mg/L**	**350 mg/L**
0,166	0,00304	0,003773	0,006917	0,0039524	0,005188	0,004368	0,004611
0,5	0,015625	0,014286	0,02	0,0138889	0,015625	0,015152	0,016129
1	0,028571	0,022222	0,026316	0,02	0,022222	0,020408	0,021277
2	0,051282	0,037037	0,040816	0,0327869	0,033898	0,032258	0,033333
3	0,071429	0,05	0,053571	0,0428571	0,042857	0,04	0,043478
4	0,088889	0,059701	0,0625	0,0519481	0,051282	0,047619	0,052632
6	0,12766	0,083333	0,082192	0,0722892	0,071429	0,065217	0,073171

Table A.27 Raw data of kinetic constants of pseudo-second order biosorption kinetic studies for different initial zinc ion concentrations

C_o (mg/L)	50	100	150	200	250	300	350
k $(mg/g)^{-1}*h^{-1}$	0,0823	0,0261	0,015	0,0199	0,0152	0,0133	0,0173

Table A.28 Raw data of biosorbed zinc ion concentrations for different initial PWS concentrations (100 mg l^{-1} Zn^{2+} concentration, pH=5, 150 rpm, T=25 ^{0}C, 64 µm)

Time(h)	**Biosorbed zinc ion concentrations (mg g^{-1})**						
	0,25 g/L	**0,5 g/L**	**1 g/L**	**1,5 g/L**	**2 g/L**	**2,5 g/L**	**3 g/L**
0	0	0	0	0	0	0	0
0,166	32	22	12	11,3333	9,5	10	9,66667
0,5	56	44	21	18,6667	17	17,2	18,6667
1	88	64	33	27,3333	26,5	29,2	26,6667
2	116	80	43	34	33	35,6	37,3333
3	136	96	55	42	38,5	40,8	46
4	156	108	64	49,3333	45	43,6	50,6667
6	168	114	69	54	49	46,8	54,6667
24	200	116	71	54,66667	50	47,2	55,33333

Table A.29 Raw data of % Zn^{2+} removals for different initial PWS concentrations (100 mg l^{-1} Zn^{2+} concentration, pH=5, 150 rpm, T=25 ^{0}C, 64 µm)

Time (h)	**% Zn^{2+} removals**						
	0,25 g/L	**0,5 g/L**	**1 g/L**	**1,5 g/L**	**2 g/L**	**2,5 g/L**	**3 g/L**
0	0	0	0	0	0	0	0
0,166	4	5,5	6	8,5	9,5	12,5	14,5
0,5	7	11	10,5	14	17	21,5	28
1	11	16	16,5	20,5	26,5	36,5	40
2	14,5	20	21,5	25,5	33	44,5	56
3	17	24	27,5	31,5	38,5	51	69
4	19,5	27	32	37	45	54,5	76
6	21	28,5	34,5	40,5	49	58,5	82
24	25	29	35,5	41	50	59	83

Table A.30 Raw data of pseudo-first order biosorption kinetic studies for different initial PWS concentrations (100 mg l^{-1} Zn^{2+} concentration, pH=5, 150 rpm, T=25 ^{0}C, 64 µm)

Time(h)	**$\ln(1-q_t/q_e)$**						
	0,25 g/L	**0,5 g/L**	**1 g/L**	**1,5 g/L**	**2 g/L**	**2,5 g/L**	**3 g/L**
0	0	0	0	0	0	0	0
0,166	-0,2113	-0,2144	-0,1911	-0,2356	-0,2155	-0,2404	-0,1946
0,5	-0,4055	-0,4877	-0,3629	-0,4242	-0,4261	-0,4581	-0,4177
1	-0,7419	-0,8242	-0,6506	-0,7056	-0,7783	-0,978	-0,669
2	-1,1727	-1,2098	-0,976	-0,9933	-1,1192	-1,43	-1,1486
3	-1,6582	-1,8458	-1,595	-1,5041	-1,5404	-2,0541	-1,8417
4	-2,6391	-2,9444	-2,6247	-2,4485	-2,5055	-2,6827	-2,6149

Table A.31 Raw data of kinetic constants of pseudo-first order biosorption kinetic studies for different initial PWS concentrations

Initial PWS concentrations (g/L)	0,25	0,5	1	1,5	2	2,5	3
k (h^{-1})	0,6228	0,6883	0,5978	0,5697	0,5915	0,6936	0,6339

Table A.32 Raw data of pseudo-second order biosorption kinetic studies for different initial PWS concentrations (100 mg l^{-1} Zn^{2+} concentration, pH=5, 150 rpm, T=25 ^{0}C, 64 µm)

Time(h)	**t/q_t**						
	0,25 g/L	**0,5 g/L**	**1 g/L**	**1,5 g/L**	**2 g/L**	**2,5 g/l**	**3 g/L**
0,166	0,00259	0,00893	0,01136	0,01724	0,02206	0,02564	0,03571
0,5	0,00377	0,01136	0,01563	0,025	0,03125	0,03704	0,05263
1	0,00692	0,02381	0,0303	0,04651	0,05455	0,0625	0,08696
2	0,00732	0,02679	0,03659	0,05882	0,07143	0,08108	0,11111
3	0,00874	0,02941	0,03774	0,06061	0,07792	0,08889	0,12245
4	0,0083	0,02907	0,03425	0,05618	0,07353	0,09174	0,12821
6	0,00859	0,02679	0,0375	0,05357	0,06522	0,07895	0,10976

Table A.33 Raw data of kinetic constants of pseudo-second order biosorption kinetic studies for different initial PWS concentrations

Initial PWS concentrations (g/L)	0,25	0,5	1	1,5	2
k $(mg/g)^{-1}*h^{-1}$	0,00695	0,00118	0,014	0,0203	0,0239

Table A.34 Raw data for different temperature experiments (1 g l^{-1} PWS concentration, 100 mg l^{-1} Zn^{2+} concentration, pH=5, 150 rpm, 64 µm)

Time (h)	**Biosorbed zinc ion concentrations (mg g^{-1})**					**Zn^{2+} removals**				
	30 ^{0}C	**35 ^{0}C**	**40 ^{0}C**	**45 ^{0}C**	**50 ^{0}C**	**30 ^{0}C**	**35 ^{0}C**	**40 ^{0}C**	**45 ^{0}C**	**50 ^{0}C**
0	0	0	0	0	0	0	0	0	0	0
0,166	15	19	23	25	30	0,15	0,19	0,23	0,25	0,3
0,5	28	30	32	36	42	0,28	0,3	0,32	0,36	0,42
1	35	39	43	49	54	0,35	0,39	0,43	0,49	0,54
2	42	46	50	57	64	0,42	0,46	0,5	0,57	0,64
3	48	51	56	62	68	0,48	0,51	0,56	0,62	0,68
4	54	57	61	65	71	0,54	0,57	0,61	0,65	0,71
6	59	62	66	68	72	0,59	0,62	0,66	0,68	0,72
24	60	62	66	70	73	0,6	0,62	0,66	0,7	0,73

Table A.35 Raw data of pseudo-first order biosorption kinetic studies for different temperature (1 g l^{-1} PWS concentration, 100 mg l^{-1} Zn^{2+} concentration, pH=5, 150 rpm, 64 µm)

Time (h)	**ln(1-q_t/q_e)**				
	30 ^{0}C	**35 ^{0}C**	**40 ^{0}C**	**45 ^{0}C**	**50 ^{0}C**
0	0	0	0	0	0
0,166	-0,2933	-0,3659	-0,4285	-0,4583	-0,539
0,5	-0,6436	-0,6614	-0,6633	-0,7538	-0,8755
1	-0,8995	-0,9916	-1,0542	-1,2751	-1,3863
2	-1,2443	-1,3545	-1,4171	-1,8216	-2,1972
3	-1,6796	-1,7292	-1,8871	-2,4277	-2,8904
4	-2,4681	-2,5177	-2,5802	-3,1209	-4,2767

Table A.36 Raw data of kinetic constants of pseudo-first order biosorption kinetic studies for different temperature

Temperature(^{0}C)	30	35	40	45	50
k (h^{-1})	0,6166	0,6391	0,6696	0,8303	0,9663

Table A.37 Raw data for different temperatures to find activation energy of biosorption with first-order kinetic constants

1/T (1/K)	3,3	3,246	3,195	3,145	3,096
ln k	-0,4835	-0,4477	-0,4011	-0,186	-0,0343

Table A.38 Raw data of pseudo-second order biosorption kinetic studies for different temperature (1 g l^{-1} PWS concentration, 100 mg l^{-1} Zn^{2+} concentration, pH=5, 150 rpm, 64 µm)

Time (h)	**t/q_t**				
	30 ^{0}C	**35 ^{0}C**	**40 ^{0}C**	**45 ^{0}C**	**50 ^{0}C**
0,166	0,01107	0,00874	0,00722	0,00664	0,00553
0,5	0,01786	0,01667	0,01563	0,01389	0,0119
1	0,02857	0,02564	0,02326	0,02041	0,01852
2	0,04762	0,04348	0,04	0,03509	0,03125
3	0,0625	0,05882	0,05357	0,04839	0,04412
4	0,07407	0,07018	0,06557	0,06154	0,05634
6	0,10169	0,09677	0,09091	0,08824	0,08333

Table A.39 Raw data of kinetic constants of pseudo-second order biosorption kinetic studies for different temperature

Temperature (^{0}C)	30	35	40	45	50
k (mg/g)$^{-1}$*h^{-1}	0,0233	0,0255	0,0264	0,0338	0,041

Table A.40 Raw data for different temperature to find activation energy of biosorption with second-order kinetic constants

1/T (1/K)	3,663004	3,663004	3,663004	3,663004	3,663004
ln k	-3,93734	-3,82585	-3,77662	-3,51325	-3,31044

Table A.41 Raw data for different flow rate fed-batch experiment (Q=0,05 L h^{-1}, C_0=100 mg l^{-1}, V_0=1 L, 3 g PWS)

Time	C-control	C-experimental	Efficiency	q
h	mg l^{-1}	mg l^{-1}	%	mg g^{-1}
0	0	0	100	0
1	4,76	0,03	99,97	1,6555
2	9,09	0,05	99,95	3,3146667
3	13,04	0,09	99,91	4,9641667
4	16,67	0,14	99,86	6,612
5	20	0,19	99,81	8,2541667
6	23,08	0,25	99,75	9,893
16	44,44	1,12	98,88	25,992
17	45,95	1,553	98,447	27,37815
18	47,37	1,77	98,23	28,88
19	48,72	2,06	97,94	30,329
20	50	2,201	97,799	31,866
21	51,22	2,381	97,619	33,373317
22	52,38	2,535	97,465	34,8915
23	53,49	2,651	97,349	36,434617
24	54,55	2,712	97,288	38,014533
25	55,56	2,987	97,013	39,42975
26	56,52	3,316	96,684	40,789733
40	66,67	16,8	83,2	49,87
41	67,21	18,165	81,835	49,862417
42	67,74	19,17	80,83	50,189
43	68,25	20,34	79,66	50,3055
44	68,75	20,94	79,06	50,997333
45	69,23	21,74	78,26	51,4475
46	69,7	22,69	77,31	51,711
47	70,15	23,23	76,77	52,394
48	70,59	23,81	76,19	53,017333
49	71,01	24,45	75,55	53,544
50	71,43	24,87	75,13	54,32
63	75,9	32,21	67,79	60,437833
64	76,19	33,23	66,77	60,144
65	76,47	33,94	66,06	60,250833
66	76,74	34,67	65,33	60,300333
67	77,01	35,13	64,87	60,726
68	77,27	35,59	64,41	61,130667
69	77,53	35,86	64,14	61,8105
70	77,78	36,32	63,68	62,19

Table A.42 Raw data for different flow rate fed-batch experiment (Q=0,1 L h^{-1}, C_0=100 mg l^{-1}, V_0=1 L, 3 g PWS)

Time	**C-control**	**C-experimental**	**Efficiency**	**q**
h	**mg l^{-1}**	**mg l^{-1}**	**%**	**mg g^{-1}**
0	0	0	100	0
1	10	0,067	99,933	3,6421
2	15,8	0,42	99,58	6,152
3	23	0,781	99,219	9,628233
4	28,3	1,242	98,758	12,62707
5	32,6	1,746	98,254	15,427
6	37	2,176	97,824	18,5728
7	41	2,563	97,437	21,78097
8	44,8	2,877	97,123	25,1538
9	48	3,117	96,883	28,4259
10	50,3	3,261	96,739	31,35933
24	69,7	17,24	82,76	59,45467
25	71,2	20,2	79,8	59,5
26	72	22,5	77,5	59,4
27	73	25	75	59,2
28	73,7	27,4	72,6	58,64667
29	74,3	29,3	70,7	58,5
30	75	31,6	68,4	57,86667
31	75,61	33	67	58,23367
32	76,19	34,2	65,8	58,786
33	76,74	35,5	64,5	59,11067
34	77,27	36,4	63,6	59,94267

Table A.43 Raw data for different flow rate fed-batch experiment (Q=0,2 L h^{-1}, C_0=100 mg l^{-1}, V_0=1 L, 3 g PWS)

Time	C-control	C-experimental	Efficiency	q
h	mg l^{-1}	mg l^{-1}	%	mg g^{-1}
0	0	0	100	0
1	16,67	0,271	99,729	6,5596
2	28,57	0,307	99,693	13,1894
3	37,5	0,674	99,326	19,64053
4	44,44	1,328	98,672	25,8672
5	50	2,521	97,479	31,65267
6	54,55	4,793	95,207	36,48847
7	58,33	7,665	92,335	40,532
8	61,54	12,685	87,315	42,341
9	64,29	14,285	85,715	46,67133
10	66,67	17,5	82,5	49,17
15	75	26,45	73,55	64,73333
16	76,19	27,94	72,06	67,55
17	77,27	30,89	69,11	68,024
18	78,26	33,56	66,44	68,54
19	79,17	35,14	64,86	70,448
20	80	35,97	64,03	73,38333
21	80,77	36,28	63,72	77,116

Table A.44 Raw data for different flow rate fed-batch experiment (Q=0,3 L h^{-1}, C_0=100 mg l^{-1}, V_0=1 L, 3 g PWS)

Time	C-control	C-experimental	Efficiency	q
h	mg l^{-1}	mg l^{-1}	%	mg g^{-1}
0	0	0	100	0
1	23,077	0,853	99,147	9,6304
2	37,5	2,167	97,833	18,84427
3	47,368	3,65	96,35	27,68807
4	54,545	8,25	91,75	33,94967
5	60	15,345	84,655	37,2125
6	64,286	20,835	79,165	40,55427
7	67,742	22,97	77,03	46,2644
8	70,588	25,77	74,23	50,79373
9	72,973	27,55	72,45	56,0217
10	75	30,67	69,33	59,10667
11	76,744	31,96	68,04	64,1904
15	81,818	33,14	66,86	89,243

Table A.45 Raw data for different flow rate fed-batch experiment (Q=0,4 L h^{-1}, C_0=100 mg l^{-1}, V_0=0,5 L, 3 g PWS)

Time	C-control	C-experimental	Efficiency	q
h	mg l^{-1}	mg l^{-1}	%	mg g^{-1}
0	0	0	100	0
1	44,44	0,379	99,621	13,2183
2	61,54	2,75	97,25	25,4757
3	70,59	6,466	93,534	36,3369
4	76,19	13,63	86,37	43,792
5	80	18,76	81,24	51,0333
6	82,76	23,81	76,19	56,985
7	84,85	28,97	71,03	61,468
8	86,49	30,34	69,66	69,2517
9	87,8	30,92	69,08	77,736
10	88,89	31,45	68,55	86,16

Table A.46 Raw data for different flow rate fed-batch experiment (Q=0,5 L h^{-1}, C_0=100 mg l^{-1}, V_0=0,5 L, 3 g PWS)

Time	C-control	C-experimental	Efficiency	q
h	mg l^{-1}	mg l^{-1}	%	mg g^{-1}
0	0	0	100	0
1	50	1,236	98,764	16,25467
2	66,67	2,5	97,5	32,085
3	75	10,136	89,864	43,24267
4	80	16,07	83,93	53,275
5	83,33	24,675	75,325	58,655
6	85,714	27,51	72,49	67,90467
7	87,5	28,56	71,44	78,58667
8	88,89	29,91	70,09	88,47
9	90	30,56	69,44	99,06667
10	90,91	30,94	69,06	109,945

Table A.47 Raw data for different initial zinc(II) concentrations fed-batch experiments (C_0=37,5 mg l^{-1}, Q=0,2 L h^{-1}, V_0=1 L, 3 g PWS)

Time	**C-control**	**C-experimental**	**Efficiency**	**q**
h	**mg l^{-1}**	**mg l^{-1}**	**%**	**mg g^{-1}**
0	0	0	100	0
1	6,25	0,039	99,896	2,4844
2	10,71	0,174	99,536	4,9168
3	14,06	0,296	99,2107	7,3408
4	16,67	0,751	97,9973	9,5514
5	18,75	1,389	96,296	11,574
6	20,45	1,795	95,2133	13,68033
7	21,88	1,996	94,6773	15,9072
8	23,08	2,529	93,256	17,81087
9	24,1	2,812	92,5013	19,8688
10	25	3,341	91,0907	21,659
15	28,13	10,06	73,1733	24,09333
16	28,57	10,45	72,1333	25,368
17	28,98	10,61	71,7067	26,94267
18	29,35	10,81	71,1733	28,428
19	29,69	10,9	70,9333	30,064
20	30	11	70,6667	31,66667

Table A.48 Raw data for different initial zinc(II) concentrations fed-batch experiments (C_0=75 mg l^{-1}, Q=0,2 L h^{-1}, V_0=1 L, 3 g PWS)

Time	**C-control**	**C-experimental**	**Efficiency**	**q**
h	**mg l^{-1}**	**mg l^{-1}**	**%**	**mg g^{-1}**
0	0	0	100	0
1	12,5	0,459	99,388	4,8164
2	21,43	0,634	99,1547	9,7048
3	28,13	0,885	98,82	14,53067
4	33,33	1,301	98,2653	19,2174
5	37,5	2,727	96,364	23,182
6	40,91	4,514	93,9813	26,6904
7	43,75	6,522	91,304	29,7824
8	46,15	10,62	85,84	30,79267
9	48,21	13,81	81,5867	32,10667
10	50	15,93	78,76	34,07
15	56,25	23,54	68,6133	43,61333
16	57,14	25,27	66,3067	44,618
17	57,95	26,68	64,4267	45,86267
18	58,69	27,34	63,5467	48,07
19	59,37	28,01	62,6533	50,176
20	60	28,67	61,7733	52,21667

Table A.49 Raw data for different initial zinc(II) concentrations fed-batch experiments (C_0=125 mg l^{-1}, Q=0,2 L h^{-1}, V_0=1 L, 3 g PWS)

Time	**C-control**	**C-experimental**	**Efficiency**	**q**
h	**mg l^{-1}**	**mg l^{-1}**	**%**	**mg g^{-1}**
0	0	0	100	0
1	20,83	0,375	99,7	8,182
2	35,71	0,872	99,3024	16,2577
3	46,87	1,84	98,528	24,016
4	55,55	4,79	96,168	30,456
5	62,5	8,635	93,092	35,91
6	68,18	13,65	89,08	39,9887
7	72,92	17,02	86,384	44,72
8	76,92	20,35	83,72	49,0273
9	80,36	23,34	81,328	53,2187
10	83,33	26,61	78,712	56,72
15	93,75	47,17	62,264	62,1067
16	95,24	49,26	60,592	64,372
17	96,59	50,67	59,464	67,3493
18	97,83	51,21	59,032	71,484
19	98,96	51,84	58,528	75,392
20	100	52,24	58,208	79,6

Table A.50 Raw data for different initial zinc(II) concentrations fed-batch experiments (C_0=175 mg l^{-1}, Q=0,2 L h^{-1}, V_0=1 L, 3 g PWS)

Time	**C-control**	**C-experimental**	**Efficiency**	**q**
h	**mg l^{-1}**	**mg l^{-1}**	**%**	**mg g^{-1}**
0	0	0	100	0
1	29,17	0,961	99,4509	11,2836
2	50	3,991	97,7194	21,4709
3	65,62	9,906	94,3394	29,7141
4	77,78	17,68	89,8971	36,06
5	87,5	26,415	84,9057	40,7233
6	95,45	31,91	81,7657	46,596
7	102,08	37,83	78,3829	51,4
8	107,69	41,33	76,3829	57,512
9	112,5	48,62	72,2171	59,6213
10	116,67	53,61	69,3657	63,06
15	131,25	83,62	52,2171	63,5067
16	133,33	86,48	50,5829	65,59
17	135,23	88,22	49,5886	68,948
18	136,96	90,18	48,4686	71,7293
19	138,54	91,46	47,7371	75,328
20	140	91,22	47,8743	81,3

Table A.51 Raw data for different initial zinc(II) concentrations fed-batch experiments (C_0=225 mg l^{-1}, Q=0,2 L h^{-1}, V_0=1 L, 3 g PWS)

Time	**C-control**	**C-experimental**	**Efficiency**	**q**
h	**mg l^{-1}**	**mg l^{-1}**	**%**	**mg g^{-1}**
0	0	0	100	0
1	37,5	6,14	97,2711	12,544
2	64,29	13,56	93,9733	23,674
3	84,37	28,145	87,4911	29,98667
4	100	37,525	83,3222	37,485
5	112,5	45,67	79,7022	44,55333
6	122,73	53,62	76,1689	50,68067
7	131,25	63,53	71,7644	54,176
8	138,46	69,51	69,1067	59,75667
9	144,64	74,84	66,7378	65,14667
10	150	78,19	65,2489	71,81
15	168,75	117,16	47,9289	68,78667
16	171,43	119,32	46,9689	72,954
17	173,86	120,68	46,3644	77,99733
18	176,09	122,11	45,7289	82,76933
19	178,12	122,79	45,4267	88,528
20	180	123,32	45,1911	94,46667

Table A.52 Raw data for different initial zinc(II) concentrations fed-batch experiments (C_0=275 mg l^{-1}, Q=0,2 L h^{-1}, V_0=1 L, 3 g PWS)

Time	**C-control**	**C-experimental**	**Efficiency**	**q**
h	**mg l^{-1}**	**mg l^{-1}**	**%**	**mg g^{-1}**
0	0	0	100	0
1	45,83	9,494	96,5476	14,5344
2	78,57	20,65	92,4909	27,02933
3	103,12	32,895	88,0382	37,45333
4	122,22	49,09	82,1491	43,878
5	137,5	65,26	76,2691	48,16
6	150	82,47	70,0109	49,522
7	160,42	97,51	64,5418	50,328
8	169,23	106,34	61,3309	54,50467
9	176,78	113,93	58,5709	58,66
10	183,33	117,83	57,1527	65,5
15	206,25	151,76	44,8145	72,65333
16	209,52	154,42	43,8473	77,14
17	212,5	156,72	43,0109	81,81067
18	215,22	158,05	42,5273	87,66067
19	217,71	159,21	42,1055	93,6
20	220	159,85	41,8727	100,25

Table A.53 Raw data for different initial PWS contents fed-batch experiments (1 g PWS, Q=0,25 L h^{-1}, C_0=200 mg l^{-1}, V_0=1 L)

Time	**C-control**	**C-experimental**	**Efficiency**	**q**
h	**mg l^{-1}**	**mg l^{-1}**	**%**	**mg g^{-1}**
0	0	0	100	0
1	40	23,92	88,04	20,1
2	66,67	44,64	77,68	33,045
3	85,71	57,47	71,265	49,42
4	100	71,77	64,115	56,46
5	111,11	84,5	57,75	59,8725
6	120	95,65	52,175	60,875
7	127,27	108,16	45,92	52,5525
8	133,33	117,47	41,265	47,58
9	138,46	125,58	37,21	41,86
10	142,86	131,21	34,395	40,775
11	146,67	137,58	31,21	34,0875
12	150	140,89	29,555	36,44
13	152,94	142,61	28,695	43,9025
14	155,56	143,48	28,26	54,36
15	157,89	144,32	27,84	64,4575

Table A.54 Raw data for different initial PWS contents fed-batch experiments (2 g PWS, Q=0,25 L h^{-1}, C_0=200 mg l^{-1})

Time	**C-control**	**C-experimental**	**Efficiency**	**q**
h	**mg l^{-1}**	**mg l^{-1}**	**%**	**mg g^{-1}**
0	0	0	100	0
1	40	15,92	92,04	15,05
2	66,67	34,64	82,68	24,0225
3	85,71	46,93	76,535	33,9325
4	100	58,18	70,91	41,82
5	111,11	70,37	64,815	45,8325
6	120	79,35	60,325	50,8125
7	127,27	88,73	55,635	52,9925
8	133,33	98,32	50,84	52,515
9	138,46	106,36	46,82	52,1625
10	142,86	112,51	43,745	53,1125
11	146,67	117,88	41,06	53,98125
12	150	121,67	39,165	56,66
13	152,94	123,19	38,405	63,21875
14	155,56	124,28	37,86	70,38
15	157,89	125,44	37,28	77,06875

Table A.55 Raw data for different initial PWS contents fed-batch experiments (3 g PWS, Q=0,25 L h^{-1}, C_0=200 mg l^{-1})

Time	**C-control**	**C-experimental**	**Efficiency**	**q**
h	**mg l^{-1}**	**mg l^{-1}**	**%**	**mg g^{-1}**
0	0	0	100	0
1	40	10,428	94,786	12,32167
2	66,67	19,71	90,145	23,48
3	85,71	33,57	83,215	30,415
4	100	48,63	75,685	34,24667
5	111,11	59,84	70,08	38,4525
6	120	68,25	65,875	43,125
7	127,27	74,46	62,77	48,40917
8	133,33	80,72	59,64	52,61
9	138,46	85,49	57,255	57,38417
10	142,86	89,46	55,27	62,3
11	146,67	92,68	53,66	67,4875
12	150	95,37	52,315	72,84
13	152,94	97,52	51,24	78,51167
14	155,56	98,44	50,78	85,68
15	157,89	99,13	50,435	93,03667

Table A.56 Raw data for different initial PWS contents fed-batch experiments (4 g PWS, Q=0,25 L h^{-1}, C_0=200 mg l^{-1})

Time	**C-control**	**C-experimental**	**Efficiency**	**q**
h	**mg l^{-1}**	**mg l^{-1}**	**%**	**mg g^{-1}**
0	0	0	100	0
1	40	7,22	96,39	10,2438
2	66,67	13,04	93,48	20,1113
3	85,71	24,88	87,56	26,6131
4	100	37,28	81,36	31,36
5	111,11	45,47	77,265	36,9225
6	120	54,77	72,615	40,7688
7	127,27	61,68	69,16	45,0931
8	133,33	66,68	66,66	49,9875
9	138,46	73,47	63,265	52,8044
10	142,86	75,68	62,16	58,7825
11	146,67	77,72	61,14	64,6406
12	150	80,96	59,52	69,04
13	152,94	82,58	58,71	74,7575
14	155,56	83,45	58,275	81,1238
15	157,89	84,02	57,99	87,7206

Table A.57 Raw data for different initial PWS contents fed-batch experiments (5 g PWS, Q=0,25 L h^{-1}, C_0=200 mg l^{-1})

Time	**C-control**	**C-experimental**	**Efficiency**	**q**
h	**mg l^{-1}**	**mg l^{-1}**	**%**	**mg g^{-1}**
0	0	0	100	0
1	40	5,24	97,38	8,69
2	66,67	9,45	95,275	17,166
3	85,71	18,33	90,835	23,583
4	100	25,51	87,245	29,796
5	111,11	33,68	83,16	34,8435
6	120	39,38	80,31	40,31
7	127,27	45,66	77,17	44,8855
8	133,33	49,26	75,37	50,442
9	138,46	54,44	72,78	54,613
10	142,86	58,61	70,695	58,975
11	146,67	62,25	68,875	63,315
12	150	65,42	67,29	67,664
13	152,94	67,85	66,075	72,3265
14	155,56	68,27	65,865	78,561
15	157,89	69,31	65,345	84,151

Table A.58 Raw data for different initial PWS contents fed-batch experiments (6 g PWS, Q=0,25 L h^{-1}, C_0=200 mg l^{-1})

Time	C-control	C-experimental	Efficiency	q
h	**mg l^{-1}**	**mg l^{-1}**	**%**	**mg g^{-1}**
0	0	0	100	0
1	40	2,713	98,6435	7,76813
2	66,67	6,068	96,966	15,1505
3	85,71	12,47	93,765	21,3617
4	100	20,86	89,57	26,38
5	111,11	27,72	86,14	31,2713
6	120	33,98	83,01	35,8417
7	127,27	40,13	79,935	39,9392
8	133,33	44,62	77,69	44,355
9	138,46	48,21	75,895	48,8854
10	142,86	52,08	73,96	52,955
11	146,67	55,63	72,185	56,9
12	150	56,79	71,605	62,14
13	152,94	58,31	70,845	67,0296
14	155,56	59,1	70,45	72,345
15	157,89	60	70	77,4963

Table A.59 Raw data of modified Bohart and Adams equation with different flow rates

$m/(Q*C_o)$	600	300	150	100	75	60
Time(h)	33,5	16,5	7,5	4,2	3,5	3

Table A.60 Raw data of modified Bohart and Adams equation with different initial zinc(II) concentrations

$m/(Q*C_o)$	400	200	120	85,71	66,67	54,55
Time(h)	18	8	5,2	3	1,55	1

Table A.61 Raw data of modified Bohart and Adams equation with different initial PWS contents

$m/(Q*C_o)$	20	40	60	80	100	120
Time(h)	0,4	0,6	1	1,5	2,05	2,8